AUGUST 1977

(NASA-CR-150519) CYCLIC AND LOW TEMPERATURE EFFECTS ON MICROCIRCUITS Final Technical Report, Aug. 1975 - Aug. 1977 (McDonnell-Douglas Astronautics Co.) 155 p HC A08/MF A01 CSCL 09A G3/33

N78-16264

Unclas 01864

CYCLIC AND LOW TEMPERATURE EFFECTS ON MICROCIRCUITS

FINAL TECHNICAL REPORT

AUGUST 1975 — AUGUST 1977

V. A. WEISSFLUG

E. V. SISUL

PREPARED FOR THE GEORGE C. MARSHALL SPACE FLIGHT CENTER,
MARSHALL SPACE FLIGHT CENTER, ALABAMA 35812

MCDONNELL DOUGLAS ASTRONAUTICS COMPANY - EAST

MCDONNELL DOUGLAS CORPORATION

UNCLASSIFIED

SECURITY CLASSIFICATION OF THIS PAGE (When Data Entered)

REPORT DOCUMENTATION PAGE		READ INSTRUCTIONS BEFORE COMPLETING FORM
1. REPORT NUMBER	2. GOVT ACCESSION NO.	3. RECIPIENT'S CATALOG NUMBER
4. TITLE (and Subtitle) CYCLIC AND LOW TEMPERATURE EFFECTS ON MICROCIRCUITS		5. TYPE OF REPORT & PERIOD COVERED FINAL TECHNICAL REPORT AUGUST 1975 - AUGUST 1977 6. PERFORMING ORG. REPORT NUMBER
7. AUTHOR(s) V. A. WEISSFLUG E. V. SISUL		8. CONTRACT OR GRANT NUMBER(s) NAS 8-31446
9. PERFORMING ORGANIZATION NAME AND ADDRESS MCDONNELL DOUGLAS ASTRONAUTICS COMPANY - EAST		10. PROGRAM ELEMENT, PROJECT, TASK AREA & WORK UNIT NUMBERS
11. CONTROLLING OFFICE NAME AND ADDRESS NATIONAL AERONAUTICS AND SPACE ADMINISTRATION GEORGE C. MARSHALL SPACE FLIGHT CENTER MARSHALL SPACE FLIGHT CENTER, ALABAMA 35812		12. REPORT DATE AUGUST 1977 13. NUMBER OF PAGES
14. MONITORING AGENCY NAME & ADDRESS(if different from Controlling Office)		15. SECURITY CLASS. (of this report) UNCLASSIFIED 15a. DECLASSIFICATION/DOWNGRADING SCHEDULE N/A

16. DISTRIBUTION STATEMENT (of this Report)

17. DISTRIBUTION STATEMENT (of the abstract entered in Block 20, if different from Report)

18. SUPPLEMENTARY NOTES

NASA MSFC CONTRACTING OFFICER'S REPRESENTATIVE
MR. F. VILLELLA
AREA CODE 205-453-2864

19. KEY WORDS (Continue on reverse side if necessary and identify by block number)

ACCELERATED TESTING
INTEGRATED CIRCUITS
RELIABILITY

20. ABSTRACT (Continue on reverse side if necessary and identify by block number)

The results of cyclic temperature operating life tests, low temperature operating life tests, and pre-/post-life device evaluations were used to evaluate the degrading effects of cyclic and low temperature environments on microcircuit reliability. The cyclic temperature operating life tests consisted of three (3) different test groups with thermal excursions of -55°C to 150°C, -25°C to 125°C and 0°C to 100°C. The low temperature operating life tests consisted of three (3) test groups at ambient temperatures of -55°C, 0°C and 125°C.

DD FORM 1 JAN 73 1473 EDITION OF 1 NOV 65 IS OBSOLETE

UNCLASSIFIED

SECURITY CLASSIFICATION OF THIS PAGE (When Data Entered)

20. ABSTRACT (Continued)

Fifty (50) each of two manufacturers' low power TTL gates and fifty (50) each of two manufacturers' linear devices were included in each test group. Device metallization systems included aluminum metallization/aluminum wire, aluminum metallization/gold wire, and gold metallization/gold wire. The pre-life and post-life evaluation included optical and scanning electron microscope examination, leak tests and bond pull tests. Fewer than 2% electrical failures were observed during the cyclic and low temperature life tests and the post-life evaluations revealed approximately 2% bond pull failures. This was insufficient failure data to permit a quantitative evaluation of cyclic and low temperature effects on microcircuit reliability. Several effects were observed and these are discussed in qualitative terms.

Reconstruction of aluminum die metallization was observed in all devices and the severity of the reconstruction appeared to be directly related to the magnitude of the temperature excursion. No electrical failures were attributed to this phenomenon. All types of bonds except the gold/gold bonds were weakened by exposure to repeated cyclic temperature stress, and the incidence of failure was related to the magnitude of the temperature excursion. Numerous devices surviving the cyclic tests exhibited zero gram failing loads during post-life pull tests, suggesting that electrical testing alone is not an adequate screen for weak bonds. No effects due to moisture or operation of microcircuits at 0°C and -55°C were observed.

PREFACE

The work described in this report was performed by the Parts Evaluation Laboratory section of the McDonnell Douglas Astronautics Company-East Engineering Reliability Department during the period between August 1975 and August 1977. The work was performed for the National Aeronautics and Space Administration, George C. Marshall Space Flight Center under Contract Number NAS8-31446. Mr. F. Villella acted as the NASA Contracting Officer's Representative. The MDAC-EAST Program Engineer was Mr. Roy Maurer. Significant technical contributions were made by Messrs. Gordon Johnson and Larry Conaway. Special thanks are due to Dr. Bob Thomas of RADC for his analysis of microcircuit package atmospheres.

TABLE OF CONTENTS

LIST OF FIGURES

LIST OF TABLES

LIST OF PAGES

1.0 INTRODUCTION

The risk of reliability degradation due to microcircuit operation in cyclic and low temperature environments is generally recognized. Repeated expansion and contraction of microcircuit materials can result in failure due to fatigue and/or mechanical overstress at material interfaces having different thermal coefficients of expansion [1,2]. Operation at low temperature, especially near the dew point of either the external or internal package atmosphere, can result in moisture related failures such as corrosion, leakage current, and surface ion drift [3,4]. Various steps are taken by microcircuit manufacturers and users to minimize the degrading effects of these environments on microcircuit reliability. Gold plated leads and gold die metallization are used to minimize corrosion effects. Passivation layers are also deposited on die surfaces as protection from moisture and ionic contaminations. Completed microcircuits are then subjected to temperature cycling, acceleration, burn-in and hermeticity tests in an attempt to screen out devices with marginal bonds, seals, glassivation and other defects.

In spite of these efforts, microcircuits still fail in operating environments, and a need exists to quantify the effects of cyclic and low temperature environments on microcircuit reliability. The intent of the study described in this report was to evaluate the effects that could be expected from prolonged operation of microcircuits in cyclic and low temperature environments.

2.0 PROGRAM DESCRIPTION

The program for evaluating cyclic and low temperature effects on microcircuits is shown in Figure 1. Included in the program are initial electrical device characterizations, pre-life evaluations of microcircuit construction features, a matrix of cyclic and low temperature operating life tests, and post-life test evaluations of microcircuit physical features. Low power TTL (54L00) and linear (741) microcircuits utilizing various internal lead wire and die metallization materials were included in the program. The device types, manufacturers and metallization systems initially selected are shown in Table 1, and are representative of Au/Au, Au/Al, Al/Al and Au beam lead metallization systems. During the initial portion of the program the Au beam lead device was eliminated because it did not meet electrical performance requirements.

2.1 Initial Electrical Characterization - Upon receipt, all devices were subjected to electrical tests at 25°C, -55°C and 125°C to characterize device performance and to eliminate devices with out-of-tolerance parameter values from subsequent evaluations. The parameters tested, test conditions and end-point limits used for these tests are shown in Tables 2 and 3 for the low power TTL device and the linear device, respectively.

2.2 Pre-Life Evaluation - Prior to subjecting microcircuits to the cyclic and low temperature life tests, a sample of ten (10) of each manufacturer's device type was subjected to fine and gross leak tests per MIL-STD-883, Method 1014 Conditions A1 and C2, external and internal optical and SEM examinations, and bond pull tests. These analyses and tests were designed to identify construction features of each device type and to establish the integrity of the wire bonds in unstressed devices. The resulting information provided a baseline for the post-life evaluations.

2.3 Cyclic and Low Temperature Life Tests - Three (3) tests groups providing different environmental stress levels were included in each of the cyclic temperature operating test (CTOT) and low temperature operating test (LTOT) portions of the program. The three temperature cycling tests were conducted in accordance with MIL-STD-883, Method 1010 for 4,000 cycles using temperature extremes of 0°C

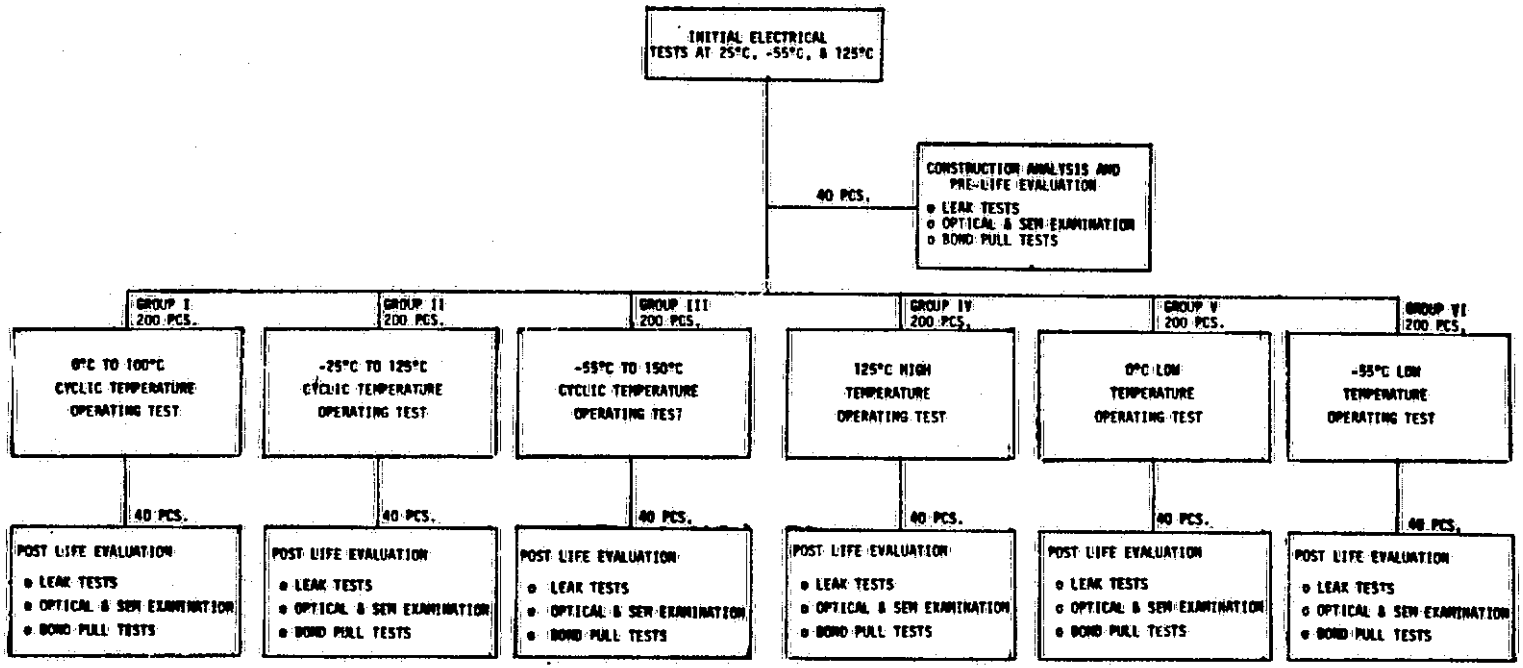

FIGURE 1. PROGRAM WORK FLOW

TABLE 1. MICROCIRCUIT TYPES

PART TYPE	PART NO.*	MANUFACTURER	INTERNAL LEAD MATERIAL	METALLIZATION MATERIAL
QUAD 2-INPUT NAND GATE	SNC54L00T	TEXAS INSTRUMENTS	GOLD	GOLD
	DM54L00F/883B	NATIONAL SEMICONDUCTOR	ALUMINUM	ALUMINUM
OPERATIONAL AMPLIFIER	LM741H/883B	NATIONAL SEMICONDUCTOR	ALUMINUM	ALUMINUM
	RM741T883B	RAYTHEON	GOLD	ALUMINUM
	RM1741BLJ	RAYTHEON	GOLD BEAM LEAD	

* All devices procured with MIL-STD-883 Class B or manufacturer's equivalent processing.

TABLE 2. 54L00 ELECTRICAL MEASUREMENTS

TEST NUMBER	TEST NAME	PIN NUMBERS 1	2	3	4	5	6	7	8	9	10	11	12	13	14	LIMITS MIN.	LIMITS MAX.	UNITS
1	V_{OH}	.7V	5.5V	-100µA	4.5V		5.5V	5.5V		5.5V	5.5V	GND	5.5V	5.5V		2.4		V
2		5.5V	.7V	-100µA			5.5V	5.5V										
3			5.5V			-100µA	.7V	5.5V										
4						-100µA	5.5V	.7V		5.5V								
5								5.5V	-100µA	.7V	5.5V							
6									-100µA	5.5V	.7V		5.5V					
7											5.5V		.7V	5.5V	-100µA			
8	V_{OH}	5.5V	5.5V										5.5V	.7V	-100µA	2.4		
9	V_{OL}	2.0V	2.0V	2mA			5.5V	5.5V		5.5V	5.5V			5.5V			.3	V
10		5.5V	5.5V			2mA	2.0V	2.0V		2.0V	2.0V			5.5V				
11		5.5V	5.5V				5.5V	5.5V	2mA	5.5V	5.5V		5.5V	5.5V				
12	V_{OL}	5.5V	5.5V		4.5V								2.0V	2.0V	2mA		.3	V
13	I_{IL}	.3V	5.5V		5.5V									5.5V		-60	180	µA
14		5.5V	.3V				5.5V											
15			5.5V				.3V	5.5V										
16							5.5V	.3V		5.5V	5.5V							
17								5.5V		.3V	5.5V		5.5V	5.5V				
18										5.5V	.3V		.3V	5.5V				
19										5.5V	5.5V		5.5V	.3V				
20	I_{IL}	5.5V	5.5V				5.5V	5.5V								-60	180	
21	I_{IH1}	2.4V	GND				GND	GND		GND	GND		GND	GND			10	
22		GND	2.4V				GND	GND		GND	GND		GND	GND				
23		GND	GND				2.4V	GND		GND	GND		GND					
24		GND	GND				GND	2.4V		GND	GND		GND					
25		GND	GND				GND	GND		2.4V	GND		GND					
26		GND	GND				GND	GND		GND	2.4V		GND					
27		GND	GND				GND	GND		GND	GND		2.4V	GND			10	
28	I_{IH1}	GND	GND				GND	GND		GND	GND		GND	2.4V			10	
29	I_{IH2}	5.5V	GND				GND	GND		GND	GND		GND	GND			100	
30		GND	5.5V				GND	GND		GND	GND		GND					
31		GND	GND				5.5V	GND		GND	GND		GND					
32		GND	GND				GND	5.5V		GND	GND		GND					
33		GND	GND				GND	GND		5.5V	GND		GND	GND				
34		GND	GND				GND	GND		GND	5.5V		GND	GND				
35		GND	GND				GND	GND		GND	GND		5.5V	GND				
36	I_{IH2}	GND	GND				GND	GND		GND	GND		GND	5.5V			100	µA
37	I_{OS}	GND	GND	GND			5.5V	5.5V		5.5V	5.5V					-3	-15	mA
38		GND	GND			GND	GND	GND		5.5V	5.5V							
39		GND	GND						GND	GND	GND							
40	I_{OS}	GND	GND										GND	GND	GND	-3	-15	
41	I_{CCL}	5.5V	5.5V				5.5V	5.5V		5.5V	5.5V		5.5V	5.5V			2.04	
42	I_{CCH}	GND	GND		5.5V		GND	GND		GND	GND	GND	GND	GND			0.80	

TABLE 3. 741 ELECTRICAL MEASUREMENTS

TEST	TEST NO.	Vcm	V_{cc}^+	V_{cc}^-	R_L	T_A = 25°C		T_A = +125°C & -55°C		UNITS
						MIN	MAX	MIN	MAX	
$V_{IO}(0)$	1	0V	+15V	-15V	∞	-5.0	5.0	-6.0	6.0	mVdc
$V_{IO}(+10)$	2	+10V				-5.0	5.0	-6.0	6.0	mVdc
$V_{IO}(-10)$	3	-10V				-5.0	5.0	-6.0	6.0	mVdc
$I_{IO}(0)$	4	0V				-200	200	-500	500	nAdc
$I_{IO}(+10)$	5	+10V				-200	200	-500	500	
$I_{IO}(-10)$	6	-10V				-200	200	-500	500	
$I_{IB}(0)$	7	0V					500		1500	
$I_{IB}(+10)$	8	+10V					500		1500	
$I_{IB}(-10)$	9	-10V					500		1500	
CMrr	10	±10V				70		70		dB
$PSrr^+$	11	0V	+10 & +15	-15V		77		77		dB
$PSrr^-$	12		+15	-10 & -15		77		77		dB
Icc	13	0V	+15V	-15V			2.8			mAdc
$Vout^+(10K)$	14				10KΩ	+12		+12		Vdc
$Vout^-(10K)$	15				10KΩ	-12		-12		
$Vout^+(2K)$	16				2KΩ	+10		+10		
$Vout^-(2K)$	17				2KΩ	-10		-10		
$A_V(2K)$	18				2KΩ	50		25		V/mV
$A_V(\infty)$	19				∞	50		25		V/mV

to 100°C, -25°C to 125°C, and -55°C to 150°C. The three (3) low temperature life tests were conducted for 2,000 hours at ambient temperatures of -55°C, 0°C, and 125°C. Device operating conditions during CTOT and LTOT were established by the biasing configurations shown in Figure 2. These circuits maintained approximately maximum rated device supply voltage and output current conditions throughout the life tests.

Periodically during the CTOT and LTOT, the devices were returned to room ambient conditions with bias applied and subjected to the 25°C, -55°C and 125°C electrical tests described for initial electrical characterization. During CTOT, electrical measurements were performed at 0, 250, 500, 1,000, 2,000, 3,000 and 4,000 cycles. During LTOT, electrical measurements were performed at 0, 250, 500, 1,000 and 2,000 hours. Generally, devices failing an electrical test were removed from the CTOT or LTOT for failure analysis. However, some devices that exhibited only marginal performance at -55°C or 125°C were left on life test to determine if further degradation would occur.

2.4 Post-Life Evaluation - Upon completion of the CTOT and LTOT, ten (10) surviving devices of each type from each test group (240 total devices) were subjected to tests and evaluations identical to those performed during the pre-life evaluations. Pre-life and post-life data were then compared to evaluate effects of the environmental stresses on non-failed devices.

2.5 Special Tests - Additional special tests that were not part of the originally planned program were also performed to evaluate the effects of internal package atmosphere upon device performance during CTOT and LTOT. These tests included gas mass spectrometer (GMS) analysis [5] of life test failures and survivors, and were performed by the USAF Rome Air Development Center.

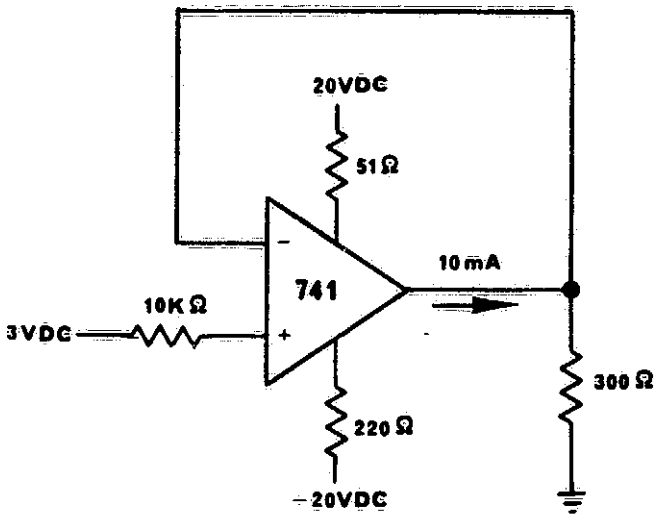

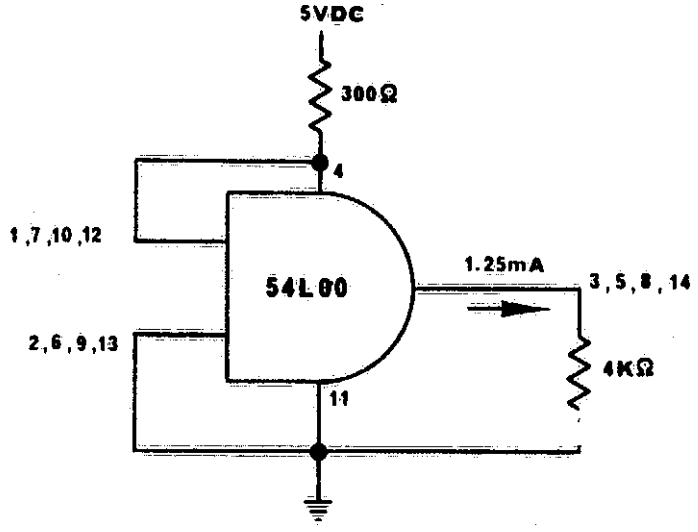

FIGURE 2. DEVICE BIAS CONFIGURATIONS

3.0 PROGRAM RESULTS

This section summarizes the results of all the tests and evaluations performed during the program. Details of the pre- and post-life evaluations are documented in Appendices A and C. Failure analysis reports for devices failing an electrical test during CTOT and LTOT are contained in Appendix B.

3.1 Initial Electrical Characterization - Approximately three hundred and fifty (350) of each of the Texas Instruments 54L00, National 54L00, National 741 and Raytheon 741 were subjected to initial electrical characterization tests. No Texas Instruments 54L00s or National 741s failed these tests. There were eleven (11) National 54L00s and thirty-one (31) Raytheon 741s devices that failed the initial electrical tests. Tables 4 and 5 provide a summary of parameter mean and standard deviation values for the Texas Instruments and National 54L00 devices meeting the electrical specification requirements. Similarly, Tables 6 and 7 summarize the National and Raytheon 741 performance characteristics. No noteworthy differences were observed between the two manufacturers' devices of the same type, and sufficient good devices were obtained to fulfill the program requirement.

3.2 Pre-Life Evaluation - One (1) device of each type was examined for the purpose of documenting construction details. A sample of ten (10) devices of each type were also subjected to hermetic seal tests, optical and SEM examinations and bond pull tests.

All of the devices utilize a SiO_2 passivated silicon die of planar epitaxial construction attached to the package with a gold-silicon eutectic. Table 8 provides other construction details and includes summaries of the leak tests and bond pull tests. No devices failed either the fine or gross leak tests. One National 54L00 bond exhibited a pull strength below the specified limit of MIL-STD-883, Method 2011 as did four (4) Raytheon 741 bonds. The limit for 0.001 inch aluminum wire is 1.5 grams and 2.0 grams for 0.001 inch gold wire. The National 54L00 Al/Al wire to die bond failure was attributed to insufficient ultrasonic energy during bonding. Three (3) of the Raytheon Au/Al wire-to-die bond failures occurred at the intermetallic region due to Kirkendall voiding. The fourth bond failure was attributed to corrosion of the pad due to contamination. This contamination was

TABLE 4. TEXAS INSTRUMENTS 54L00 INITIAL ELECTRICAL CHARACTERIZATION

PARAMETER	END-POINT LIMITS		T_A=25°C		T_A=125°C		T_A=-55°C		UNITS
	MIN.	MAX.	MEAN	SIGMA	MEAN	SIGMA	MEAN	SIGMA	
V_{OH}	2.4		2.755	0.068	2.772	0.078	2.690	0.066	Vdc
V_{OL}		0.3	0.155	0.015	0.176	0.020	0.132	0.013	Vdc
I_{OS}	-1	-15	-6.538	0.247	-5.844	0.240	-5.152	0.782	mA
I_{IH1}		10	0.379	0.233	0.609	0.365	0.214	0.158	µA
I_{IH2}		100	0.513	0.333	0.818	0.503	0.296	0.245	µA
I_{IL}		-0.18	-0.096	0.005	-0.083	0.005	-0.102	0.005	mA
I_{CCL}		2.04	1.155	0.062	1.079	0.061	1.192	0.063	mA
I_{CCH}		0.8	0.429	0.022	0.420	0.025	0.456	0.024	mA

TABLE 5. NATIONAL SEMICONDUCTOR 54L00 INITIAL ELECTRICAL CHARACTERIZATION

PARAMETER	END-POINT LIMITS		T_A=25°C		T_A=125°C		T_A=-55°C		UNITS
	MIN.	MAX.	MEAN	SIGMA	MEAN	SIGMA	MEAN	SIGMA	
V_{OH}	2.4		2.855	0.082	2.877	0.099	2.787	0.076	Vdc
V_{OL}		0.3	0.122	0.021	0.143	0.030	0.102	0.017	Vdc
I_{OS}	-1	-15	-8.906	0.497	-7.750	0.497	-9.417	0.465	mA
I_{IH1}		10	1.224	0.922	1.924	1.425	0.774	0.628	µA
I_{IH2}		100	1.772	1.827	2.874	2.877	1.053	1.366	µA
I_{IL}		-0.18	-0.116	0.014	-0.102	0.014	-0.124	0.014	mA
I_{CCL}		2.04	1.413	0.160	1.287	0.149	1.466	0.150	mA
I_{CCH}		0.8	0.508	0.060	0.470	0.050	0.541	0.058	mA

TABLE 6. NATIONAL SEMICONDUCTOR 741 INITIAL ELECTRICAL CHARACTERIZATION

PARAMETER	END-POINT LIMITS		T_A=25°C		T_A=125°C		T_A=-55°C		UNITS
	MIN.	MAX.	MEAN	SIGMA	MEAN	SIGMA	MEAN	SIGMA	
V_{IO}	-5.0	5.0	-0.105	0.679	0.278	0.848	-0.057	0.716	mVdc
V_{IO+}	-5.0	5.0	-0.121	0.648	0.251	0.827	-0.122	0.661	mVdc
V_{IO-}	-5.0	5.0	-0.059	0.731	0.341	0.893	0.008	0.794	mVdc
I_{IO}	-200	200	-0.574	3.834	-6.708	7.344	0.410	12.000	nAdc
I_{IO+}	-200	200	-0.700	4.376	-5.159	13.851	0.485	13.442	nAdc
I_{IO-}	-200	200	-0.729	3.470	-7.176	5.337	1.368	10.667	nAdc
I_{IB}		500	51.727	10.495	51.254	16.242	78.285	16.775	nAdc
I_{IB+}		500	62.490	12.287	89.885	33.938	93.716	19.687	nAdc
I_{IB-}		500	44.266	9.224	15.028	7.552	67.796	14.726	nAdc
CMRR	70		106.497	9.011	104.238	10.701	102.809	8.187	dB
PSRR+	77		99.651	3.426	94.125	1.978	106.574	11.033	dB
PSRR-	77		100.305	5.575	94.408	6.703	108.765	10.488	dB
I_{CC}		2.8	2.067	0.113	1.712	0.097	2.244	0.120	mAdc
V_{O+}	+12		14.141	0.098	14.296	0.096	14.012	0.107	Vdc
V_{O-}	-12		-12.740	0.082	-13.344	0.091	-12.322	0.065	Vdc
V_{O+2}	+10		13.918	0.094	13.889	0.104	13.803	0.094	Vdc
V_{O-2}	-10		-12.428	0.101	-12.930	0.088	-12.065	0.069	Vdc
AV2K	50		2314.205	5313.117	1312.577	2844.100	894.327	3942.928	mV/V
AV	50		150.858	14.873	274.831	377.430	1546.645	4024.596	mV/V

TABLE 7. RAYTHEON 741 INITIAL ELECTRICAL CHARACTERIZATION

PARAMETER	END-POINT LIMITS		T_A=25°C		T_A=125°C		T_A=-55°C		UNITS
	MIN.	MAX.	MEAN	SIGMA	MEAN	SIGMA	MEAN	SIGMA	
V_{IO}	-5.0	5.0	-0.070	1.399	0.018	1.899	0.245	1.519	mVdc
V_{IO+}	-5.0	5.0	0.036	1.505	-0.089	1.820	0.143	1.402	mVdc
V_{IO-}	-5.0	5.0	-0.034	1.451	0.165	1.989	0.352	1.636	mVdc
I_{IO}	-200	200	-6.434	20.552	-5.539	11.139	3.072	42.422	nAdc
I_{IO+}	-200	200	23.245	44.030	-11.779	19.435	-2.480	58.891	nAdc
I_{IO-}	-200	200	-12.912	24.273	0.745	5.451	2.581	31.896	nAdc
I_{IB}		500	29.513	16.061	26.897	11.670	69.565	53.797	nAdc
I_{IB+}		500	38.667	24.805	52.431	21.985	85.998	77.944	nAdc
I_{IB-}		500	23.893	13.200	4.079	9.293	57.924	44.123	nAdc
CMRR	70		108.231	8.242	98.185	8.683	102.995	10.972	dB
PSRR+	77		99.399	9.784	101.670	9.844	97.382	8.867	dB
PSRR-	77		96.346	8.290	98.548	9.497	99.563	8.998	dB
I_{CC}		2.8	1.983	0.286	1.619	0.237	2.237	0.312	mAdc
V_{O+}	+12		14.189	0.091	14.352	0.092	14.051	0.084	Vdc
V_{O-}	-12		-12.884	0.073	-13.379	0.076	-12.409	0.077	Vdc
V_{O+2}	+10		13.960	0.084	14.047	0.087	13.839	0.100	Vdc
V_{O-2}	-10		-12.532	0.082	-12.834	0.063	-12.133	0.106	Vdc
AV2K	50		1441.074	5073.516	392.632	997.826	895.239	5551.934	mV/V
AV	50		123.951	74.697	271.472	958.411	321.072	747.606	mV/V

TABLE 8. PRE-LIFE EVALUATION SUMMARY

	TEXAS INSTRUMENTS 54L00	NATIONAL SEMICONDUCTOR 54L00	NATIONAL SEMICONDUCTOR 741	RAYTHEON 741
PACKAGE TYPE	14-PIN FLATPACK	14-PIN FLATPACK	8-PIN CAN	8-PIN CAN
LID SEAL	WELD	SOLDER	WELD	WELD
LEAD SEAL	GLASS	GLASS	GLASS	GLASS
EXTERNAL LEAD MATERIAL	GOLD-PLATED KOVAR	GOLD-PLATED KOVAR	GOLD-PLATED KOVAR	GOLD-PLATED KOVAR
INTERCONNECTION WIRE	GOLD	ALUMINUM	ALUMINUM	GOLD
METALLIZATION	GOLD	ALUMINUM	ALUMINUM	ALUMINUM
WIRE BONDS:				
DIE	THERMOCOMPRESSION BALL	ULTRASONIC	ULTRASONIC	THERMOCOMPRESSION BALL
POST/FRAME	THERMOCOMPRESSION STITCH	ULTRASONIC	ULTRASONIC	THERMOCOMPRESSION STITCH
WIRE PULL TEST				
MEAN (GRAMS)	5.17	3.39	3.75	4.75
SIGMA (GRAMS)	0.98	0.86	0.45	1.48

not observed in any of the other devices examined, and no attempt was made to identify the nature of the contaminate. As previously stated, Appendix A contains the complete construction details and pre-life evaluation reports which discuss these failures in more detail.

3.3 Cyclic and Low Temperature Life Tests - Tables 9 and 10 provide failure summaries for the LTOT and CTOT respectively. The failure percentage for LTOT was 0.8% and CTOT was 3.0%. Tables 11 through 14 are failure mode and mechanism summaries for each device type and include the Table 9 and 10 failures plus test induced failures. All failures are discussed in Appendix B.

LTOT produced only five (5) valid device failures, three (3) Raytheon 741s, one (1) National 741 and one (1) T.I. 54L00. The three (3) Raytheon 741 LTOT failures in Group VI (-55°C) were initially marginal devices which drifted in and out of the specification value for input offset voltage (V_{IO}) or power supply rejection ratio (PSRR) during the LTOT. Because these devices did not exhibit strong failure indications and were very close to the specification limit initially, they were discounted as being indicators of low temperature effects. The remainder of the LTOT produced only two (2) additional failures, a shorted MOS capacitor in a National 741 and a surface related failure in a Texas Instruments 54L00. These two (2) failures were in Group IV (125°C) and are typical of the types of failures observed during high temperature testing. Previous high temperature operating tests with similar devices [6,7] indicated that the frequency of failure occurrence declines as the ambient temperature is reduced. The Group IV (125°C) result of 1.0% failures is in keeping with this trend. The Group V (0°C) and VI (-55°C) were expected to produce failures due to moisture related mechanisms that occur less frequently or do not occur at ambient temperature above 25°C. No failures of this type were observed.

The CTOT groups produced seventeen (17) failures compared to the five (5) generated in the LTOT groups. Two factors accounted for this. The first factor is that the hot cycle of Group III was 150°C, the highest temperature experienced by the parts in this program. The nine (9) surface instability failures in Group III were probably a direct result of this temperature. The second factor was the temperature cycling itself. Five (5) bond related failures were observed in

TABLE 9. LOW TEMPERATURE OPERATING TEST FAILURE SUMMARY

TEST GROUP	MANUFACTURER	PART TYPE	METALLIZATION SYSTEM	CUMULATIVE NUMBER OF FAILURES AT HOURS OF TEST			
				250	500	1000	2000
GROUP IV	TEXAS INST.	54L00	Au./Au.	0	0	0	1
125°C	NATIONAL	54L00	Al./Al.	0	0	0	0
	NATIONAL	741	Al./Al.	0	0	1	1
	RAYTHEON	741	Au./Al.	0	0	0	0
GROUP V	TEXAS INST.	54L00	Au./Au.	0	0	0	0
0°C	NATIONAL	54L00	Al./Al.	0	0	0	0
	NATIONAL	741	Al./Al.	0	0	0	0
	RAYTHEON	741	Au./Al.	0	0	0	0
GROUP VI	TEXAS INST.	54L00	Au./Au.	0	0	0	0
-55°C	NATIONAL	54L00	Al./Al.	0	0	0	0
	NATIONAL	741	Al./Al.	0	0	0	0
	RAYTHEON	741	Au./Al.	2	3	3	3

TABLE 10. CYCLIC TEMPERATURE OPERATING TEST FAILURE SUMMARY

TEST GROUP	MANUFACTURER	PART TYPE	METALLIZATION SYSTEM	CUMULATIVE NO. OF FAILURES AT CYCLES OF TEST					
				250	500	1000	2000	3000	4000
GROUP I	TEXAS INST.	54L00	Au./Au.	0	0	0	0	0	0
0°C TO 100°C	NATIONAL	54L00	Al./Al.	0	0	0	0	0	0
	NATIONAL	741	Al./Al.	0	0	0	0	0	0
	RAYTHEON	741	Au./Al.	1	1	1	1	1	1
GROUP II	TEXAS INST.	54L00	Au./Au.	0	0	0	0	0	0
-25°C TO 125°C	NATIONAL	54L00	Al./Al.	0	0	0	0	0	1
	NATIONAL	741	Al./Al.	0	0	0	0	0	0
	RAYTHEON	741	Au./Al.	0	0	0	0	0	1
GROUP III	TEXAS INST.	54L00	Au./Au.	0	0	2	3	5	7
-55°C TO 150°C	NATIONAL	54L00	Al./Al.	0	0	0	0	2	2
	NATIONAL	741	Al./Al.	0	0	0	0	1	2
	RAYTHEON	741	Au./Al.	1	1	1	1	3	3

TABLE 11. TEXAS INSTRUMENTS 54L00 FAILURE MODE SUMMARY

	A. FAILED PARAMETER OR SYMPTOMS B. FAILURE MODE C. FAILURE MECHANISM D. CAUSE OF FAILURE	QUANTITY OF FAILURES AND TIME OF FAILURE (HOURS OR CYCLES) BY TEST GROUP					
		I	II	III	IV	V	VI
		0°C TO 100°C	-25°C TO 125°C	-55°C TO 150°C	125°C LIFE	0°C LIFE	-55°C LIFE
SURFACE INSTABILITY	A. EXCESSIVE I_{IH1} AT -55°C B. INTER-EMITTER LEAKAGE DUE TO AN INCREASE IN THE PARASITIC LATERAL h_{FE} C. INVERSION OF THE BASE OF THE INPUT TRANSISTOR DUE TO CHARGE MIGRATION D. MOBILE IONIC CONTAMINATION			2@1000 1@2000 2@3000 2@4000	1@2000		
TEST ERROR	A. OPEN AND SHORTED INPUTS B. MELTED STRIPES AND SHORTED JUNCTIONS C. ELECTRICAL OVERSTRESS D. SHORTED PROGRAM CARD CONDUCTORS DUE TO MOISTURE INDUCED CORROSION		6@250	3@250		3@500	
	A. OPEN PIN @ 125°C B. NONE (RETEST OK) C. NONE (RETEST OK) D. FAULTY TEST SOCKET			1@3000			
	TOTAL NUMBER OF FAILED PARTS	0	6	11	1	3	0

TABLE 12. NATIONAL SEMICONDUCTOR 54L00 FAILURE MODE SUMMARY

	A. FAILED PARAMETER OR SYMPTOMS B. FAILURE MODE C. FAILURE MECHANISM D. CAUSE OF FAILURE	QUANTITY OF FAILURES AND TIME OF FAILURE (HRS OR CYCLES) BY TEST GROUP					
		I	II	III	IV	V	VI
		0°TO 100°C	-25 TO 125°C	-55 TO 150°C	125°C LIFE	0°C LIFE	-55°C LIFE
MECHANICAL FAILURES	A. OPEN PIN B. BROKEN WIRE BOND C. FATIGUE D. AU-AI INTERMETALLICS DUE TO DEVICE PROCESSING OR PRECONDITIONING		1 @ 4000	1 @ 3000			
MECHANICAL FAILURES	A. SHORTED PIN B. WIRE-DIE SHORT C. SAGGING OF ALUMINUM WIRE D. MISPLACED BOND AND INSUFFICIENT WIRE-TO-DIE CLEARANCE			1 @ 3000			
TEST ERROR	A. OPEN AND SHORTED INPUTS B. MELTED STRIPES AND SHORTED JUNCTIONS C. ELECTRICAL OVERSTRESS D. SHORTED PROGRAM CARD CONDUCTORS DUE TO MOISTURE INDUCED CORROSION		3 @ 250				3 @ 250
	TOTAL NUMBER OF FAILED PARTS	0	4	2	0	0	3

TABLE 13. NATIONAL SEMICONDUCTOR 741 FAILURE MODE SUMMARY

	A. FAILED PARAMETER OR SYMPTIONS B. FAILURE MODE C. FAILURE MECHANISM D. CAUSE OF FAILURE	QUANTITY OF FAILURES AND TIME OF FAILURE (HRS OR CYCLES) BY TEST GROUP					
		I	II	III	IV	V	VI
		0 TO 100°C	-25 TO 125°C	-55 TO 150°C	125°C LIFE	0°C LIFE	-55°C LIFE
MECHANICAL FAILURES	A. LATCHED NEGATIVE			1 @ 3000	1 @ 1000		
	B. SHORTED MOS CAPACITOR						
	C. ALUMINUM MIGRATION THROUGH OXIDE PINHOLE						
	D. PHOTOLITHOGRAPHIC ERROR						
SURFACE INST. FAILURE	A. A_V (2K) AND A_V (∞)			1 @ 4000			
	B. NOT ESTABLISHED						
	C. SURFACE INSTABILITY						
	D. IONIC CONTAMINATION						
	TOTAL NUMBER OF FAILED PARTS	0	0	2	1	0	0

TABLE 14. RAYTHEON 741 FAILURE MODE SUMMARY

	A. FAILED PARAMETER OR SYMPTOMS B. FAILURE MODE C. FAILURE MECHANISM D. CAUSE OF FAILURE	QUANTITY OF FAILURES AND TIME OF FAILURE (HRS OR CYCLES) BY TEST GROUP					
		I	II	III	IV	V	VI
		0 TO 100°C	-25 TO 125°C	-55 TO 150°C	125°C LIFE	0°C LIFE	-55°C LIFE
MECHANICAL FAILURES	A. OPEN PIN B. LIFTED BALL BOND C. FRACTURED SILICON D. OVERBONDING			1 @ 3000			
	A. SHORTED PINS B. LIFTED BALL BOND C. KIRKENDALL VOIDING IN Au_2Al_5 D. BONDING ERROR			1 @ 3000			
	A. LATCHED NEGATIVE B. SHORTED MOS CAPACITOR C. ALUMINUM MIGRATION THROUGH OXIDE PINHOLES D. PHOTOLITHOGRAPHIC ERROR	1 @ 250					
SURFACE INSTABILITY FAILURES	A. PRIMARILY V_{IO} AND PSRR B. PROBABLY INPUT STAGE DEGRADATION C. ION DRIFT OR CHARGE SEPARATION D. MOBILE IONIC CONTAMINATION		1 @ 4000	1 @ 250			2 @ 250 1 @ 500
TEST ERROR	A. CATASTROPHIC AT -55°C B. OPEN PIN 7 C. NONE D. INTERMITTENT TEST SET INTERFACE				1 @ 250		
	A. PSRR OR VOUT AND AV AT -55°C B. NOT DETERMINED C. NOT DETERMINED D. PROBABLY A TEST PROBLEM	3 @ 4000		1 @ 2000			
	TOTAL NUMBER OF FAILED PARTS	4	1	4	1	0	3

the CTOT groups, one (1) in Group II (-25°C to 125°C) and four (4) in Group III (-55°C to 150°C), while none were observed in the LTOT groups. Although the bond related failures were due to different causes, the temperature cycling probably aggravated them to the point of failure. This indicates that as the range of the temperature cycle is increased, more bond related failures will occur. With the exception of these bond related failures, the CTOT, as was the case with LTOT, did not produce failures due to mechanisms which were anticipated at ambient temperatures below 25°C.

3.4 Post-Life Evaluation - At the completion of CTOT and LTOT, ten (10) survivors of each type and from each group were evaluated and tested. This data, in conjunction with the pre-life evaluation data, was used to determine the effects of the environmental stresses on non-failed devices.

The leak tests performed in the pre-life and post-life evaluations did not indicate any important degradation in package hermeticity. No device failed the fine or gross leak test during the pre-life evaluations. During post-life evaluations, two (2) National 54L00s and one (1) Raytheon 741 exhibited gross leaks, and one (1) Raytheon 741 exhibited a fine leak.

The optical and SEM examinations also revealed no degradation of the package markings, external lead finish, internal lead dress, and die attach. With the exception of the Group III National 741, no devices showed any sign of degradation of the glassivation as a result of environmental testing. Nine (9) of the Group III National 741 devices contained cracks in the glassivation over the MOS capacitor. Because this was only observed in the Group III devices, the probable cause was a thermal expansion mismatch between the glass and the large aluminum area of the capacitor and the 205°C thermal excursion, during the -55°C to 150°C temperature cycling. This degradation was not responsible for any electrical failure.

The metallization of all devices was unaffected by the LTOT. CTOT, however, produced evidence of aluminum reconstruction [2] (Figure 3) in the three (3) device types with aluminum metallizations. The reconstruction was especially noticeable in the -55°C to 150°C test. Aluminum reconstruction can result in increased sheet resistivity and can promote electromigration [2], but no electrical

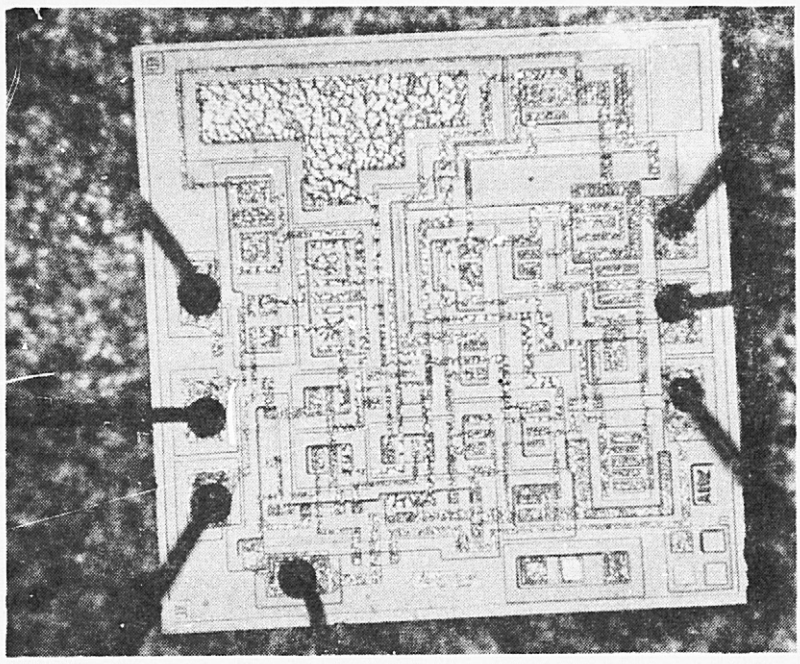

a) METALLIZATION WITH GLASSIVATION REMOVED

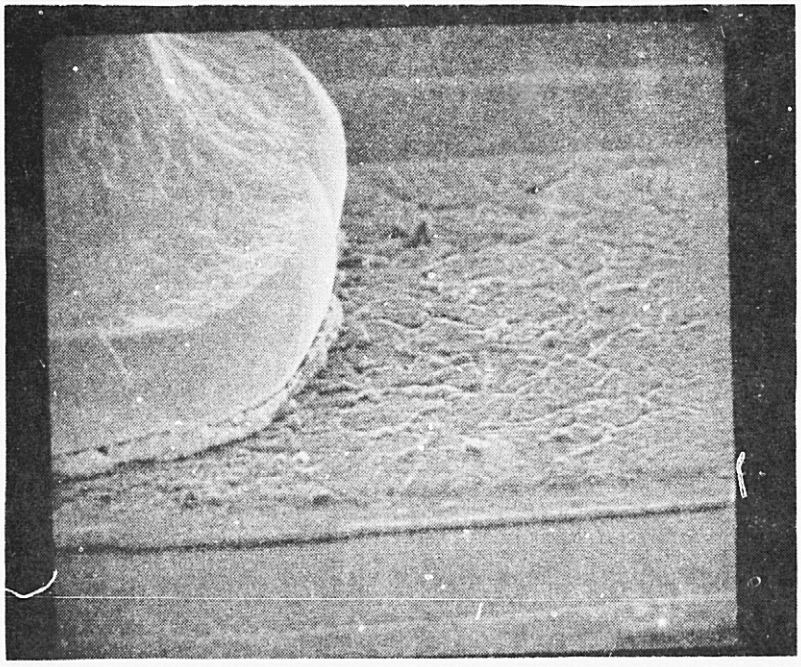

b) SEM PHOTO OF ALUMINUM RECONSTRUCTION

FIGURE 3. EXAMPLES OF ALUMINUM RECONSTRUCTION

failures resulted from aluminum reconstruction. The aluminum beneath the glassivation was slightly reconstructed and the unglassivated aluminum in the area of the bond pads was reconstructed more severely. However, no bond failure was attributed to this mechanism, and no other anomalous metallization conditions were observed. Additional details and photographs of the aluminum reconstruction are contained in the Appendix C post-life evaluation reports.

All internal interconnecting wires of the samples of each device type from each group were pull tested to destruction and the failing force recorded. These results are summarized in Appendix C. Of the 2,506 wires pulled to destruction, 46 exhibited failing loads below the 1.5 or 2.0 grams specified in MIL-STD-883. In fact, the failing loads of ten (10) of the 46 bond failures were less than 0.1 grams. Table 15 relates the failure mode, cause, and type of bond to part type and test group.

The seven (7) Group III National 741 bond failures were heel fractures attributed to weakening caused by flexure of the wire during temperature cycling. In addition, electromigration may have been a contributing factor because all seven (7) failures occurred at either pin 6 (output) or pin 7 (V+).

Twelve (12) National 54L00s from various groups contained twenty (20) ultrasonic bonds which failed at the lead frame due to brittle fracture at the heel. Intermetallic growth was observed at the point of fracture and gold rich intermetallics were found under the entire foot of the bond. In view of this, the aluminum bonds of five of the pre-life evaluation samples were chemcially removed and the lead frames were examined for the presence of intermetallics. All seventy (70) bonds contained gold-rich intermetallics indicating that the reaction originated during device processing or preconditioning. The bonds were probably weakened by continued growth of intermetallics during elevated temperature life (Group IV, 125°C) and by flexing of the wire at the heel in conjunction with the existing brittle intermetallics during temperature cycling (Groups II and III). Low temperature life (Groups V and VI) could not have caused continued growth or flexure of wire, yet seven (7) bonds exhibited low pull strength due to the presence of

TABLE 15. POST-LIFE BOND PULL FAILURE SUMMARY

A. DESCRIPTION OF BOND FAILURE B. CAUSE C. TYPE OF BOND	QUANTITY OF FAILED BONDS									
	5610		740		GROUP I	GROUP II	GROUP III	GROUP IV	GROUP V	GROUP VI
	TEXAS INST.	NATIONAL	NATIONAL	RAYTHEON						
A. DIE BOND HEEL FRACTURE B. WEAKENED BY FLEXURE DURING TEMP. CYCLING C. Al-Al ULTRASONIC BOND			7				7			
A. LEAD FRAME BOND HEEL FRACTURE B. WEAKENED BY INTERMETALLIC GROWTH C. Au-Al WIRE ULTRASONIC BOND		20				1	9	3	5	2
A. DIE BOND LIFT-OFF FROM PAD B. INSUFFICIENT ULTRASONIC ENERGY C. Al-Al ULTRASONIC BOND		2					1			1
A. DIE BOND LIFT-OFF FROM PAD B. UNDERBONDING C. Au-Al THERMAL COMPRESSION BOND				11	2	1	3	5		
A. DIE BOND PAD SEPARATION FROM SiO_2 PASSIVATION B. INSUFFICIENT ADHESION C. Au-Al THERMALCOMPRESSION BOND				2			2			
A. DIE BOND FRACTURE AT THE INTERMETALLIC REGION B. KIRKENDALL VOIDING C. Au-Al THERMALCOMPRESSION BOND				4		1	1	2		

intermetallics. Apparently, the temperature cycling stresses experienced by the parts during insertion and removal from low temperature and during electrical testing at 25°C, -55°C and 125°C was sufficient to aggravate bonds weakened by the existing intermetallic growth.

The remaining bonds that failed were found to have fabrication or bonding error anomalies as their primary cause of failure. These conditions may have been aggravated by LTOT or CTOT, but no evidence was found to substantiate this.

3.5 Special Tests - GMS analysis was performed on two (2) Texas Instruments 54L00 Group III (-55°C to 150°C) devices and a Raytheon 741 Group III device which failed electrically during CTOT. Two (2) survivors of each part type from Group III were also subjected to GMS analysis. Table 16 provides the results of these analyses. Although the internal package atmosphere of the Raytheon 741s contains a high percentage of water vapor (2.6% and 6.8%), no failures were found to have resulted from this condition.

TABLE 16. GMS ANALYSIS RESULTS

	GASEOUS IMPURITIES, % (V/V)						
	HYDROGEN	CARBON DIOXIDE	WATER VAPOR	OXYGEN	ARGON	PUMP OIL	FREON
FAILED DEVICES							
T.I. 54L00 S/N 272	0.2	0.1	0.0429	0	0.0422	0	0
T.I. 54L00 S/N 291	0.0435	0.1	0.0439	0	0.0181	0	0
RAY. 741 S/N 314	0.0209	2.0	6.8	1.0	0.4	0	0
SURVIVORS							
T.I. 54L00 S/N 243	0.1	0.2	0.0344	0.0006	0.0386	0	0
T.I. 54L00 S/N 244	0.2	0.1	0.1	0	0.0220	0	0
NAT. 54L00 S/N 464	0.9	0.4	0.1	0	0.0172	0.0027	0.0005
NAT. 54L00 S/N 465	0.0384	0.4	0.2	0.0126	0.0280	0.0051	0.0023
NAT. 741 S/N 262	0.0244	0.2	0.0411	0.0039	0.0316	0	0
NAT. 741 S/N 305	0.0264	0.2	0.0147	0	0.0326	0	0
RAY. 741 S/N 313	0.0249	2.2	4.9	0.0338	0.3	0	0
RAY. 741 S/N 315	0.0247	0.8	2.6	0.0008	0.2	0	0

4.0 DATA CORRELATION AND EVALUATION

Upon completion of 4,000 temperature cycles and 2,000 hours of low temperature operation, the microcircuits exhibited fewer than 2% electrical failures. This precluded the quantification of effects in terms of the environmental conditions. In its place, the data and observations obtained from the program were examined for qualitative trends which resulted from the environmental conditions.

4.1 Cyclic Temperature Effects - Seventeen (17) electrical failures were generated from the 600 devices subject to CTOT, of which fourteen (14) were from Group III (-55°C to 150°C), two (2) from Group II (-25°C to 125°C) and one (1) from Group I (0°C to 100°C). Nine (9) Group III failures and one (1) Group II failure were surface related and resulted from ionic contamination accelerated to failure by the high temperature interval of the temperature cycle. Two (2) 741 devices failed due to oxide pinholes in their MOS capacitor. This mechanism was probably not induced by the temperature cycling. The remaining five (5) CTOT failures were bond related. In each case, failure analysis indicated the cause of failure to be either processing or bonding error. However, the temperature cycling was probably a contributory factor to the parts failure, since four (4) of these failures were in Group III, one (1) in Group II and none in Group I.

The post-life evaluations revealed that all of the CTOT devices with aluminum metallization exhibited aluminum reconstruction. Although no devices failed electrically as a result of this mechanism, aluminum reconstruction can result in increased sheet resistivity and can promote electromigration.

Bond pull tests that were performed on survivors of CTOT also produced very few failures. Twenty-eight (28) bonds failed from the 1,260 wires that were tested. Twenty-three (23), however, were from Group III survivors indicating that the cyclic temperature contributed to their failure. Five (5) of these CTOT bond pull failures occurred at less than 0.1 gram although they had passed electrical testing. This indicates that electrical testing alone is not a good screen for faulty bond detection.

The Texas Instruments 54L00, which utilizes the Au/Au metallization system, exhibited no degradation in the post-life evaluations as well as no bond pull failures. The cyclic temperature conditions of this program appears to have had no effect on these devices.

4.2 Low Temperature Effects - Five (5) electrical failures were experienced during LTOT. Three (3) of these, as discussed in paragraph 3.3, were discounted as indicators of effects of low temperature. The remaining two (2) failures were from the 125°C group. Therefore, the electrical testing of the LTOT devices revealed no degrading effects induced by low temperature operation of the microcircuits. Post-life visual examinations also revealed no evidence of aluminum reconstruction.

As was the case with the CTOT bond pull test, few failures were observed in the LTOT survivors. Eighteen (18) bonds failed from the 1,260 wires that were tested. There is no strong indication that the low life test temperatures contributed to these failures. The temperature cycling stresses inherent in tri-temperature electrical tests probably contributed to these bond failures. Five (5) of the LTOT bond pull failures occurred at less than 0.1 gram.

4.3 Effects of Package Atmosphere - GMS analysis of several survivors and failed devices was conducted to determine the water vapor content of the parts. The Texas Instruments 54L00 failures and survivors demonstrated no important differences in atmospheric content. The water vapor content of the failed device was less than one surviving device and more than the other. Although acceptable levels of moisture are not known [8], the Raytheon 741 devices (one failure and two survivors) all were found to contain water vapor percentages (2.6% to 6.8%) much higher than any of the other devices. However, none of the Raytheon 741 failures from CTOT or LTOT were directly attributed to the high water vapor content of the parts. GMS analysis of National 54L00 and 741 devices that survived the life tests revealed no noteworthy conditions.

High water vapor content alone does not mean that the devices must eventually fail, rather it is one of the ingredients which can contribute to failure mechanisms such as corrosion and ionic drift [4]. Other environmental conditions like ionic contamination and applied voltage as well as the integrity of the glassivation are partners in these failure mechanisms. Therefore, it is not contradictory to observe high moisture content in the Raytheon 741 devices and find no failures due to moisture related mechanisms.

5.0 CONCLUSIONS AND RECOMMENDATIONS

Insufficient failures were observed during the program to quantify the effects of operating microcircuits in cyclic and low temperature environments. The following general conclusions and recommendations, however, can be made from the observations of the program:

Effect of Cyclic Operation - The effect of operating microcircuits in cyclic temperature environments is to: a) contribute to the failure of microcircuits containing fabrication or processing errors such as oxide pinholes, underbonded wire bonds, excessive intermetallic growth at Au/Al bond interfaces, and contamination, b) degrade the strength of aluminum ultrasonic bonds, and c) induce reconstruction of aluminum metallization. The microcircuits containing fabrication or processing errors were devices that had escaped the MIL-STD-883 Class B screening tests, indicating that more stringent process controls or screens are required. However, additional temperature cycling does not appear to be an effective screening technique. Most of the observed failures occurred after several thousand cycles. In addition, the failures due to ionic contamination were accelerated only by the high temperature portion of the cycle, and a high temperature (>200°C) burn-in would be more effective for these types of failures. Additional temperature cycles will also degrade the strength of "good" aluminum ultrasonic bonds. If additional temperature cycles are employed as a screen, a subsequent constant acceleration test should also be performed to ensure detection of very weak bonds (0.0 to 0.1 grams).

An all gold metallization system appears less susceptible to wire bond failure/degradation due to temperature cycling, since none of the T.I. Au/Au bonds exhibited any mechanical problem or degradation. However, the T.I. device exhibited the highest number of surface related failures, and this may be related to the Ti-W-Au metallization [6].

The aluminum reconstruction noted after 4,000 cycles between -55°C and 150°C did not cause any device failure, and is probably not a severe reliability risk for most applications. However, for applications requiring reliable operation for greater than 4,000 cycles, or in environments with wider temperature extremes, additional tests and investigations should be performed.

Low Temperature Effects - The effect of operating microcircuits at temperatures below 25°C appears to be negligible from the results of this study. All of the device failures and weak bonds encountered during LTOT were the results of microcircuit fabrication or processing errors (oxide pinholes, underbonded wire bonds, and excessive intermetallic growth). None of the failures were attributed to mechanisms unique to low temperature operation. Moisture related failures were expected, especially with the high moisture content Raytheon 741 devices. However, none were observed. Other contaminants and/or device defects are required to induce failures at low operating temperatures. The moisture levels and concentrations of other contaminants required to induce microcircuit failure are not well understood, and additional moisture related studies are recommended.

6.0 REFERENCES

[1] F. Villella and M. F. Nowakowski, "Investigation of Fatigue Problems in 1-mil Diameter Thermocompression and Ultrasonic Bonding of Aluminum Wire". NASA TM-X-64566 (1970).

[2] E. Philofsky, K. Ravi, E. Hall, J. Black, "Variables Affecting Thermally Induced Surface Reconstruction in Aluminum Metal", Ninth Annual Reliability Physics Symposium Proceedings, Las Vegas, Nevada, 1971, pp. 120-128.

[3] D. S. Peck and C. H. Zierdt, Jr., "Temperature-Humidity Acceleration of Metal-ElectrolysisFailure in Semiconductor Devices", Eleventh Annual Reliability Physics Symposium Proceedings, Las Vegas, Nevada, 1973, pp. 146-152.

[4] S. C. Kolesar, "Principles of Corrosion", Twelfth Annual Reliability Physics Symposium Proceedings, Las Vegas, Nevada, 1974, pp. 155-167.

[5] R. W. Thomas, "Microcircuit Package Gas Analysis", Fourteenth Annual Reliability Physics Symposium Proceedings, Las Vegas, Nevada, 1976, pp. 283-294.

[6] G. M. Johnson, "Accelerated Test Techniques for Microcircuits", MDC E1208, January, 1975.

[7] G. M. Johnson, "Evaluation of Microcircuit Accelerated Test Techniques", RADC-TR-218, July, 1976.

[8] D. E. Meyer, "Miniature Moisture Sensors for In-Package Use by the Microelectronics Industry", Thirteenth Annual Reliability Physics Symposium Proceedings, Las Vegas, Nevada, 1975, pp. 48-52.

APPENDIX A

CONSTRUCTION DETAILS AND PRE-LIFE EVALUATIONS

TABLE OF CONTENTS

APPENDIX A1

CONSTRUCTION DETAILS AND PRE-LIFE EVALUATIONS OF

THE TEXAS INSTRUMENTS SNC54L00T

QUAD 2-INPUT NAND GATE

DATE CODE 7519

I. CONSTRUCTION DETAILS (Based on one sample)

A. PACKAGE

1. Type: 14-Pin Flatpack - Figure A1
2. Weight: 0.13 gram
3. Materials:
   a) Lid and Case: Gold-Plated Kovar
   b) Leads: Kovar, Gold-Plated Internal & External
   c) Seals: Glass and Weld

B. INTERNAL GEOMETRY - Figure A2

1. Interconnections
   a) Type: Gold Wire
   b) Diameter: 0.001 inch
   c) Bonds:
      - o Gold-Gold Thermocompression Ball at the Die - Figure A3
      - o Gold-Gold Thermocompression Stitch at the Lead Frame - Figure A4
2. Die
   a) Type: Silicon, planar epitaxial
   b) Scribe Method: Mechanical
   c) Attach Method: Gold Eutectic
   d) Geometry and Electrical Schematic: Figures A5 and A6
   e) Glassivation: Silicon dioxide
3. Metallization
   a) Type: Multilayer - TiW/Au/TiW
   b) Thickness: TiW Top Layer = 1,000Å
      Au Main Conductor = 12,000Å
      TiW Barrier Layer = 2,000Å

II. PRE-LIFE EVALUATIONS (Based on ten parts)

A. HERMETICITY

1. Fine Leak Rates: 0.34 to 0.62 (Mean=0.45) x 10^{-8} STD CC OF He/Sec.
2. Gross Leakers: None

B. INTERNAL EXAMINATIONS

1. Surface Quality: Good
2. Metallization Quality: Good - No defects, good step coverage, continuous barrier metal layer as documented in Figures A7 through A9.

C. PULL TESTS (140 Wires)

1. Mean Pull Strength: 5.17 grams
2. STD Deviation: 0.98 gram (.19$\bar{X}$)
3. Range: 2.0 to 7.9 grams
4. Weak Bonds: None, all breaks occurred in the wire or in the neckdown area above the ball at the specified minimum limit of 2.0 grams (MIL-STD-883) or more.

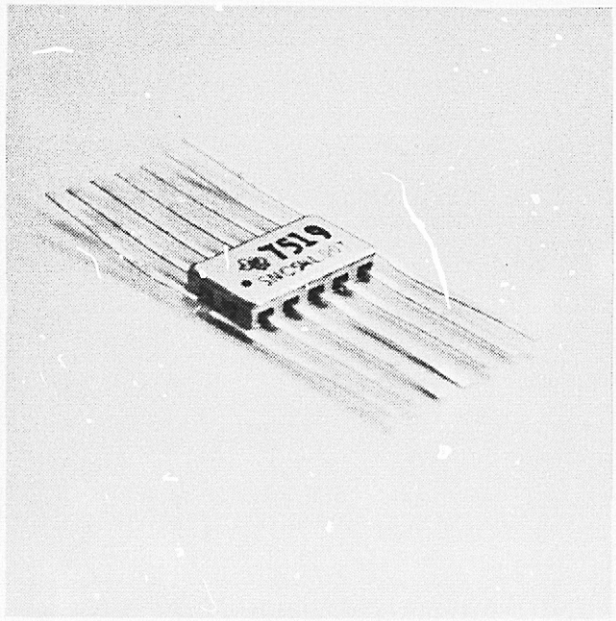

3.5X S/N 661

FIGURE A1. TEXAS INSTRUMENTS SNC54LOOT PACKAGE

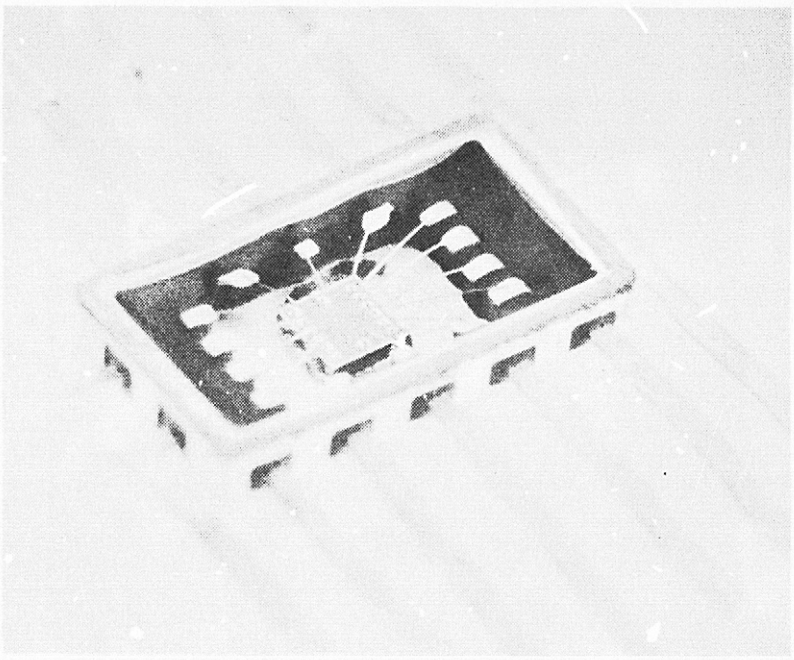

9X S/N 661

FIGURE A2. INTERNAL GEOMETRY

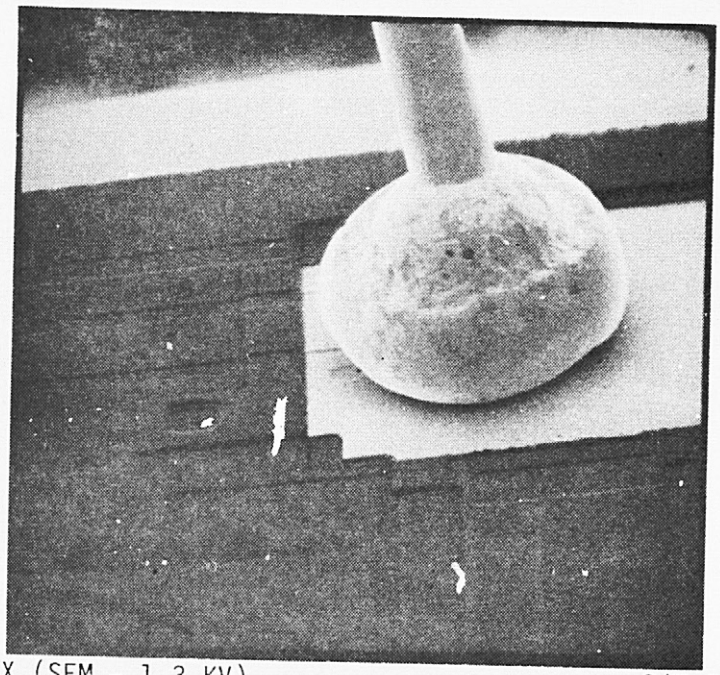

475X (SEM - 1.3 KV) S/N 661

FIGURE A3. WIRE BOND AT THE DIE

500X (SEM - 1.3 KV) S/N 661

FIGURE A4. WIRE BOND AT THE LEAD FRAME

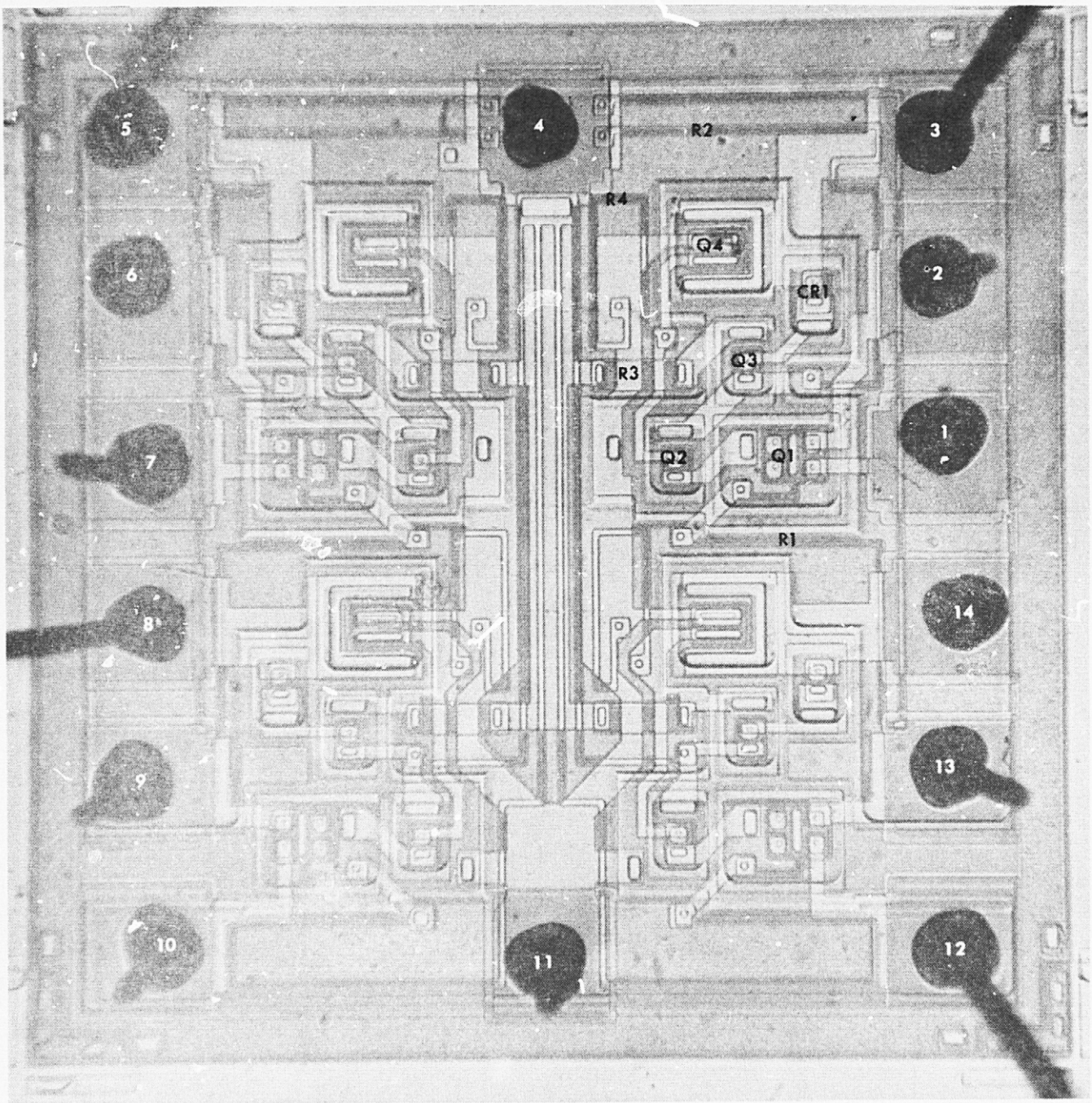

150X S/N 685

FIGURE A5. DIE GEOMETRY

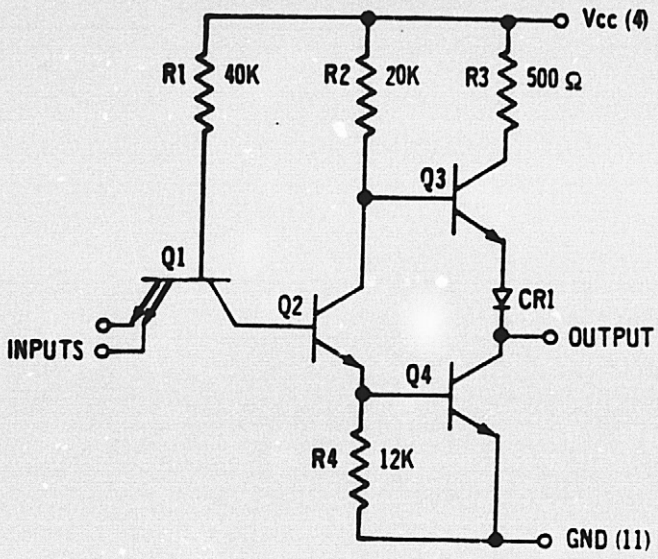

a) Electrical Schematic of One Gate

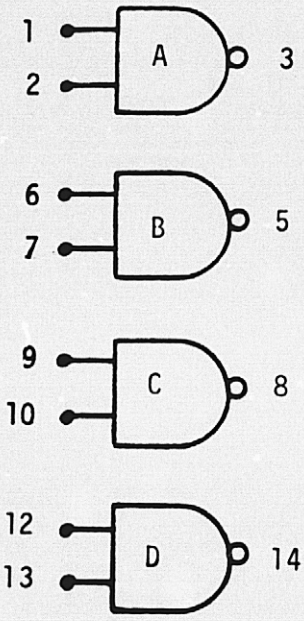

b) Block Diagram

FIGURE A6. SCHEMATIC DIAGRAMS OF THE SNC54L00T

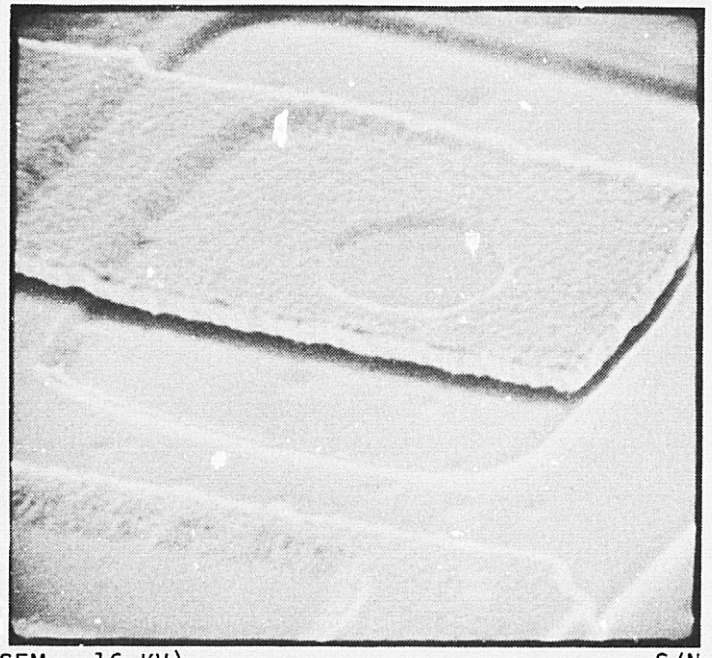

1700X (SEM - 16 KV) S/N 685

FIGURE A7. EXAMPLE OF METALLIZATION QUALITY AND STEP COVERAGE (GLASSIVATION REMOVED).

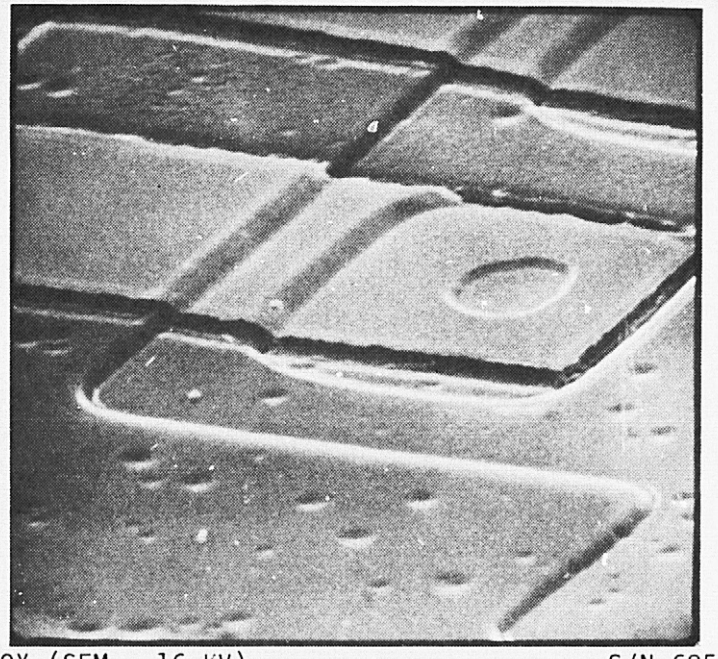

1500X (SEM - 16 KV) S/N 685

FIGURE A8. EXAMPLE OF TiW BARRIER METAL QUALITY AND STEP COVERAGE (TOP TiW AND Au LAYERS REMOVED).

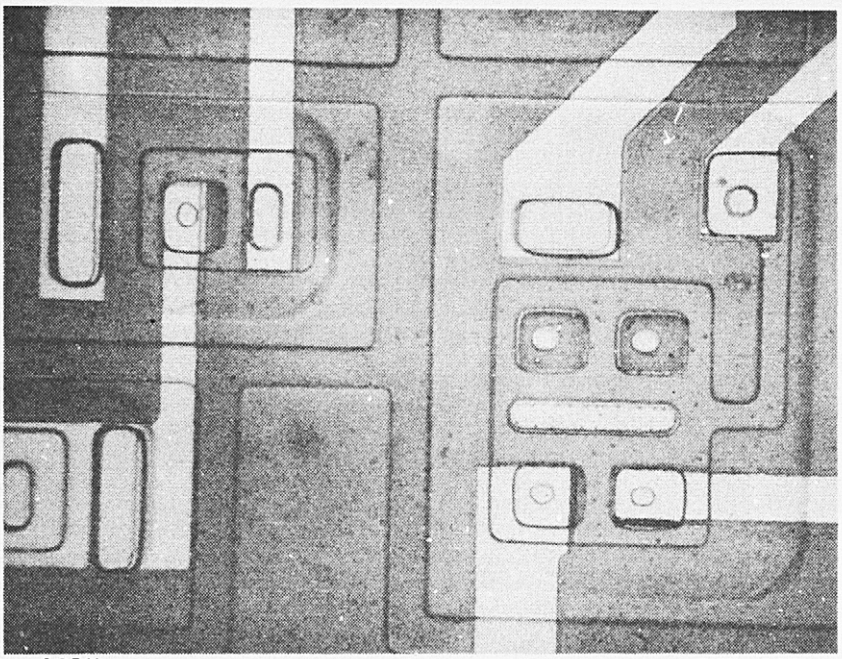

491X S/N 685

FIGURE A9. OPTICAL MICROGRAPH OF TiW BARRIER METAL LAYER

APPENDIX A2

CONSTRUCTION DETAILS AND PRE-LIFE EVALUATIONS

OF THE

NATIONAL SEMICONDUCTOR DM54L00F/883B

QUAD 2-INPUT NAND GATE

DATE CODE 7446

I. CONSTRUCTION DETAILS (Based on one sample)

A. PACKAGE

1. Type: 14-Pin Flatback - Figure A10
2. Weight: 0.26 gram
3. Materials:
   a) Lids and solder frame: Gold-Plated Kovar
   b) Leads: Kovar, Gold-Plated External and Internal
   c) Seals: Solder and Glass

B. INTERNAL GEOMETRY - Figure A11

1. Interconnections:
   a) Type: Aluminum Wire
   b) Diameter: 0.001 inch
   c) Dress: Smooth loops, maximum height of loop is at the bond to the frame indicating the use of reverse or "backwards" bonding (first bond is made at frame, second at the die).
   d) Bonds:
      - o Aluminum-Aluminum Ultrasonic at the Die - Figure A12
      - o Aluminum-Gold Ultrasonic at the Frame - Figure A13
2. Die:
   a) Type: Silicon, Planar Epitaxial
   b) Scribe Method: Mechanical
   c) Attach Method: Gold Eutectic
   d) Geometry and Electrical Schematic: Figures A14 and A15
   e) Glassivation: Silicon Dioxide
3. Metallization:
   a) Type: Aluminum
   b) Thickness: Approximately 12,000Å
   c) Structure: Fine Grain

II. PRE-LIFE EVALUATIONS (Based on ten sampeles)

A. HERMETICITY

1. Fine Leak Rates: 0.46 to 1.13 (Mean=0.81) $x.10^{-8}$ STD CC of He/Sec
2. Gross Leakers: None

B. INTERNAL EXAMINATIONS

1. Surface Quality: Fair - Three of ten parts examined contained contamination on top of the glassivation which remained in place after a nominal gas blow as illustrated in Figure A16. In two of the parts, the debris appeared to be transparent flakes that had accumulated at the edges of the metal stripes as shown in Figures A17 and A18. In the third part, the debris appeared to be a build-up of residue trapped at the edges of the stripes as shown in Figures A19 and A20. None of the contamination should pose a problem provided the glassivation remains intact.
2. Metallization Quality: No defects, good step coverage, and very little reordering (grain growth) from glassivation operation as documented in Figures A21 through A26.

C. PULL TESTS (140 Wires)

1. Mean Pull Strength: 3.39 grams
2. Std. Deviation: 0.86 gram ($.25\overline{X}$)
3. Range: 0.7 gram to 6.0 grams
4. Weak Bonds: Only one bond exhibited a pull strength of less than the specified minimum limit of 1.5 grams (MIL-STD-883). The pin 6 bond of S/N 314 lifted from the pad at the die of a force of 0.7 gram. The bond probably had received insufficient ultrasonic energy since welding occurred only around the extreme periphery as shown in Figure A27. One other bond of S/N 314 and two bonds of S/N 315 lifted in this same manner, but these bonds failed at acceptable levels (1.8 to 2.6 grams). All other breaks occurred either in the wire or at the neckdown area (heel) of the post or die bond at values ranging from 1.6 to 6.0 grams.

3.5X S/N 295

FIGURE A10. NATIONAL 54LOOF PACKAGE

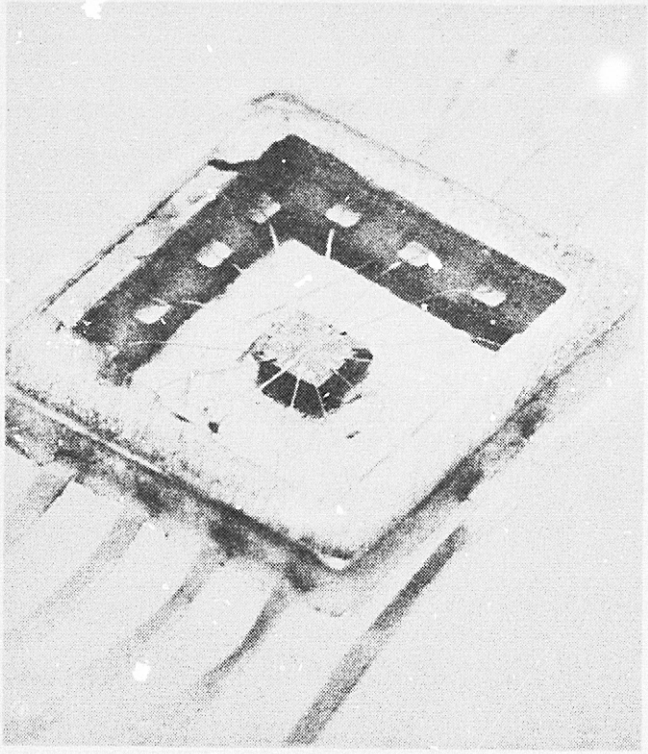

9X S/N 295

FIGURE A11. INTERNAL GEOMETRY

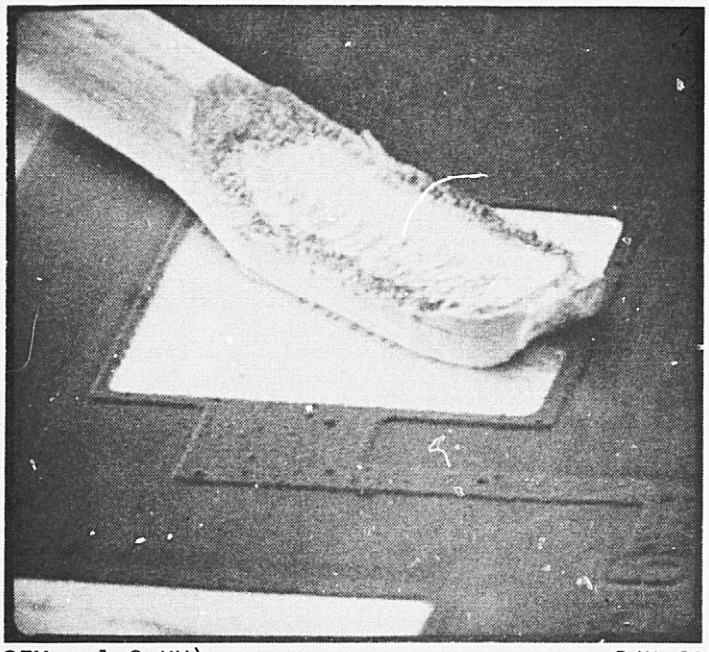

450X (SEM - 1.2 KV) S/N 695

FIGURE A12. WIRE BOND AT THE DIE

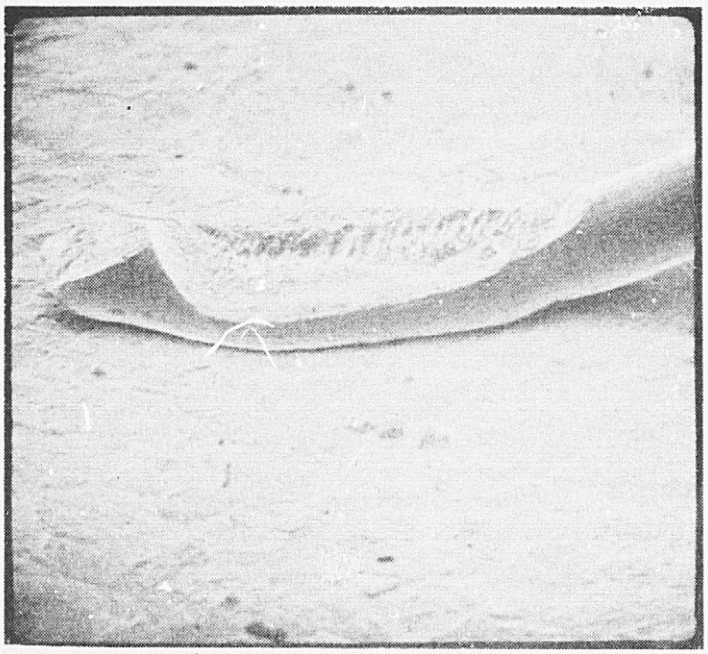

400X (SEM - 1.2 KV) S/N 695

FIGURE A13. WIRE BOND AT THE LEAD FRAME

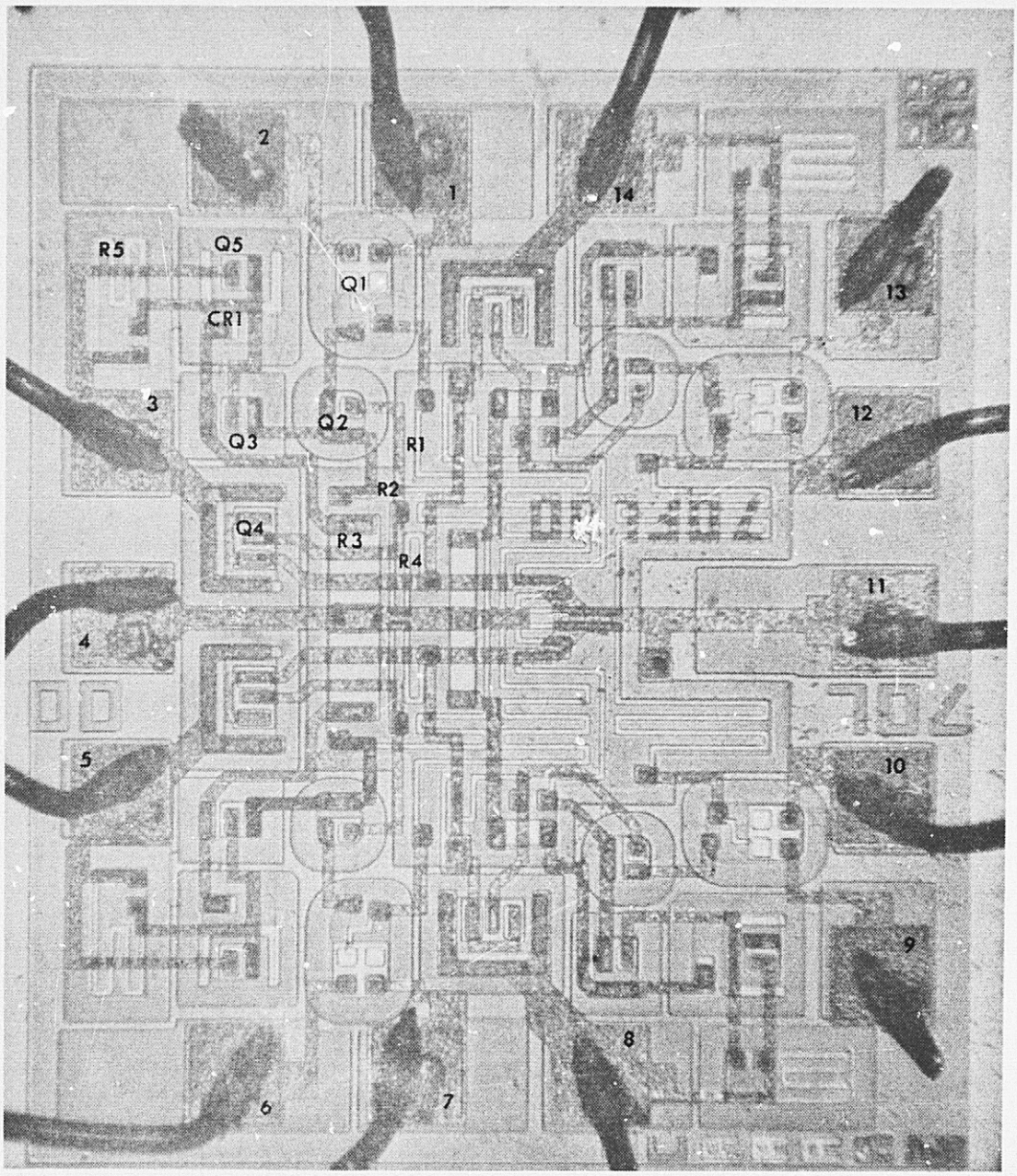

154X S/N 305

FIGURE A14. DIE GEOMETRY

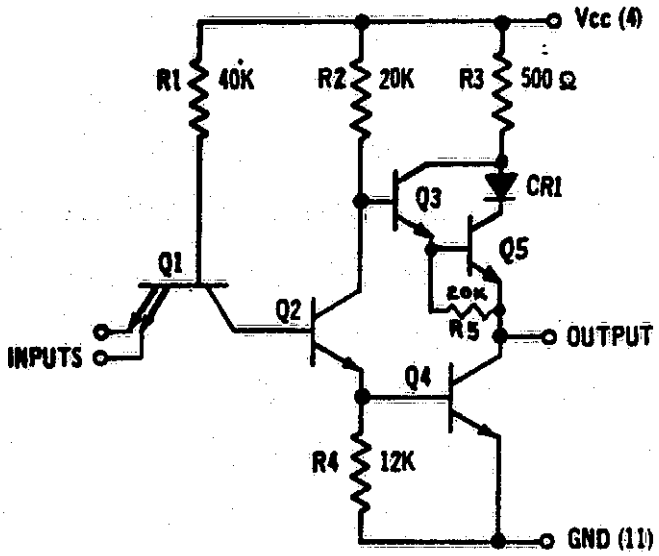

a) Electrical Schematic of One Gate

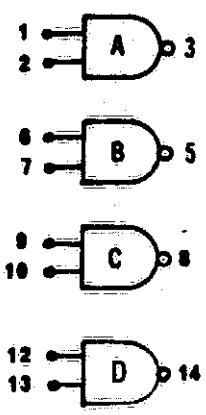

b) Block Diagram

FIGURE A15. SCHEMATIC DIAGRAMS OF THE DM54L00F

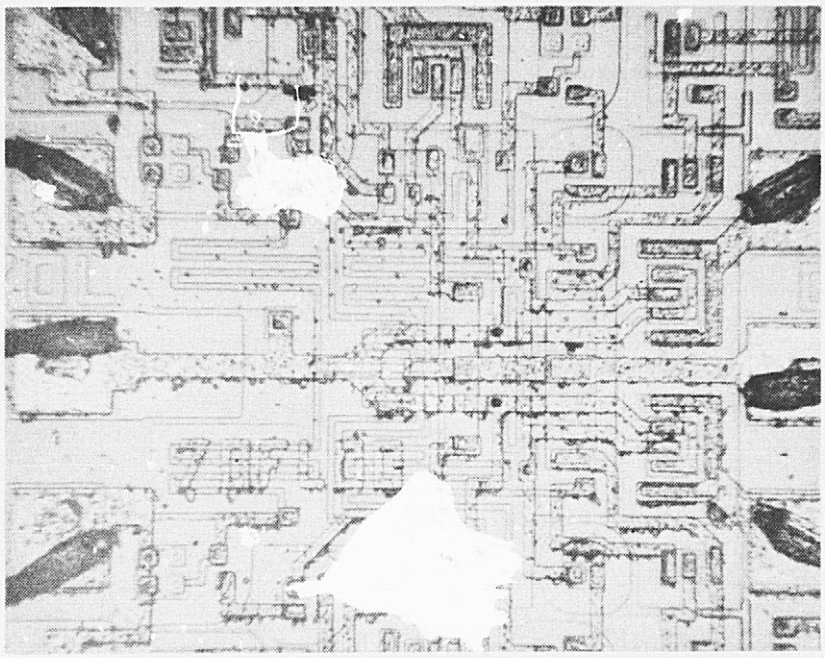

70X S/N 313

FIGURE A16. EXAMPLE OF DIE WITH ACCUMULATION OF CONTAMINATION ALONG THE EDGES OF THE METAL STRIPES.

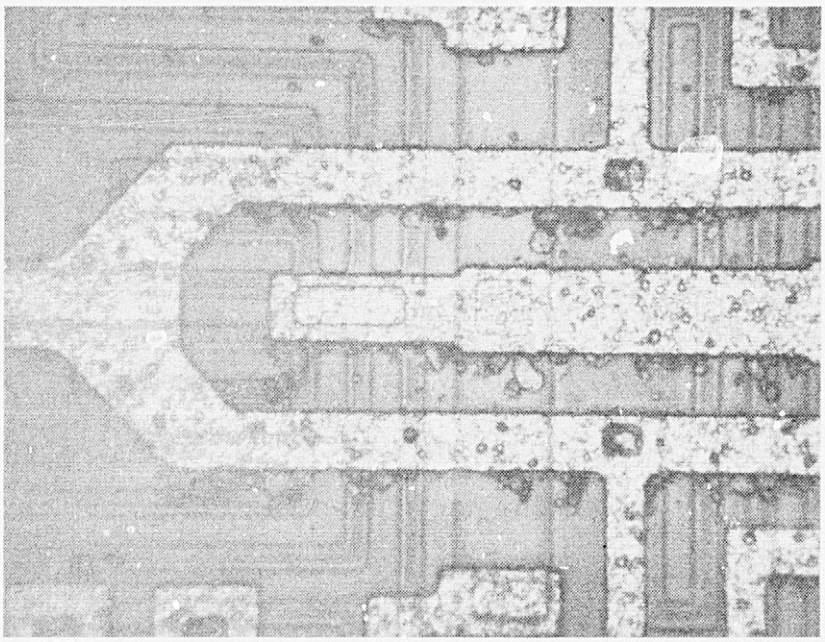

491X S/N 313

FIGURE A17. EXAMPLE OF THE TRANSPARENT, FLAKE-TYPE CONTAMINATION.

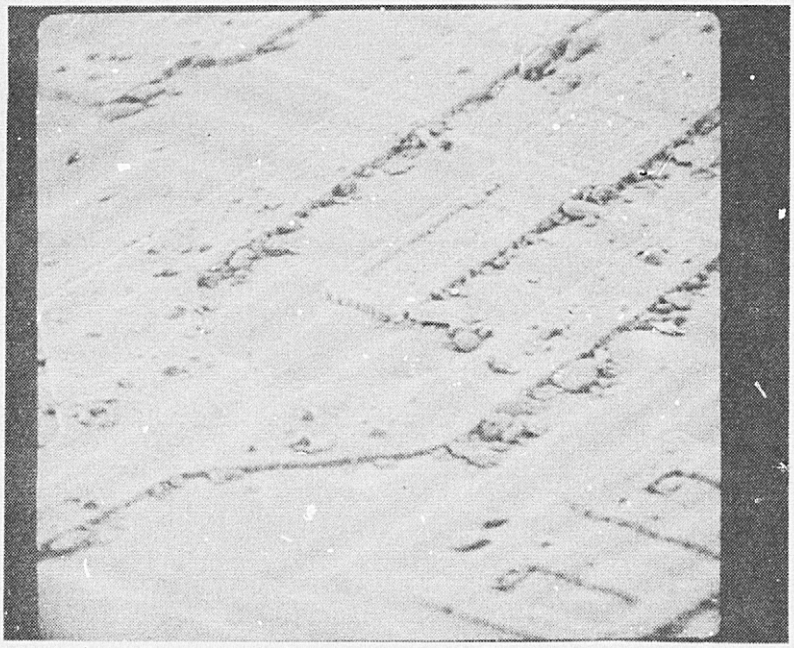

600X (SEM - 1.3 KV) S/N 313

FIGURE A18. SEM PHOTO OF THE FLAKES SHOWN IN FIGURE A17.

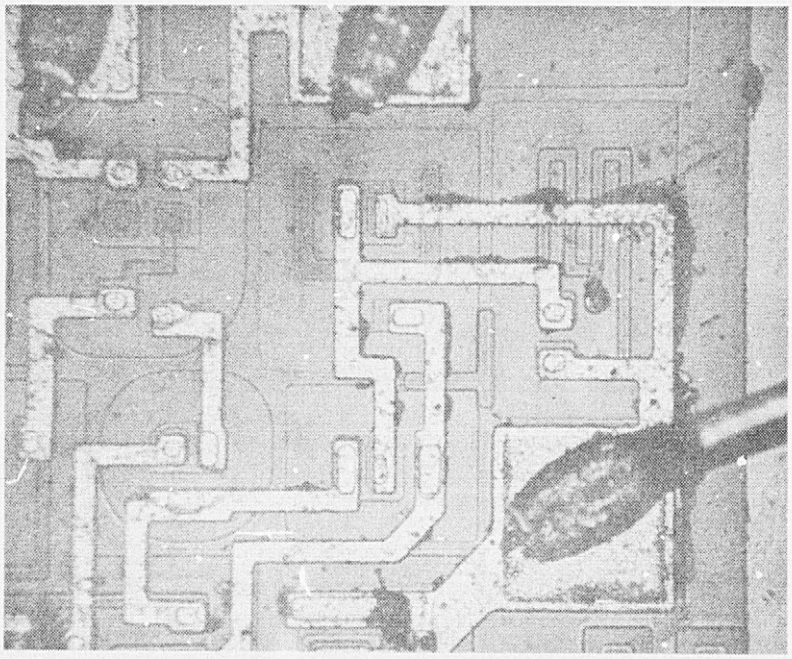

247X S/N 311

FIGURE A19. OPTICAL PHOTOGRAPH OF THE RESIDUE-TYPE CONTAMINATION

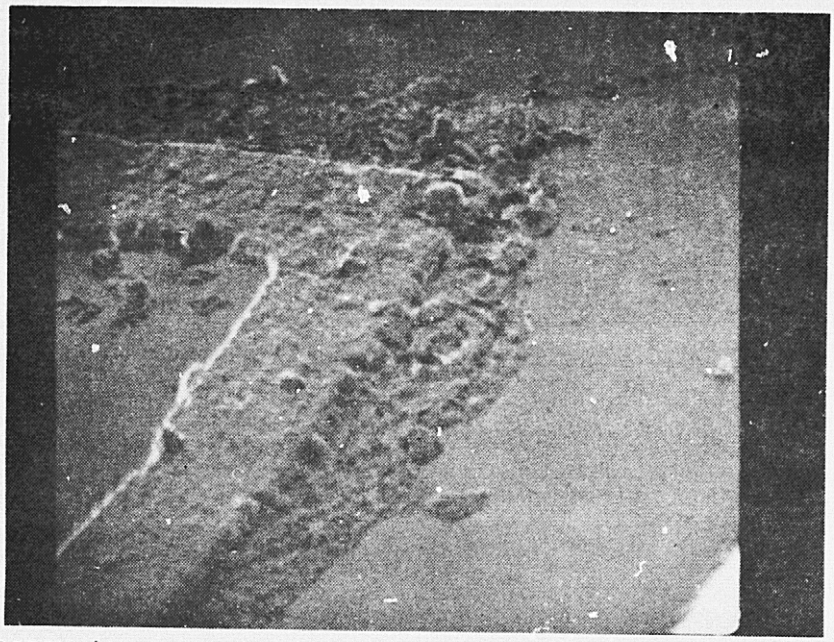

1000X (SEM - 1.3 KV) S/N 311

FIGURE A20. SEM CLOSE-UP OF THE CONTAMINATION SHOWN IN FIGURE A19.

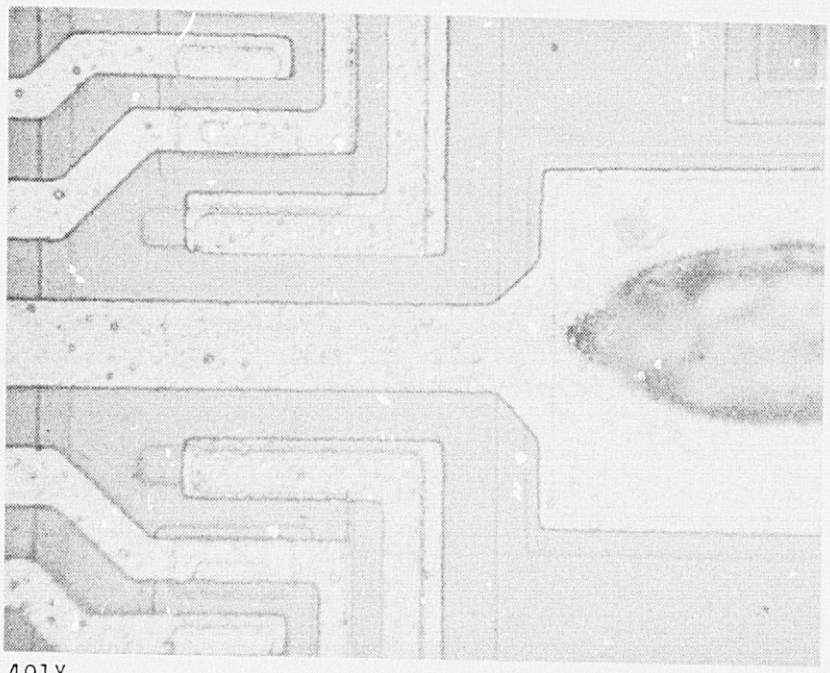

491X S/N 695

FIGURE A21. Vcc (PIN 4) METALLIZATION STRIPE (PRIOR TO GLASSIVATION REMOVAL).

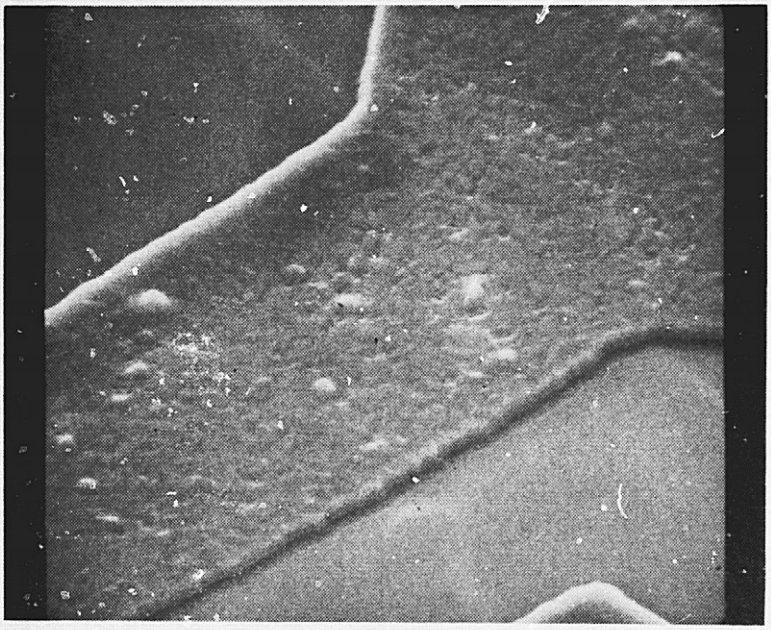

2500X (SEM - 16 KV) S/N 695

FIGURE A22. SEM VIEW OF Vcc STRIPE AFTER GLASSIVATION REMOVAL.

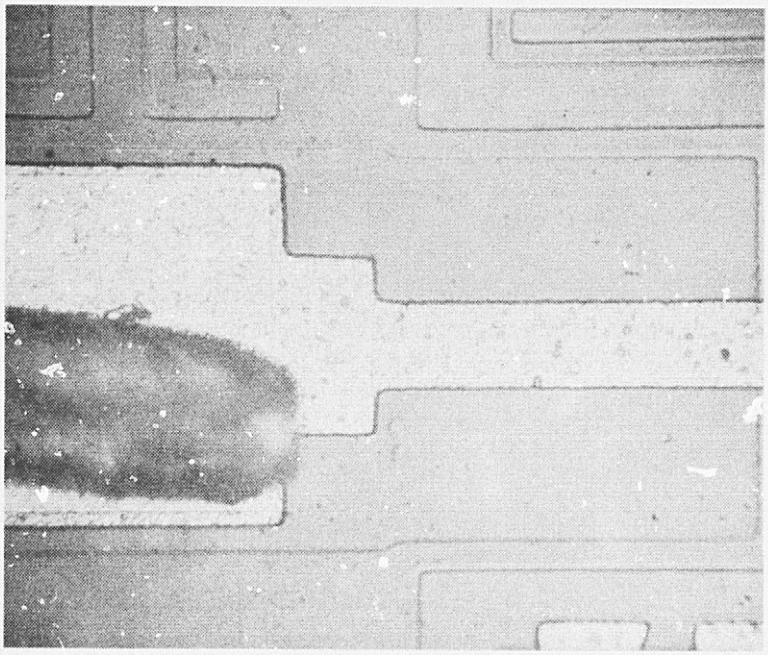

491X S/N 695

FIGURE A23. GROUND (PIN 11) METALLIZATION STRIPE (PRIOR TO GLASSIVATION REMOVAL).

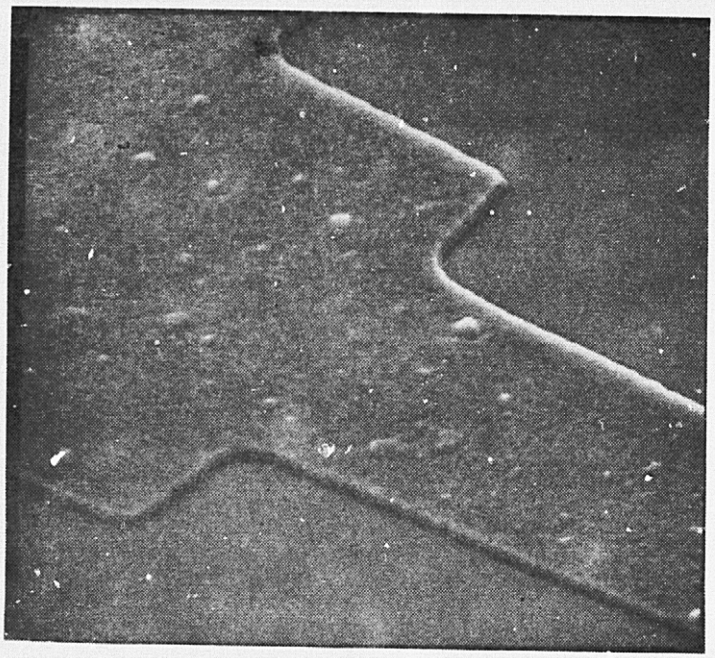

1500X (SEM - 16KV) S/N 695

FIGURE A24. SEM VIEW OF GROUND STRIPE AFTER GLASSIVATION REMOVAL.

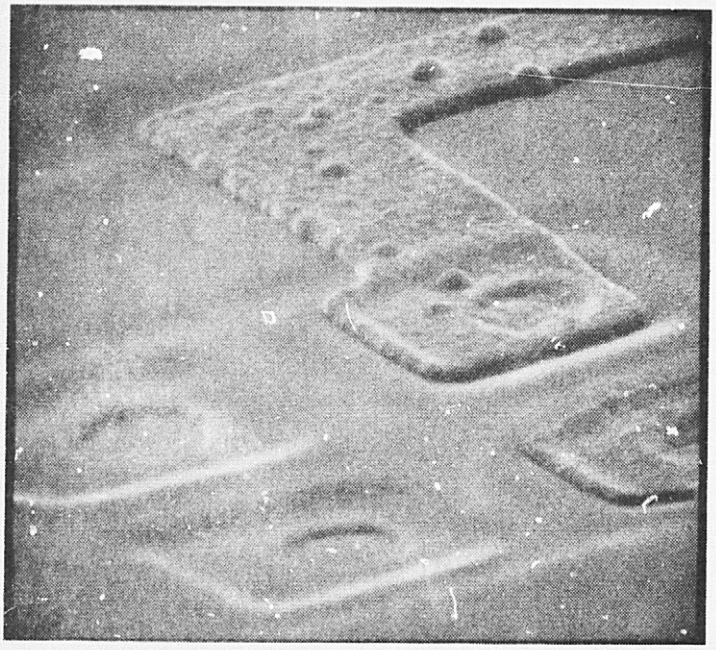

1500X (SEM - 1.3 KV) S/N 695

FIGURE A25. EXAMPLE OF GRAIN GROWTH (BUMPS) AND STEP COVERAGE (PRIOR TO GLASSIVATION REMOVAL).

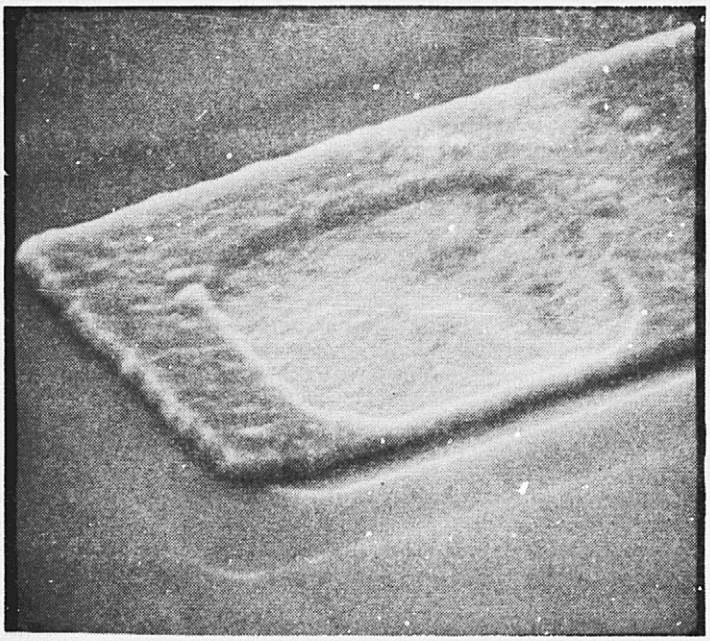

2000X (SEM - 16 KV) S/N 695

FIGURE A26. EXAMPLE OF STEP COVERAGE (AFTER GLASSIVATION REMOVAL).

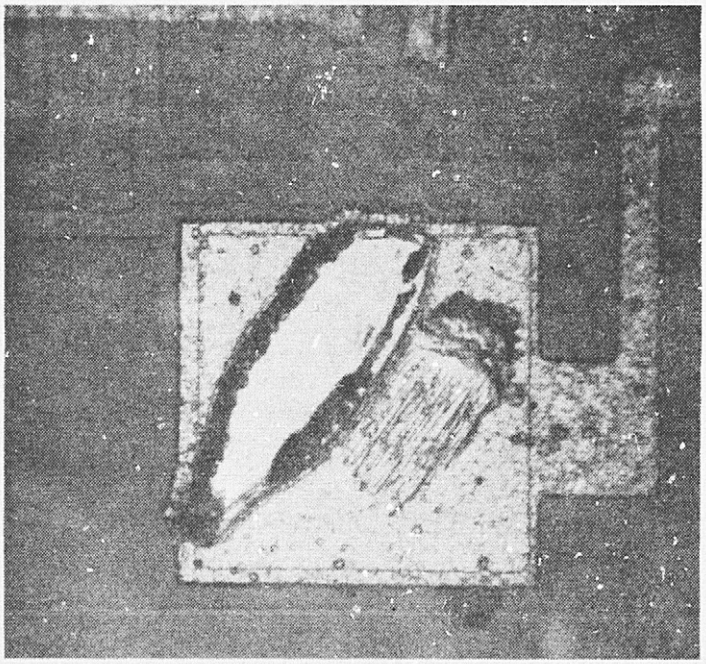

491X S/N 314

FIGURE A27. LIFT-OFF PATTERN OF PIN 6 WIRE BOND

APPENDIX A3

CONSTRUCTION DETAILS AND

PRE-LIFE EVALUATION OF THE

NATIONAL SEMICONDUCTOR LM741H/883B

OPERATIONAL AMPLIFIER

DATE CODE 7545

I. CONSTRUCTION DETAILS (Based on one sample)

A. PACKAGE

1. Type: 8-Pin Can - Figure A28
2. Weight: 0.94 gram
3. Materials:
   a) Lid: Kovar
   b) Header and Leads: Gold-Plated Kovar, External and Internal
   c) Seal: Glass and Weld

B. INTERNAL GEOMETRY - Figure A29

1. Interconnections
   a) Type: Aluminum Wire
   b) Diameter: 0.001 inch
   c) Dress: The wires appeared to have been hand dressed or subjected to a nondestructive pull test as shown in Figure A30.
   d) Bonds:
      - o Aluminum-Aluminum Ultrasonic at the Die - Figure A31
      - o Aluminum-Gold Ultrasonic at the Posts - Figure A32
2. Die
   a) Type: Silicon, planar epitaxial
   b) Scribe Method: Mechanical
   c) Attach Method: Gold Eutectic
   d) Geometry and Electrical Schematic: Figures A33 and A34
   e) Glassivation: Silicon Dioxide
3. Metallization
   a) Type: Aluminum
   b) Thickness: Approximately 13,000Å
   c) Structure: Fine Grain

II. PRE-LIFE EVALUATIONS (Based on ten parts)

A. HERMETICITY

1. Fine Leak Rates: All less then 3.8×10^{-8} STD CC of He/Sec
2. Gross Leakers: None

B. INTERNAL EXAMINATIONS

1. Surface Quality: Good
2. Metallization Quality: Good - No defects, good step coverage, and only minor reordering from glassivation operation as documented in Figures A35 through A39.

C. PULL TESTS (70 Wires)

1. Mean Pull Strength: 2.75 grams
2. STD Deviation: 0.45 gram (.16 $\bar{X}$)
3. Range: 2.0 to 4.0 grams
4. Weak Bonds: None - All breaks occurred at the heel of the bond at the die at forces greater than the specified minimum limit (MIL-STD-883) of 1.5 grams.

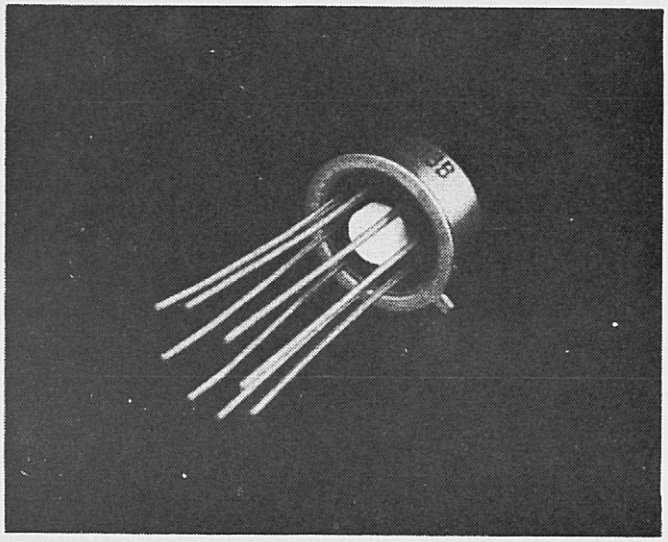

2.6X S/N 685

FIGURE A28. NATIONAL LM741H PACKAGE

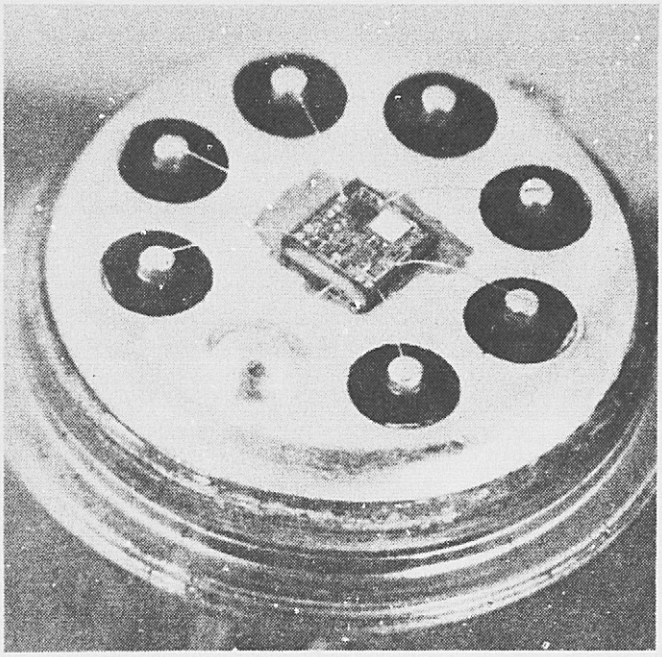

10X S/N 685

FIGURE A29. INTERNAL GEOMETRY

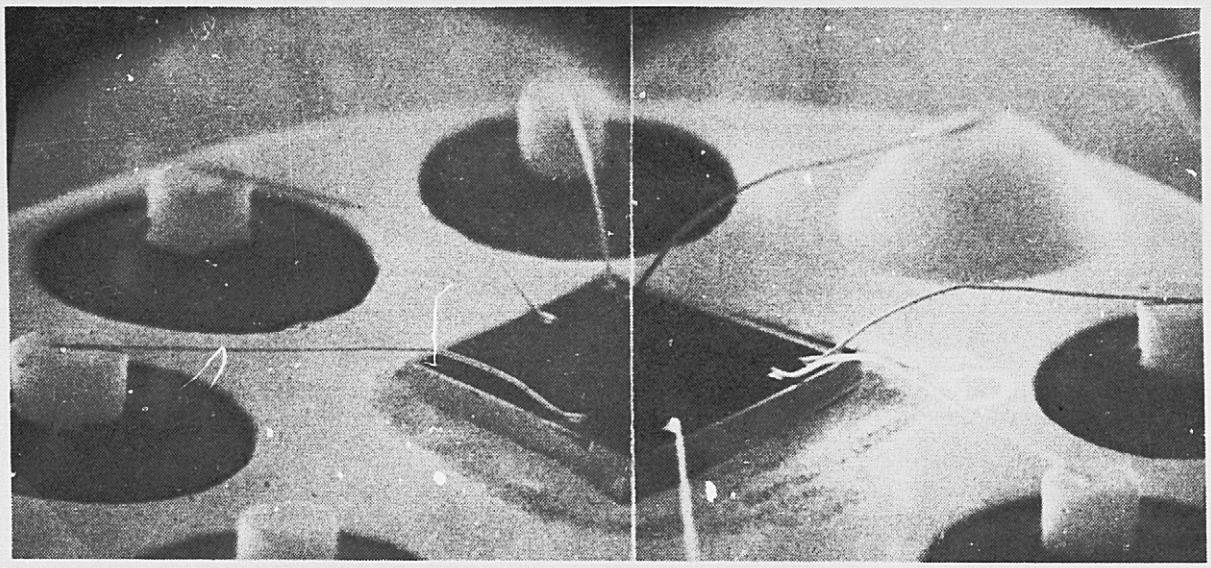

25X S/N 685

FIGURE A30. COMPOSITE SEM PHOTO OF THE LEAD WIRE DRESS. THE KINKS IN THE WIRES AT MID SPAN INDICATE THAT THEY PROBABLY HAD BEEN PULL TESTED.

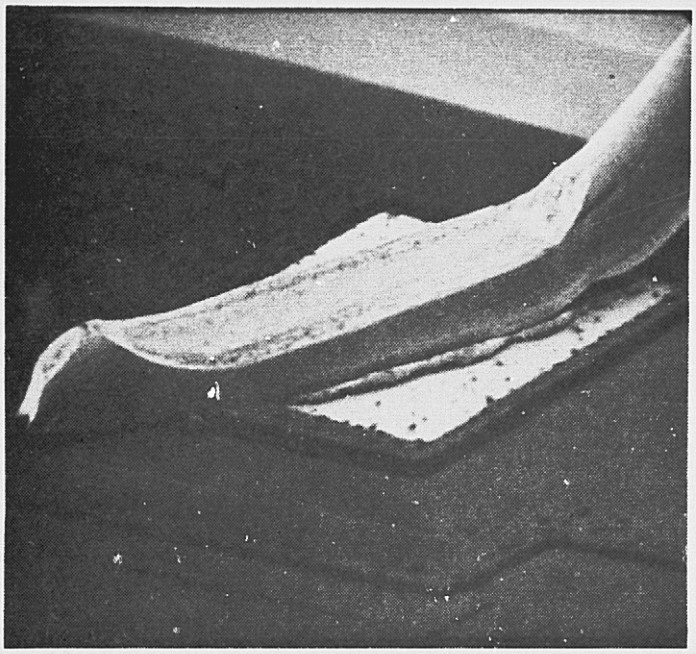

300X (SEM - 1.3 KV) S/N 685

FIGURE A31. WIRE BOND AT THE DIE

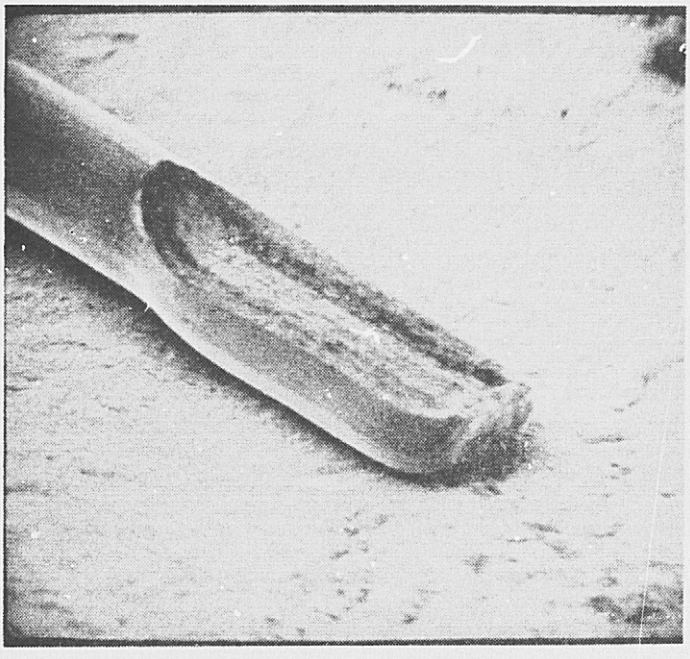

300X (SEM - 1.3 KV) S/N 685

FIGURE A32. WIRE BOND AT THE POST

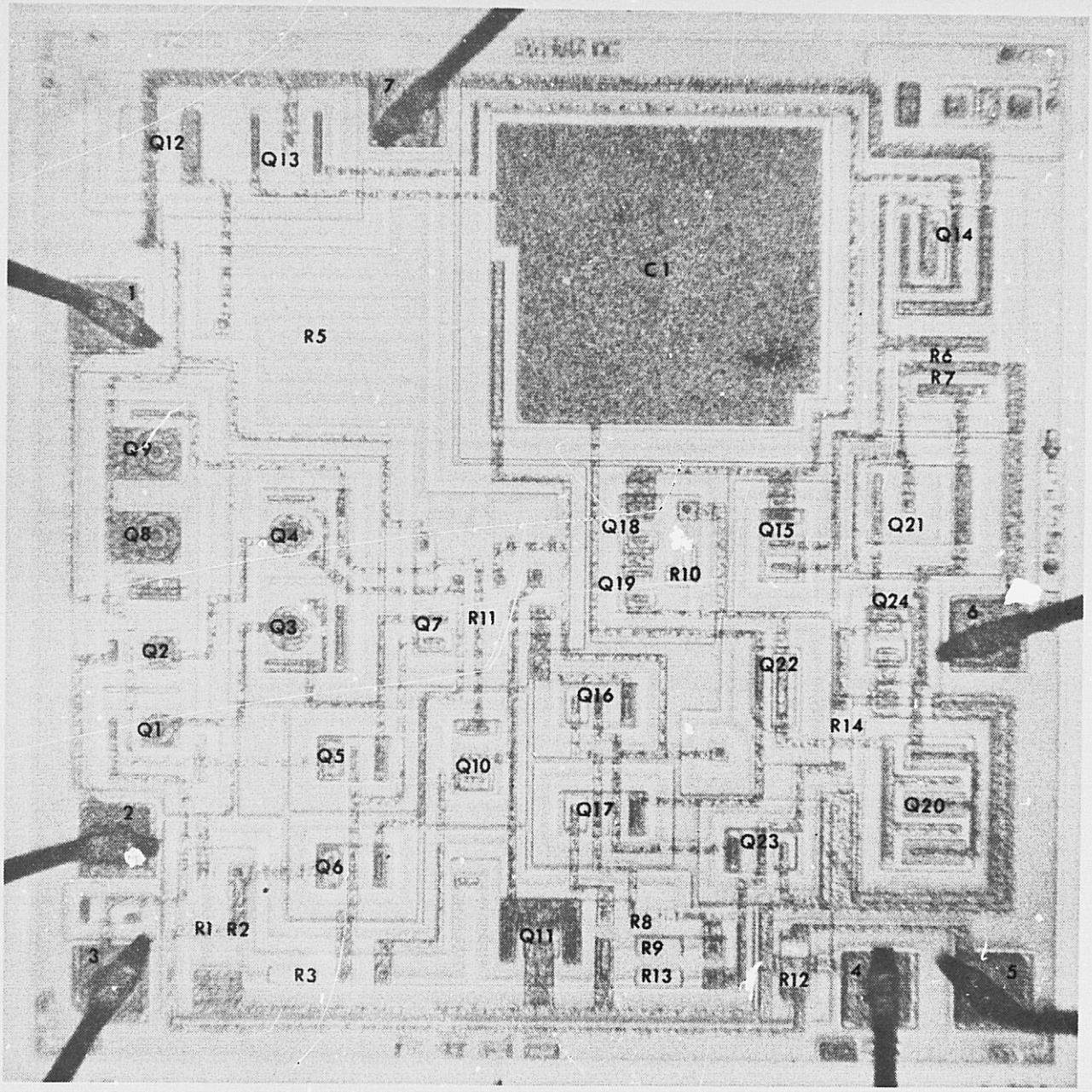

130X

S/N 685

FIGURE A33. DIE GEOMETRY

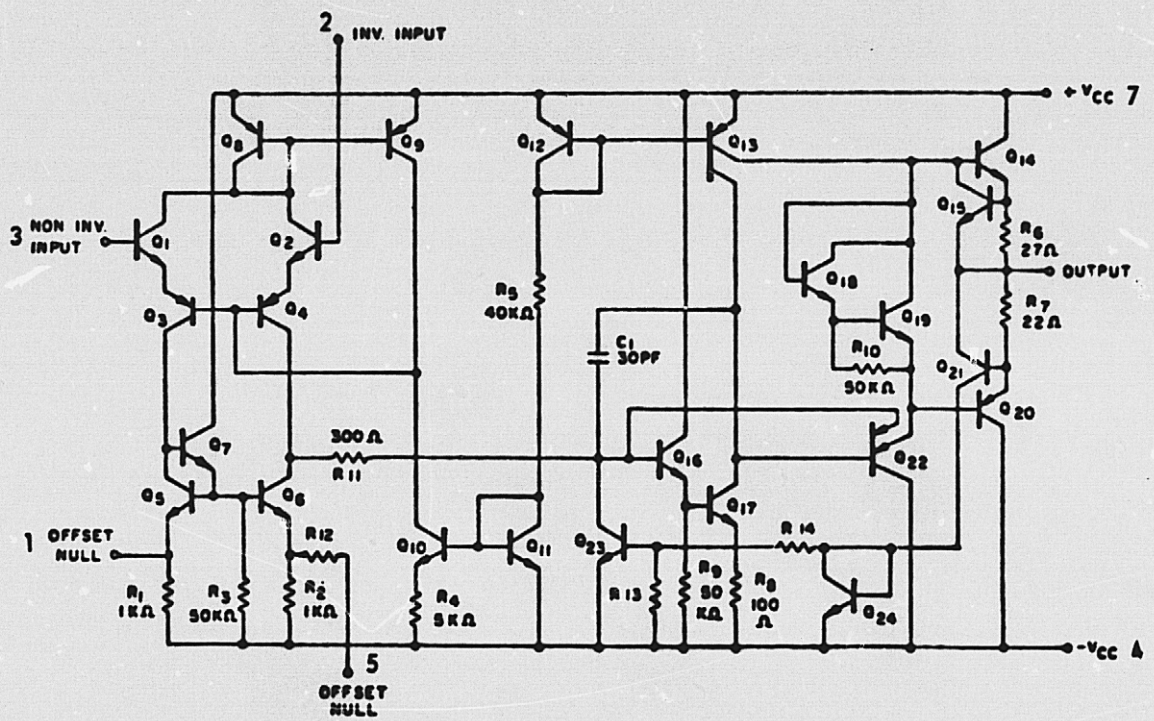

FIGURE A34. ELECTRICAL SCHEMATIC OF THE LM741H

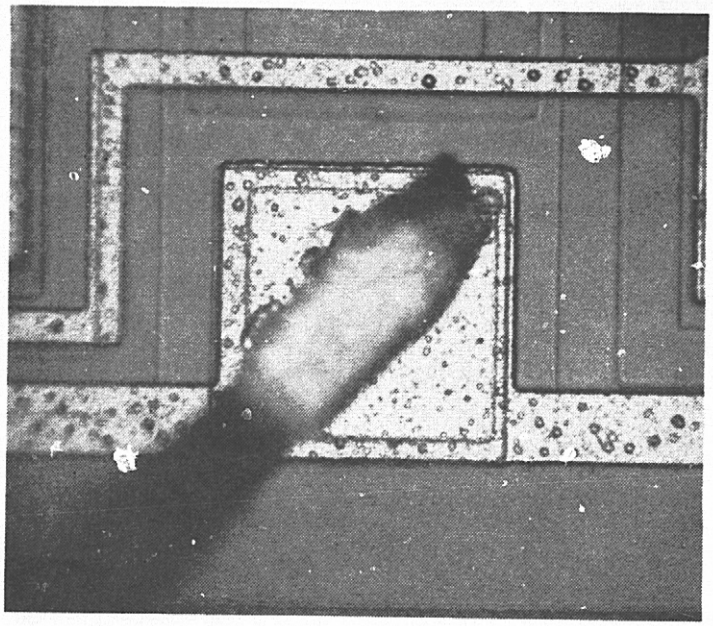

395X S/N 685

FIGURE A35. +V (PIN 7) METALLIZATION (PRIOR TO GLASS REMOVAL).

200X (SEM - 16 KV) S/N 685

FIGURE A36. SEM VIEW OF +V METALLIZATION AFTER GLASS REMOVAL

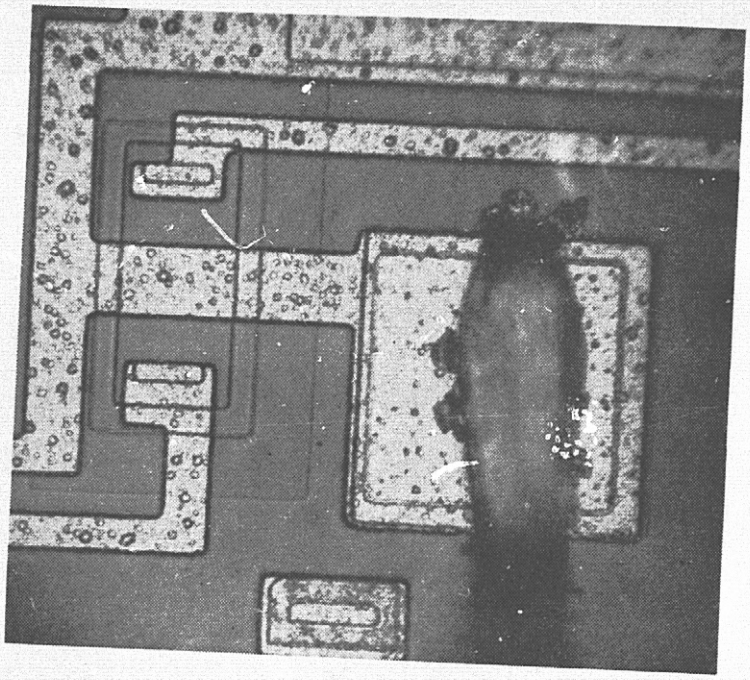

395X S/N 685

FIGURE A37. -V (PIN 4) METALLIZATION (PRIOR TO GLASS REMOVAL).

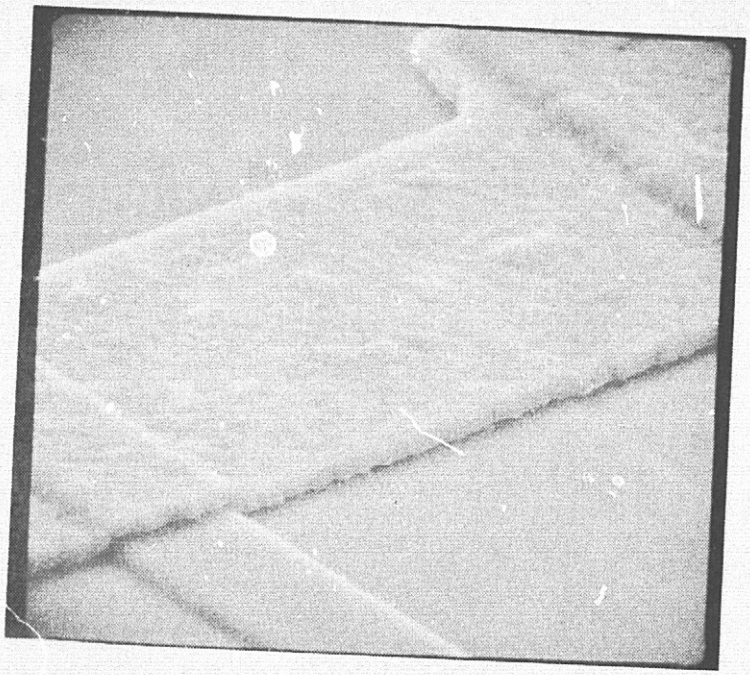

200X (SEM - 16KV) S/N 685

FIGURE A38. SEM VIEW OF -V METALLIZATION AFTER GLASS REMOVAL

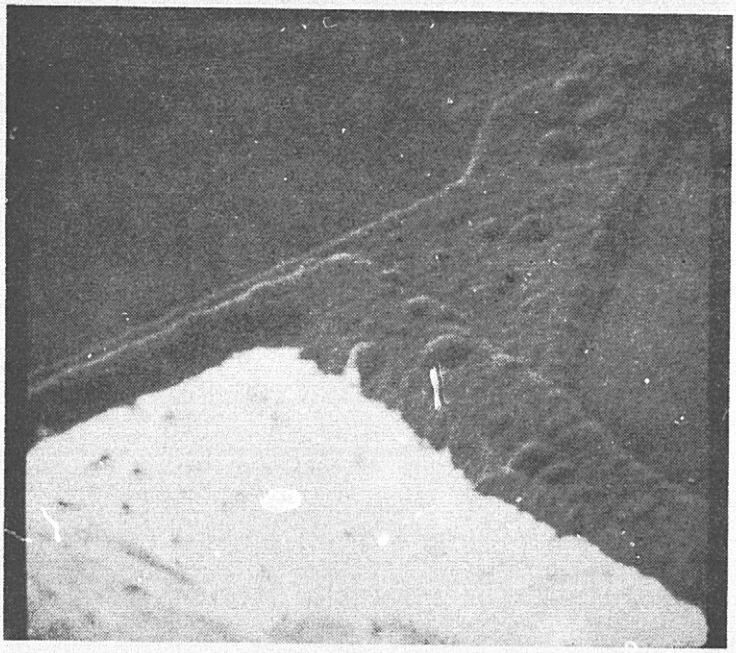

1500X (SEM - 1.e KV) S/N 685

FIGURE A39. METALLIZATION AT BOND PAD OPENING (PRIOR TO GLASS REMOVAL) SHOWING MINOR GRAIN GROWTH (BUMPS).

APPENDIX A4

CONSTRUCTION DETAILS AND

PRE-LIFE EVALUATION OF THE

RAYTHEON RM741T883B

OPERATIONAL AMPLIFIER

DATE CODE 5737

I. CONSTRUCTION DETAILS (Based on one sample)

A. PACKAGE

1. Type: 8-Pin Can - Figure A40
2. Weight: 0.86 gram
3. Materials:
   a) Lid: Kovar
   b) Header and Leads: Gold-Plated Kovar, External and Internal
   c) Seal: Glass and Weld

B. INTERNAL GEOMETRY - Figure A41

1. Interconnections
   a) Type: Gold Wire
   b) Diameter: 0.001 inch
   c) Bonds:
      - o Gold-Aluminum Thermocompression Ball at the Die - Figure A42
      - o Gold-Gold Thermocompression Wedge at the Post - Figure A43
2. Die
   a) Type: Silicon, planar epitaxial
   b) Scribe Method: Mechanical
   c) Attach Method: Gold Eutectic
   d) Geometry & Electrical Schematic: Figures A44 and A45
   e) Glassivation: Silicon Dioxide
3. Metallization
   a) Type: Aluminum
   b) Thickness: Approximately 10,000Å
   c) Structure: Fine Grain

II. PRE-LIFE EVALUATIONS (Based on ten parts)

A. HERMETICITY

1. Fine Leak Rates: 1.06 to 1.46 (Mean=1.22) X 10^{-8} STD CC of He/Sec
2. Gross Leakers: None

B. INTERNAL EXAMINATIONS

1. Surface Quality: Good
2. Metallization Quality: Good - No defects, good step coverage, and very little reordering (grain growth) from glassivation operation as documented in Figures A46 through A50.

C. PULL TESTS (70 Wires)

1. Mean Pull Strength: 4.75 grams
2. STD Deviation: 1.48 grams (.31 $\bar{X}$)
3. Range: 0.2 to 7.8 grams
4. Weak Bonds: Four bonds exhibited a pull strength of less than the specified minimum limit of 2.0 grams (MIL-STD-883). The pin 5 ball bond of S/N 611 lifted from the die pad at a force of 0.2 gram. Pad aluminum had lifted from the SiO_2 and the bond area was contaminated as shown in Figure A51 and the die contained a large stain as shown in Figure A52. Thus, this failure probably resulted from corrosion of the pad caused by the contamination. The pin 3 ball of S/N 623 lifted from the pad at 1.2 grams and the pin 4 and the pin 7 balls of S/N 624 lifted from the pads at 0.9 and 1.3 grams, respectively. These three bonds lifted at the Au/Al interface and showed very little sign of intermetallic formation as illustrated in Figure A53. Thus, these failures were attributed to underbonds probably caused by insufficient heat or dwell time during the bonding operation. One other bond, pin 7 of S/N 622, lifted in this same manner, but this bond failed at an acceptable level of 2.7 grams. All of the other breaks occurred either in the wire or at a neckdown area at values ranging from 3.2 to 7.8 grams.

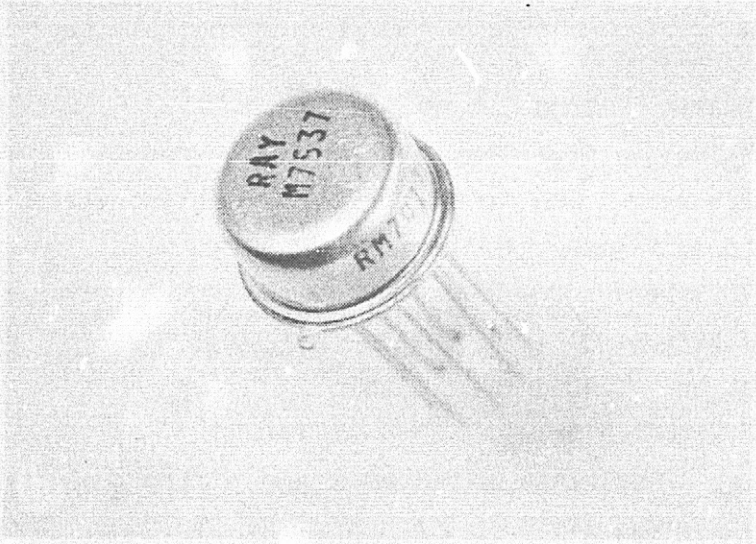

3.5X S/N 605

FIGURE A40. RAYTHEON RM741T PACKAGE

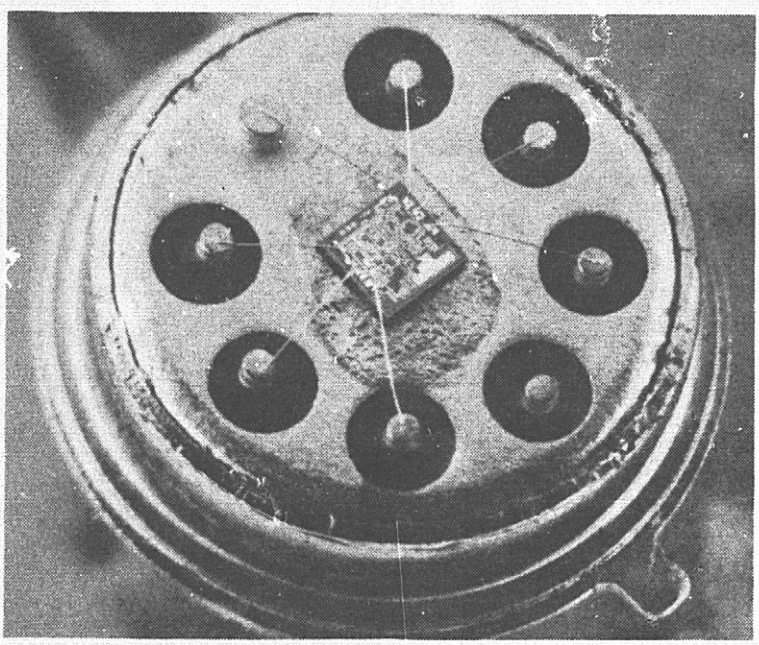

9X S/N 605

FIGURE A41. INTERNAL GEOMETRY

495X (SEM - 1.2 KV) S/N 605

FIGURE A42. WIRE BOND AT THE DIE

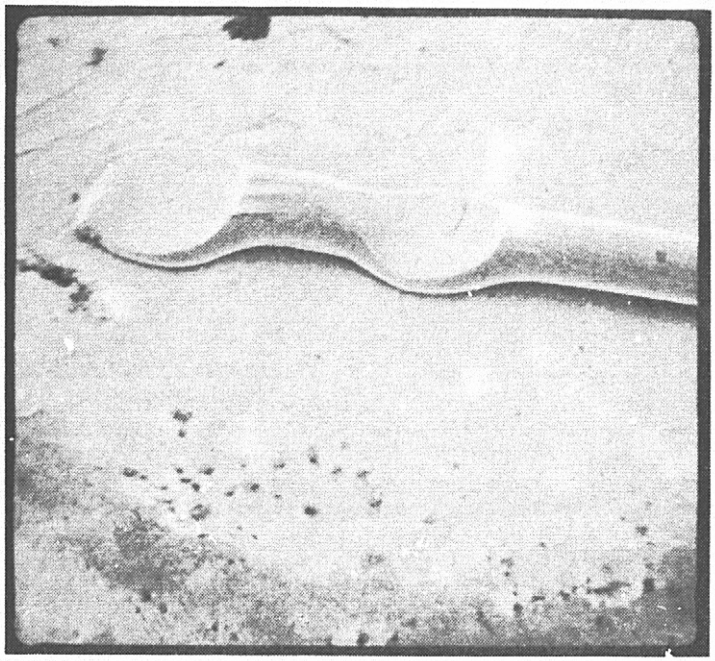

379X (SEM - 1.2 KV) S/N 605

FIGURE A43. WIRE BOND AT THE POST

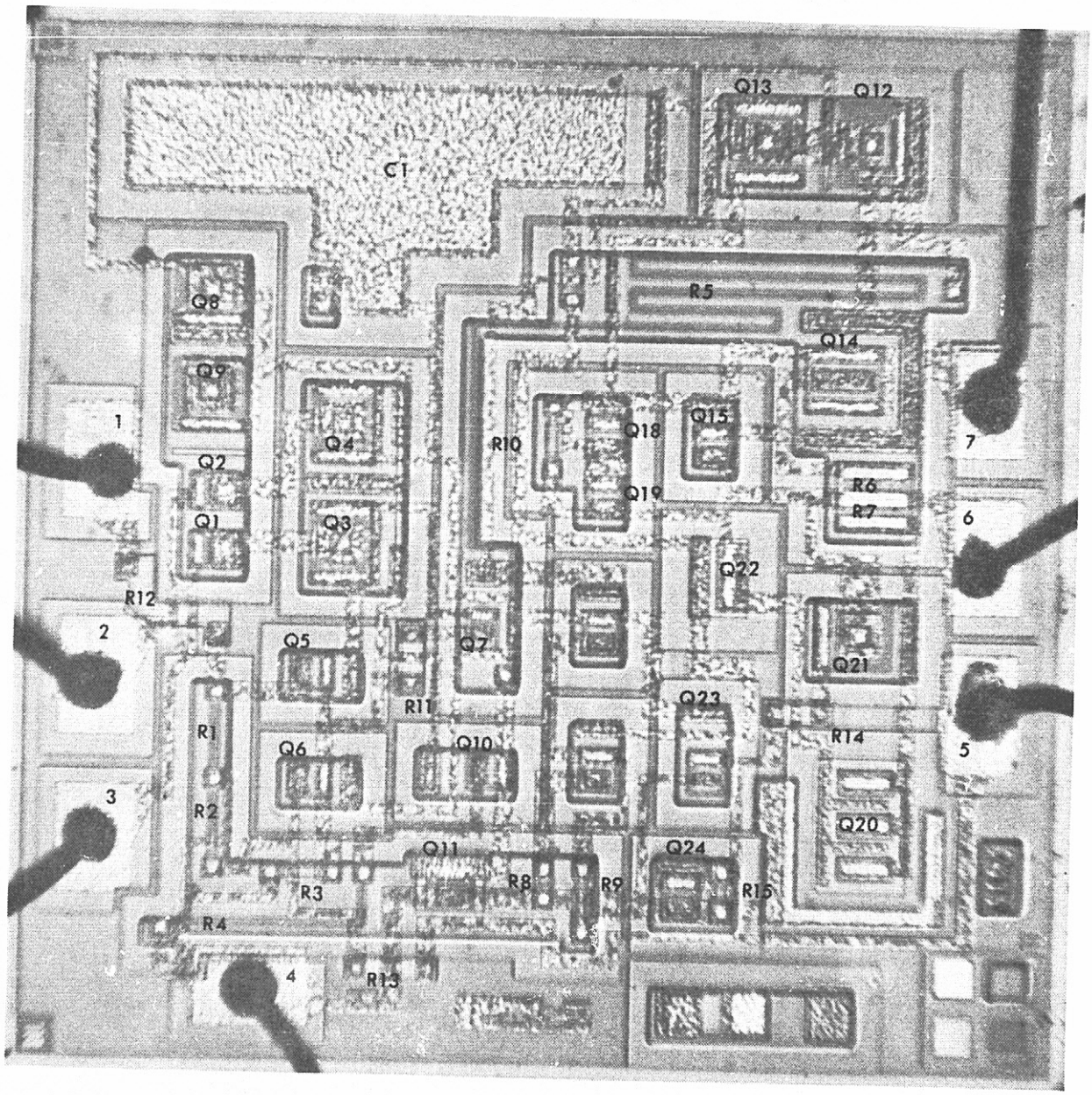

125X

S/N 605

FIGURE A44. DIE GEOMETRY

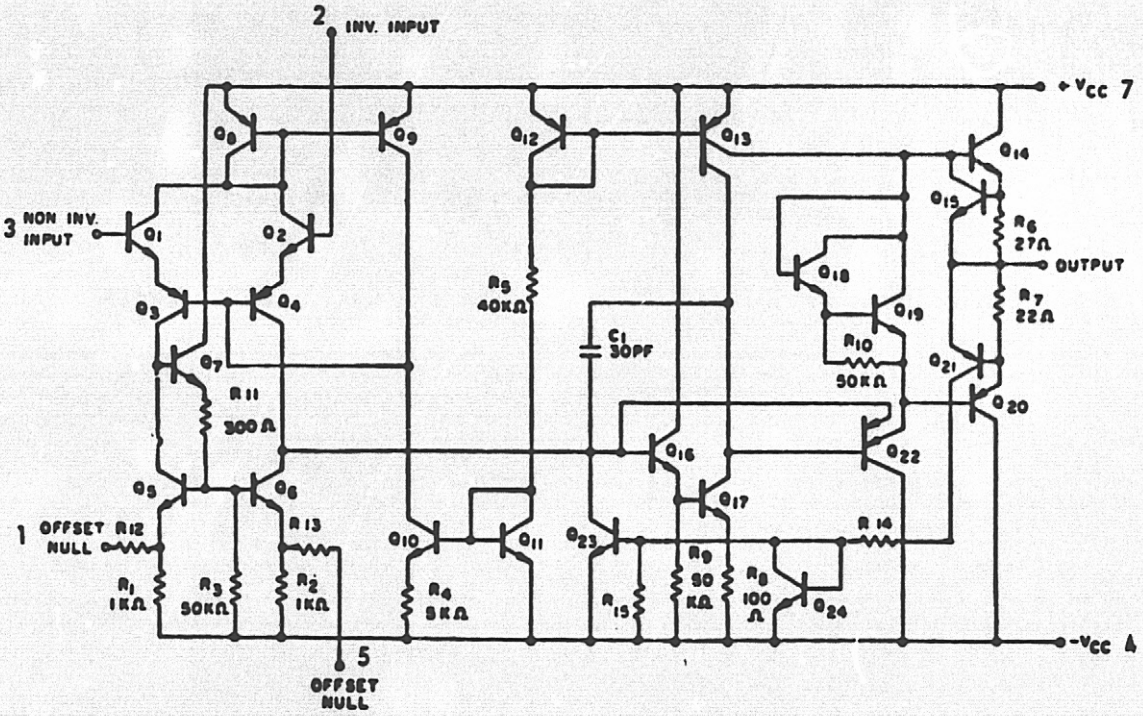

FIGURE A45. ELECTRICAL SCHEMATIC OF THE RM741T.

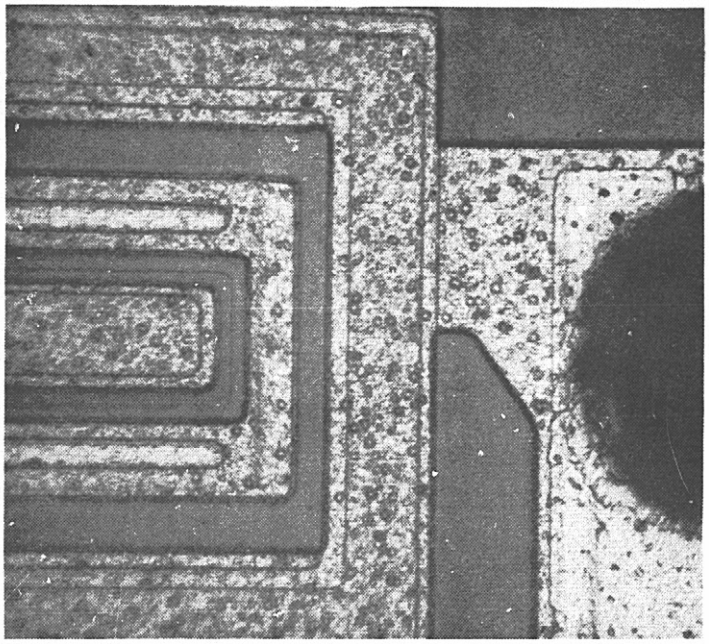

491X S/N 615

FIGURE A46. V+ (PIN 7) METALLIZATION (PRIOR TO GLASS REMOVAL).

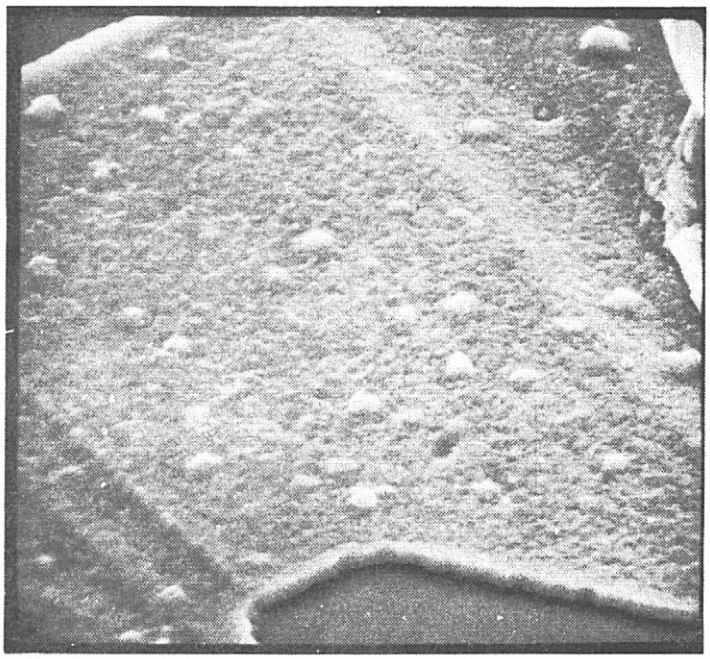

1300X (SEM - 16 KV) S/N 615

FIGURE A47. SEM VIEW OF V+ METALLIZATION AFTER GLASS REMOVAL.

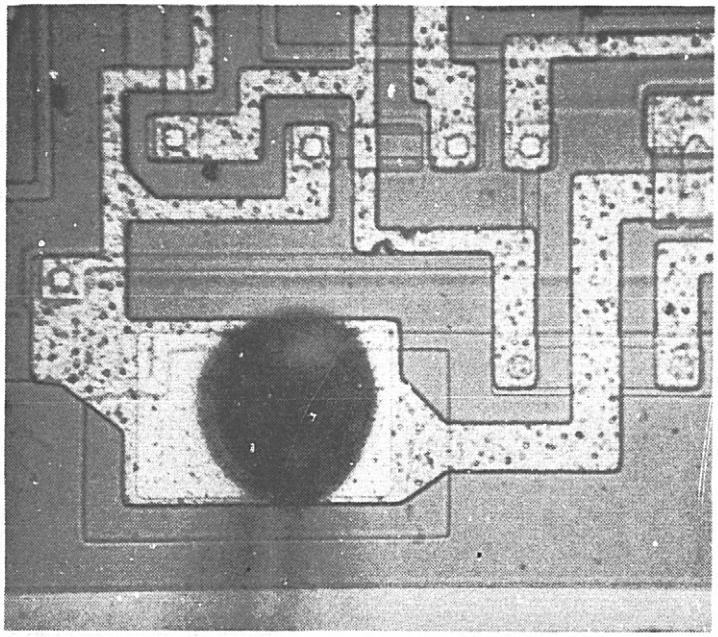

247X S/N 615

FIGURE A48. V- (PIN 4) METALLIZATION STRIPES (PRIOR TO GLASS REMOVAL).

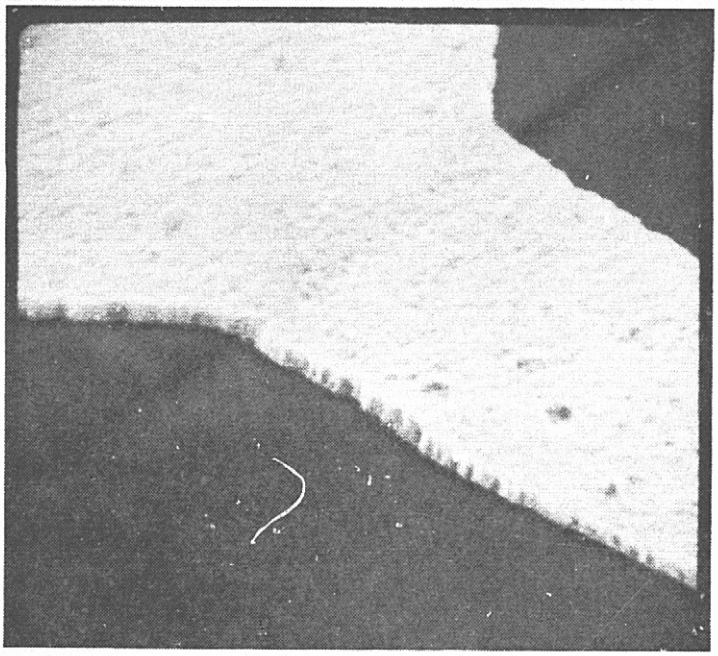

300X (SEM - 1.3 KV) S/N 615

FIGURE A49. SEM VIEW OF ONE OF THE V- STRIPES AFTER GLASS REMOVAL.

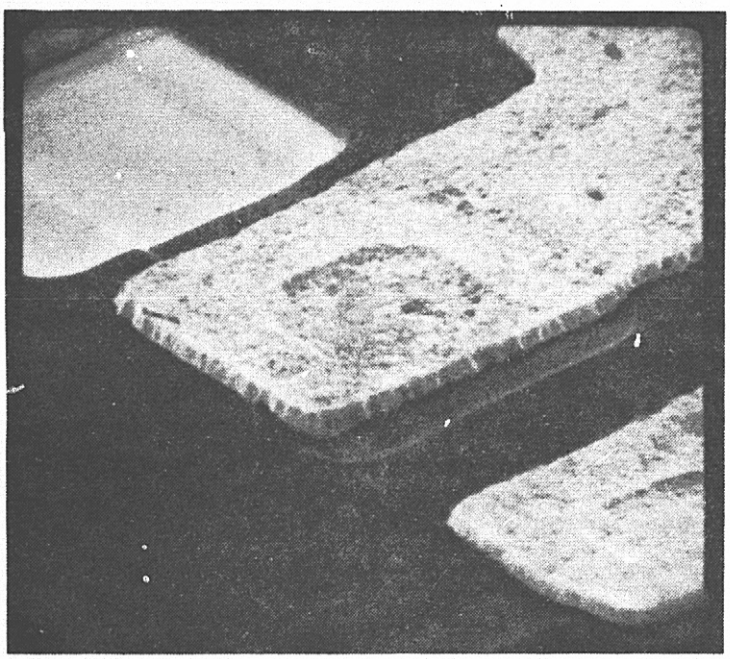

1500X (SEM - 1.3 KV) S/N 015

FIGURE A50. EXAMPLE OF STEP COVERAGE (GLASS REMOVED).

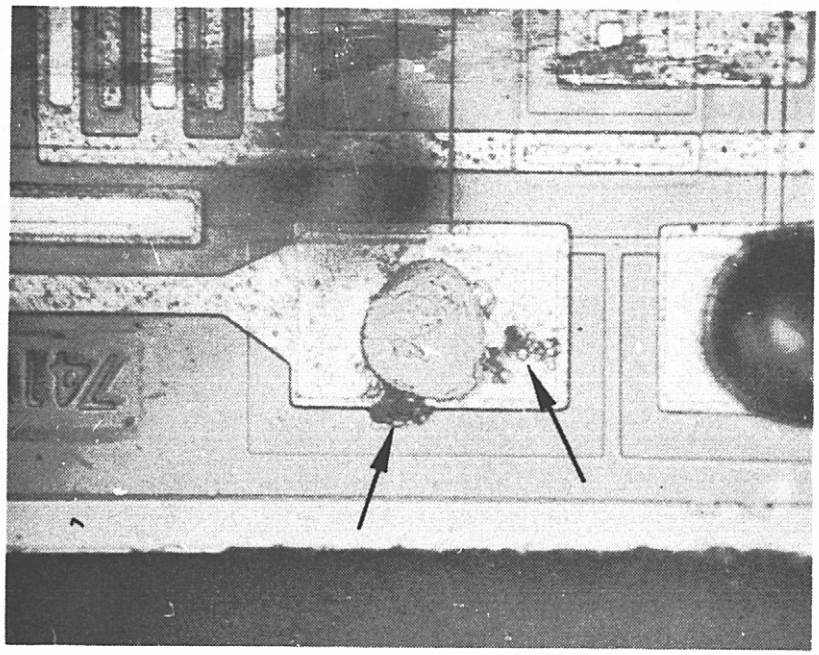

247X S/N 611

FIGURE A51. LIFT-OFF PATTERN OF THE PIN 5 BOND. ARROWS DENOTE THE CONTAMINATION.

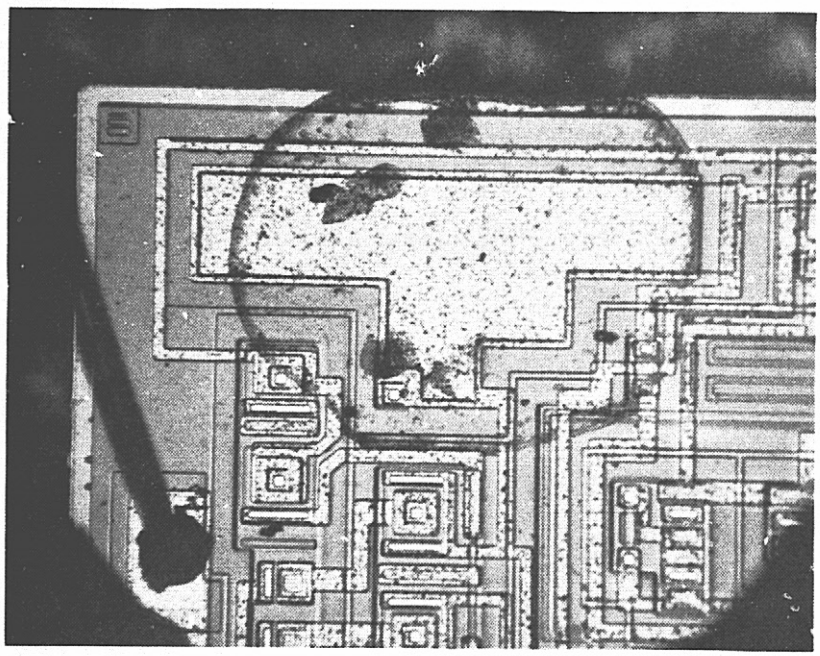

132X S/N 611

FIGURE A52. LARGE STAIN OVER THE MOS CAPACITOR

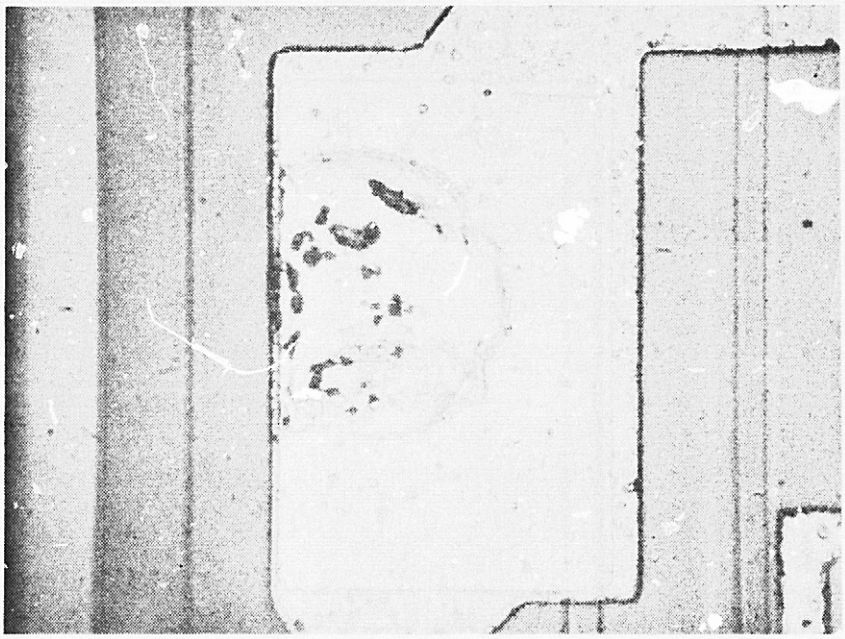

491X S/N 62

FIGURE A53. LIFT-OFF PATTERN OF THE PIN 5 BOND. NOTE THAT, ALTHOUGH THE BALL HAD DEFORMED THE PAD, VERY LITTLE INTERMETALLIC GROWTH (DARK SPOTS) OCCURED.

APPENDIX B

FAILURE ANALYSIS REPORTS

TABLE OF CONTENTS

APPENDIX B1

FAILURE ANALYSIS REPORT

FOR THE

TEXAS INSTRUMENTS SNC54L00T

QUAD 2-INPUT NAND GATE

TEXAS INSTRUMENTS 54L00 FAILURE ANALYSIS - Twenty (20) parts failed during the LTOT and CTOT tests. Following is a discussion of the failure analysis of these failures.

SURFACE INSTABILITY FAILURES - Eight (8) parts failed due to excessive I_{IH1} at one or two inputs. Seven of the parts failed at the -55°C measurement temperature, three at 125°C and three at 25°C. A complete breakdown of the failures by serial number, failed input and measurement temperature is given in Table B1. The -55°C measurement was the most effective test for detection of this failure mechanism. Normally, the input leakage current is highest at 125°C and lowest at -55°C as shown in Table B2, column II. In the failed condition; however, the leakage was greatest at -55°C and least at 25°C as shown in column III, Table B2. This trend was observed in every failed part. The cause of this behavior was not determined.

Curve tracer tests of the parts that were failed at room temperature established that the high input currents were due to inter-emitter transistor action. The excessive I_{IH} saturated with increasing input voltage (channeled characteristic) and I_{IH} was excessive only with bias applied to V_{CC} (with V_{CC} open, the input leakage was negligible). This meant that the lateral parasitic (NPN) h_{FE} between the emitter diffusions of the TTL input transistor (Q1) had increased during stress. The failures were bake recoverable (see column IV of Table B2 for post bake mean values) indicative of a surface instability mechanism. Therefore, the h_{FE} increase was attributed to inversion of the p-type base region around the n+ input emitters due to the accumulation, from drift of mobile ions, of a net positive charge in or over a passivation layer above the base as illustrated in Figure B1. The inverted region effectively increased the size of the emitters which narrows the inter-emitter spacing (lateral base widths) causing h_{FE} to increase.

TEST ERRORS - Twelve (12) parts failed catastrophically at all three measurement temperatures due to shorted and open inputs. Each part contained melted open input stripes and flash-over shorts between the input emitter diffusions as illustrated in Figure B2. The damage indicated that the inputs were electrically overstressed by an inadvertent differential overvoltage generated across each input pair. Subsequent investigation disclosed that the overvoltage was caused

by short-circuits between conductors on the power supply program cards. It was discovered that moisture accumulated on the cards after exposure to low temperatures and this resulted in the formation of resistive paths between the conductors due to electrolytic corrosion. The 54L00 supply line shorted to the higher voltage linear device supply line resulting in an overvoltage condition on the inputs of some of the 54L00 devices. The problem was corrected by applying an acrylic resin over the conductors to seal them from the moisture and removing the linear device supply line from the 54L00 Program Cards.

One Group III part failed at 3,000 hours at the +125°C measurement temperature. The symptoms indicated that pin 14 (output) was open. The part was left on test and did not fail or show any sign of degradation thereafter. At the end of the test, the part was bench tested at high temperature, was delidded and examined, and the pin 14 wire was pull tested. These tests disclosed no intermittent condition or other explanation for the 3,000 hour failure. Therefore the failure was attributed to an intermittent condition in the test socket at high temperature.

TABLE B1. SUMMARY OF I_{IH1} FAILURES

TEST GROUP	TIME OF FAILURE	PART S/N	FAILED INPUTS	TEMPERATURES AT WHICH THE INPUTS WERE FAILED		
				-55°C	25°C	+125°C
III	1000 CYCLES	252	PIN 1	X		X
			PIN 2	X	X	X
		314	PIN 1	X		X
			PIN 7	X	X	X
	2000 CYCLES	272	PIN 6	X		
	3000 CYCLES	234	PIN 6	?	X	?
		291	PIN 2	X		
	4000 CYCLES	241	PIN 9	X		X
			PIN 10	X		X
		245	PIN 6	X		
IV	2000 HOURS	353	PIN 13	X		

? = VALUE UNKNOWN BECAUSE PIN 7 OF THE TEST SOCKET WAS INTERMITTENTLY OPEN

TABLE B2. I_{IH1} VS. MEASUREMENT TEMPERATURE

MEASUREMENT TEMPERATURE	MEAN I_{IH1} OF ALL TEST PARTS PRIOR TO STRESS	MEAN I_{IH1} OF THE 11 FAILED INPUTS AT THE TIME OF FAILURE	MEAN I_{IH1} OF 9 [1/] FAILED INPUTS AFTER A 16 HR, 200°C BAKE
+125°C	.609 µA	12.97 µA	.318 µA
+25°C	.379 µA	9.29 µA	.237 µA
-55°C	.214 µA	17.42 µA	.166 µA

1/ S/Ns 272 AND 291 WERE NOT BAKED (SENT TO RADC FOR GMS ANALYSIS)

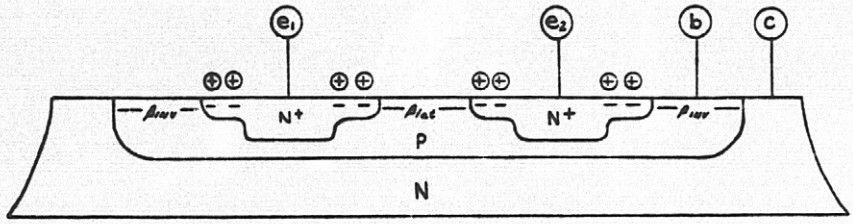

FIGURE B1. DIFFUSION PROFILE OF INPUT TRANSISTOR SHOWING INVERTED BASE REGION OF LATERAL NPN TRANSISTOR

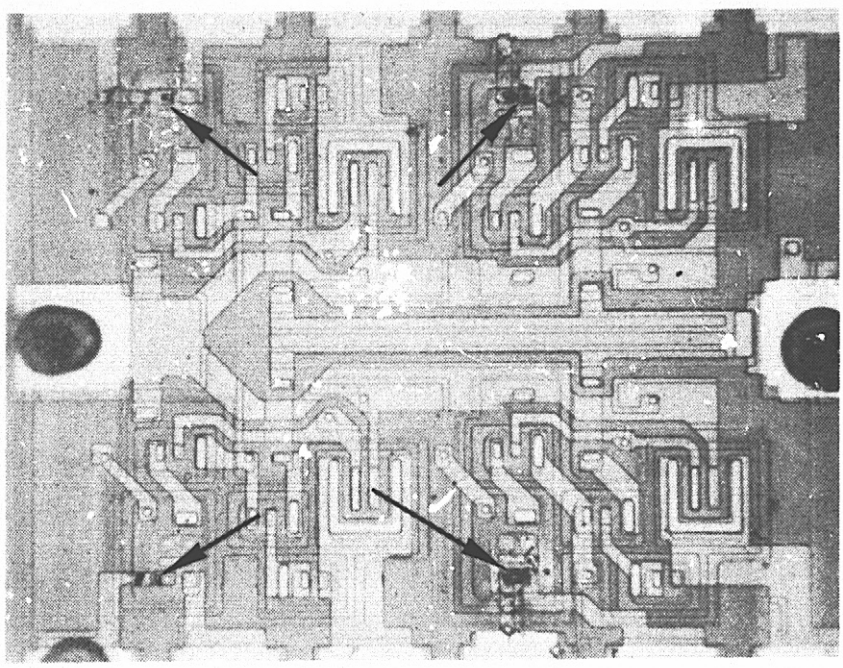

105X S/N 311

FIGURE B2. DIE PHOTO SHOWING THE DAMAGED INPUTS (ARROWS).

APPENDIX B2

FAILURE ANALYSIS REPORT

FOR THE

NATIONAL SEMICONDUCTOR DM54L00F/883B

QUAD 2-INPUT NAND GATE

NATIONAL SEMICONDUCTOR 54L00 FAILURE ANALYSIS - Nine (9) parts failed during LTOT and CTOT tests. Following is a discussion of the failure analysis of these failures.

BROKEN WIRE BONDS - Two (2) parts failed due to an open pin at the 25°C and -55°C measurement temperatures. The opens were traced to a broken Al-Au ultrasonic wire bond at the lead frame. Each failure was due to brittle fracture of the heel as illustrated in Figure B3. Examination of the other bonds in the package disclosed that several were on the verge of failure as illustrated in Figures B4 and B5. Removal of the bond feet by dissolving the aluminum in sodium hydroxide revealed that the lead frames were covered with gold-rich intermetallic growth under each foot, as illustrated in Figure B6. Further investigation (discussed in the post-life evaluation section) established that the intermetallics were generated during device processing or preconditioning. These findings indicate that because of the existing brittle intermetallics the bonds were susceptible to flexure fatigue at the heel and broke as the wires flexed during temperature cycling.

WIRE DIE SHORT - One (1) part failed at all three measurement temperatures due to a 50 ohm short from pin 1 to ground. The pin 1 aluminum interconnect wire had shorted to the unpassivated edge of the substrate (ground). This was caused primarily by a combination of slight bond misplacement toward the edge of the die, as shown in Figure B7, and the inherent shallow angle of departure of the wire from the ultrasonic bond.

ELECTRICAL OVERSTRESS - Six (6) parts failed catastrophically at all three measurement temperatures due to shorted and open inputs. Each part contained melted open input stripes and flashover shorts between the input emitter diffusions as illustrated in Figure B8. The damage indicated that the inputs were electrically overstressed by an inadvertent differential overvoltage generated across each input pair. Subsequent investigations disclosed that the overvoltage was caused by short-circuits between conductors on the power supply program cards. This is the same problem that had caused the overstress of the Texas Instruments 54L00s and is discussed in detail in the analysis report of that device.

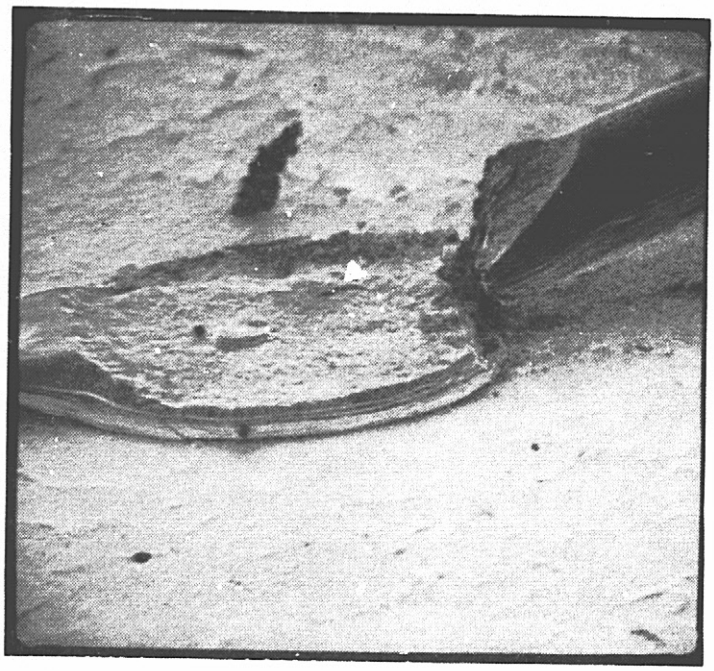

600X S/N 24

FIGURE B3. SEM PHOTO OF AN OPEN LEAD FRAME WIRE BOND AT PIN 7

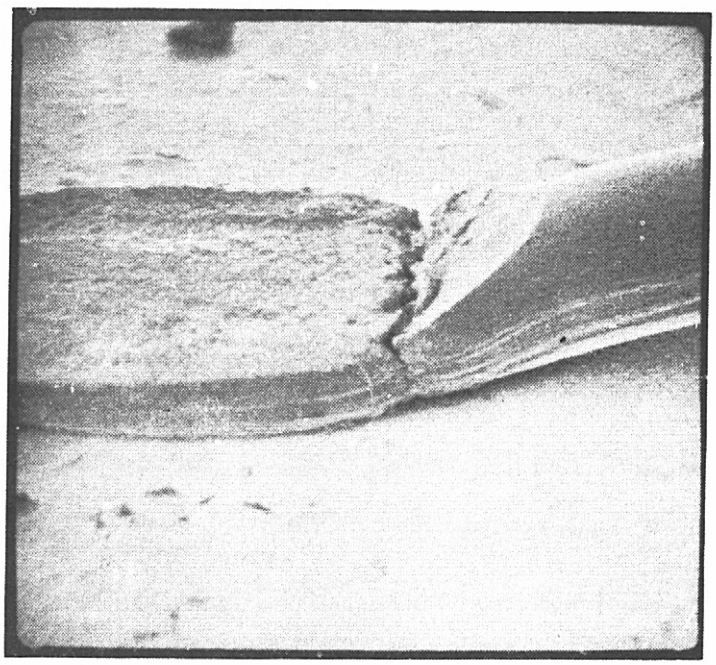

750X S/N 24

FIGURE B4. SEM PHOTO OF A CRACKED WIRE BOND AT PIN 1.

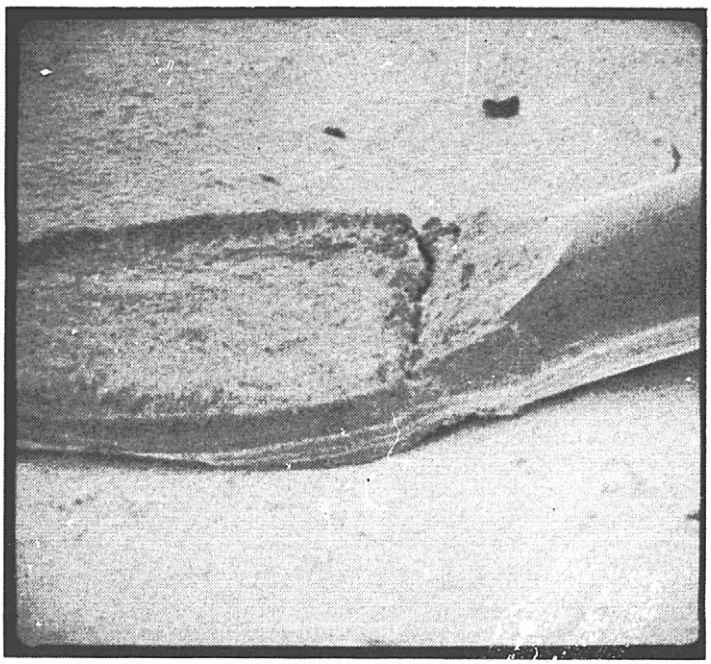

750X S/N 24

FIGURE B5. SEM PHOTO OF A CRACKED WIRE BOND AT PIN 12.

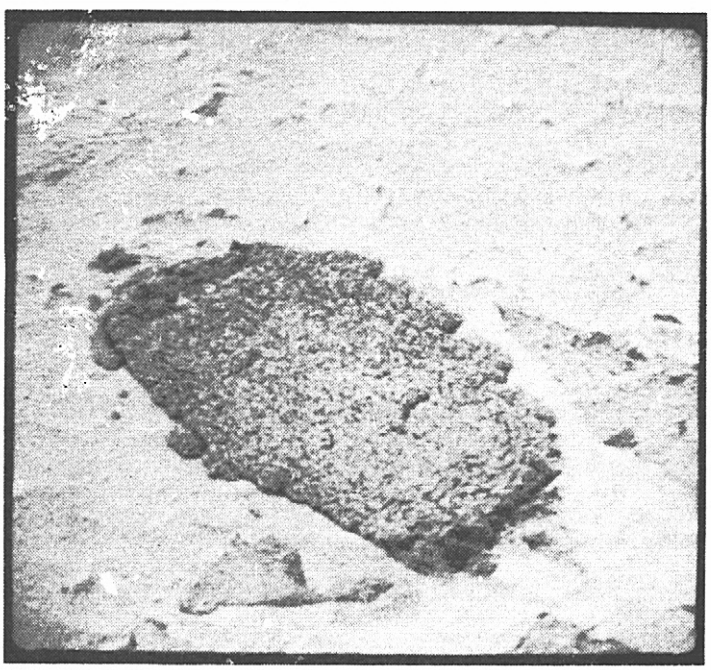

1000X S/N 24

FIGURE B6. INTERMETALLICS ON THE PIN 12 LEAD FRAME REVEALED BY DISSOLVING THE BOND FOOT.

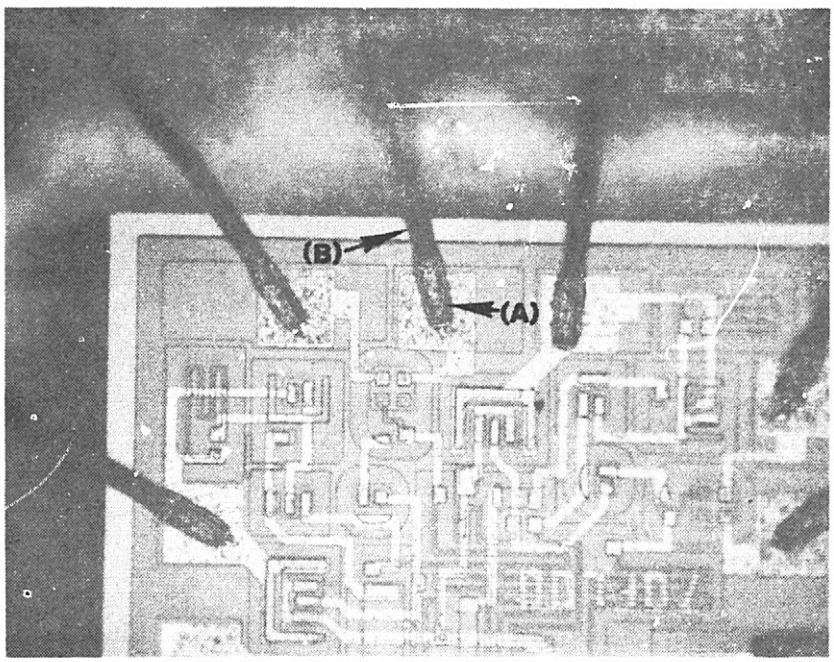

105X S/N 463

FIGURE B7. MISPLACED PIN 1 WIRE BOND (A) SHOWING THE LOCATION OF THE WIRE-DIE SHORT (B)

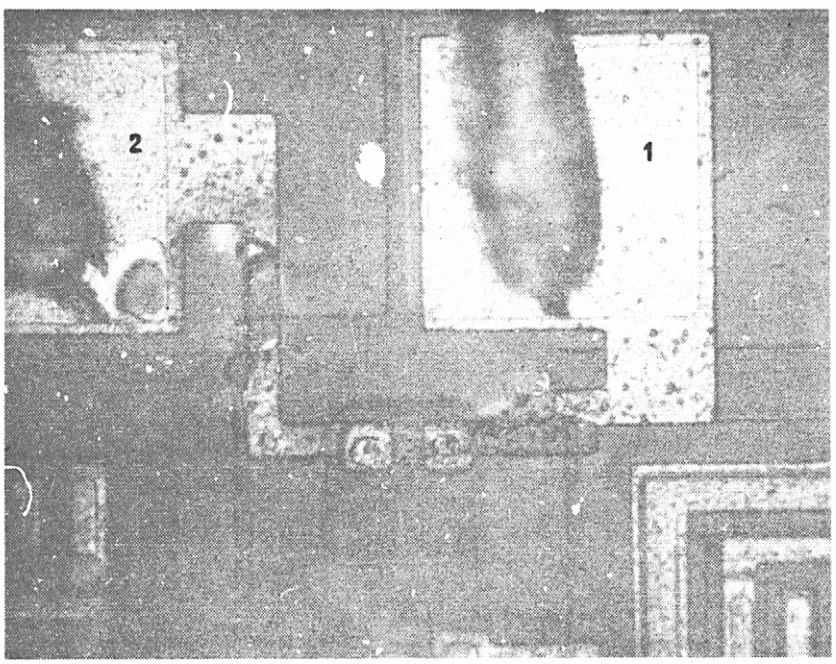

400X S/N 335

FIGURE B8. EXAMPLE OF TYPICAL DAMAGE SUSTAINED BY AN INPUT PAIR

APPENDIX B3

FAILURE ANALYSIS REPORT

FOR THE

NATIONAL SEMICONDUCTOR LM741H/883B

OPERATIONAL AMPLIFIER

NATIONAL SEMICONDUCTOR 741 FAILURE ANALYSIS - Three (3) parts failed during CTOT and CTOT tests. Following is a discussion of the failure analysis of these failures.

SHORTED MOS CAPACITOR - Two parts were latched negative at all three measurement temperatures. The failures were traced to a short (9 ohms and 20 ohms) in the internal 30 picofarad MOS compensating capacitor, C1. Removal of the aluminum electrode revealed, in each instance, a pinhole in the SiO_2 dielectric as shown in Figures B9 and B10. The failure mechanism involved migration of aluminum through the pinhole during stress and the pinholes most likely were caused by pinholes in the photoresist polymer during contact window etching.

SURFACE INSTABILITY - One part exhibited low A_V (2K) and A_V (∞) at the 25°C and the 125°C measurement temperatures. The part recovered when baked for 16 hours at 200°C, indicative of a surface instability mechanism. Therefore, this failure was attributed to mobile ionic contamination or charges in or on the passivation.

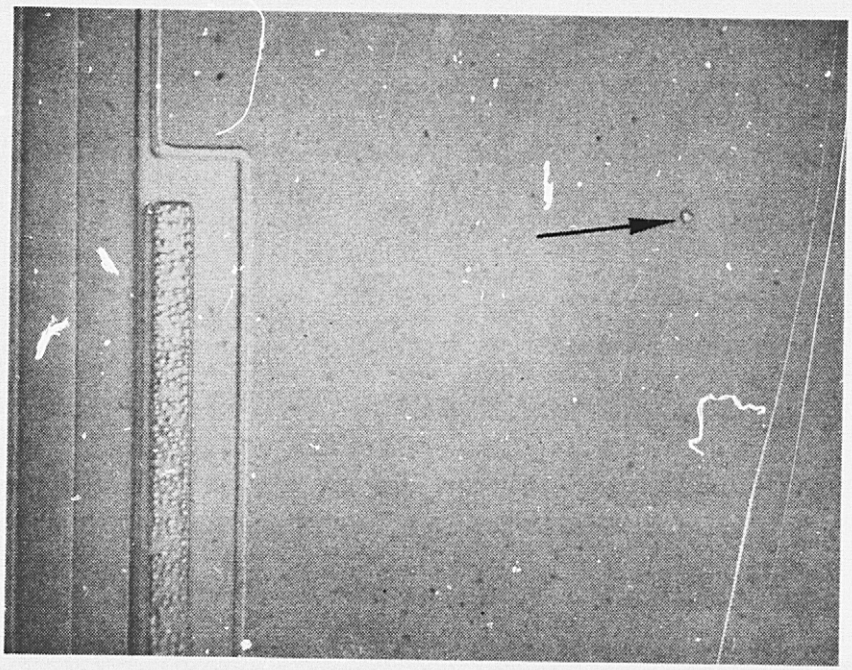

359X S/N 264

FIGURE B9. PINHOLE (ARROW) IN THE SiO_2 DIELECTRIC OF C1

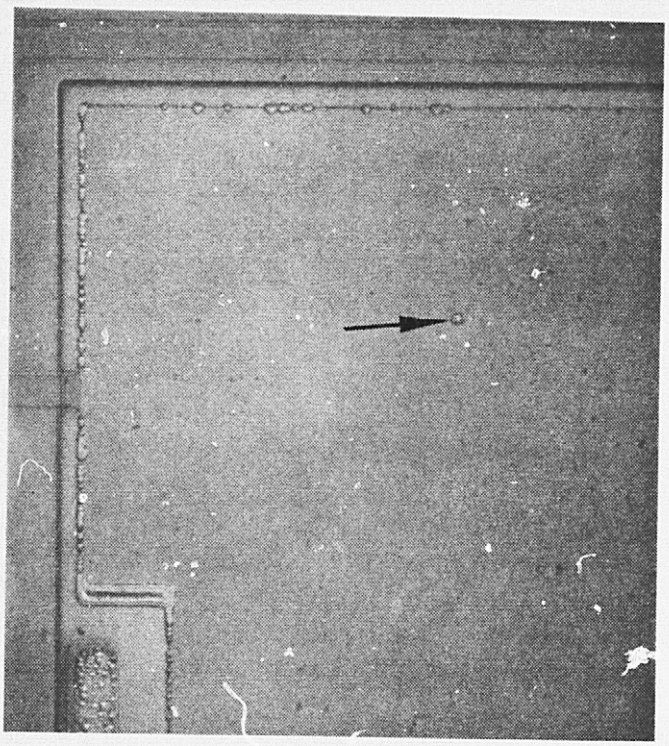

395X S/N 414

FIGURE B10. PINHOLE (ARROW) IN THE SiO_2 DIELECTRIC OF C1

APPENDIX B4

FAILURE ANALYSIS REPORT

FOR THE

RAYTHEON RM741T883B

RAYTHEON 741 FAILURE ANALYSIS - Thirteen (13) parts failed during LTOT and CTOT tests. Following is a discussion of the failure analysis of the failures.

LIFTED BALL BONDS - One (1) Group III part, S/N 312, exhibited an open pin 6 at the 25°C and the -55°C measurement temperatures and one (1) Group III part, S/N 311, exhibited a short-circuit between pin 7 and pin 6 at all three measurement temperatures. Both failures were traced to lifted Au-Al ball bonds. S/N 312 contained a lifted pin 6 wire bond at the die. Examination of the pin 6 bond pad disclosed a hole in the aluminum pad and a crater in the exposed silicon substrate as shown in Figure B11. This indicated that the substrate had been damaged by excessive bonding tool force or velocity. S/N 311 contained a lifted pin 7 wire bond at the die and the dangling pin 7 wire had shorted to the pin 6 wire. Examination of the pad disclosed that it was covered with gold-colored intermetallics as shown in Figure B12. This indicated that the failure was due to Kirkendall voiding in Au_2Al_5. In view of the results of the post-life pull tests (Appendix C4), the excessive intermetallic growth in this instance was probably caused by an isolated bonding error.

SHORTED MOS CAPACITOR - One (1) Group I part was latched negative at all three measurement temperatures. The failure was traced to a 100 ohm short in the 30 picofarad MOS compensating capacitor, C1. Removal of the aluminum electrode disclosed two pinholes in the SiO_2 dielectric as shown in Figure B13. The failure mechanism involved migration of aluminum through the oxide pinholes during temperature cycling and the pinholes most likely were caused by pinholes in the photoresist polymer during contact window etching.

SURFACE INSTABILITY - Three (3) Group VI (-55°C life) parts failed marginally either V_{IO} or PSRR at -55°C or +125°C. As shown in Table B3, in each instance the failed parameter was marginal upon receipt and drifted only slightly to an out of specification value. The parts were left on test and the failed parameters drifted in and out of specification. The perameters that were out of tolerance at the end of the test (2,000 hours) could be brought back within tolerance by baking the part. One (1) Group II part and one (1) Group III part exhibited catastrophic V_{IO} values at 25°C which completely recovered when baked. Therefore, these five failures were attributed to a surface related instability mechanism such as mobile ion

drift or charge separation probably caused by contamination in or on the passivation over the input stage of the amplifier. Fine and gross leak tests of the parts disclosed no loss of hermeticity and optical examinations after delidding disclosed no significant anomaly.

TEST ERRORS - One (1) Group IV part failed catastrophically at 250 hours at the -55°C measurement temperature. The symptoms indicated that pin 7 (V+) was open. The part was left on test and did not fail or show any sign of degradation thereafter. At the end of the test, the part was bench tested at low temperature, was delidded and examined, and the pin 7 wire was pull tested. This disclosed no intermittent condition or other explanation for the 250 hour failure. Therefore the failure was attributed to an intermittent connection in the test socket at low temperature.

Four (4) parts failed PSRR or V_{OUT} + (10K) and AV (2K) at the -55°C measurement temperature only and recovered when retested or left on test. As shown in Table B4, the failed parameters showed no sign of significant degradation prior to failure and after recovering returned to essentially the same values as prior to failure. The value of I_{IO} (+10v) at -55°C of the parts which failed PSRR is also listed in the table because it is indicative of the balance of the input stage and because it serves to illustrate the abruptness of the failure and recovery. Fine and gross leak tests of the parts disclosed no loss of hermeticity and optical examinations of the three Group III parts after delidding disclosed no significant anomaly. Consequently, it is believed that these failures probably were caused by a condition external to the part, such as accumulation of moisture across the input pins during the low temperature test, rather than by any part deficiency.

TABLE B3. HISTORY OF THE FAILED PARAMETERS OF THE GROUP VI MARGINALLY FAILED PARTS

S/N	PARAMETER	SPECIFIED LIMIT	PARAMETER VALUES (FAILED VALUES ARE UNDERLINED)				
			PRESTRESS	250 HRS	500 HRS	1000 HRS	2000 HRS
592	V_{IO} (-10) @ -55°C	±6 mV	+5.303 mV	+6.453 mV	+2.352 mV	+5.349 mV	+6.397 mV ⚠
593	V_{IO} (+10) @ 125°C	±6 mV	-5.887 mV	-6.107 mV	-6.119 mV	-2.629 mV	-2.500 mV
	V_{IO} (0) @ 125°C	±6 mV	-5.974 mV	-6.123 mV	6.096 mV	-2.159 mV	-2.038 mV
	V_{IO} (-10) @ 125°C	±6 mV	-5.992 mV	-6.046 mV	-5.992 mV	-1.781 mV	-1.781 mV
601	PSRR + @ 125°C	77 dB Min.	79.10 dB	82.77 dB	62.43 dB	79.77 dB	69.54 dB ⚠
	PSRR - @ 125°C	77 dB Min.	80.47 dB	85.08 dB	62.65 dB	81.78 dB	70.12 dB ⚠

⚠ Within specification after an 18 hour, 200°C bake.

TABLE B4. HISTORY OF THE FAILED PARAMETERS OF THE FOUR PARTS WHICH FAILED AND RECOVERED ABRUPTLY

S/N	GROUP	PARAMETER	SPECIFIED LIMIT	PARAMETER VALUES (FAILED VALUES ARE UNDERLINED)					
				PRESTRESS	1000 CYC	2000 CYC	3000 CYC	4000 CYC	RETEST
171	I	PSRR - @ -55°C (I_{IO} [+10] @ -55°C)	77 dB MIN ±500 nA	117.75 dB 1.9 nA	115 dB -1.3 nA		103 dB 0.6 nA	75.65 dB -302 nA	103 dB .85 nA
173	I	PSRR - @ - 55°C (I_{IO} [+10] @ -55°C)	77 dB MIN ±500 nA	117.75 dB 0.5 nA	101 dB 2.0 nA		105 dB -1.6 nA	76.92 dB 241 nA	101 dB -2.7 nA
215	I	VOUT + (10K) @ -55°C AV (2K) @ -55°C	+12V MIN 25 V/mV MIN	14.06B 129 V/mV	14.06V 150 V/mV		13.90V 137 V/mV	11.95V .6 V/mV	14.05V 134 V/mV
3.4	III	PSRR + @ -55°C PSRR - @ -55°C (I_{IO} [+10] @ -55°C)	77 dB MIN 77 dB MIN ±500 nA	98.12 dB 92.26 dB 4.4 nA	96.77 dB 90.69 dB -22.1 nA	73.32 dB 72.67 dB 139 nA	96.04 dB 91.03 dB 3.1 nA	97.74 dB 92.21 dB .9 nA	⚠

⚠ Sent to RADC for GMS analysis.

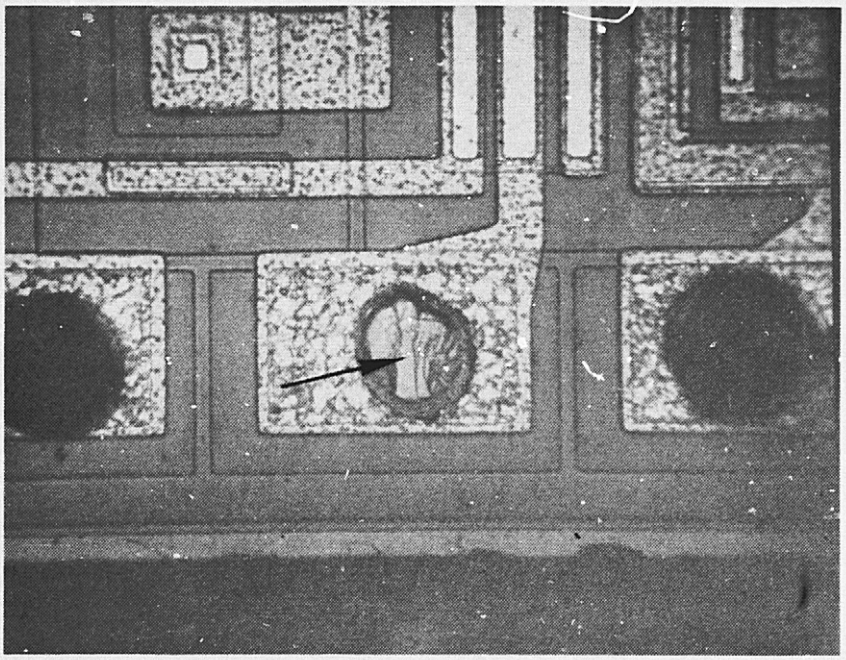

247X S/N 312, GROUP III

FIGURE B11. LIFT-OFF PATTERN OF THE PIN 6 BOND SHOWING THE CRATER (ARROW) IN THE SILICON.

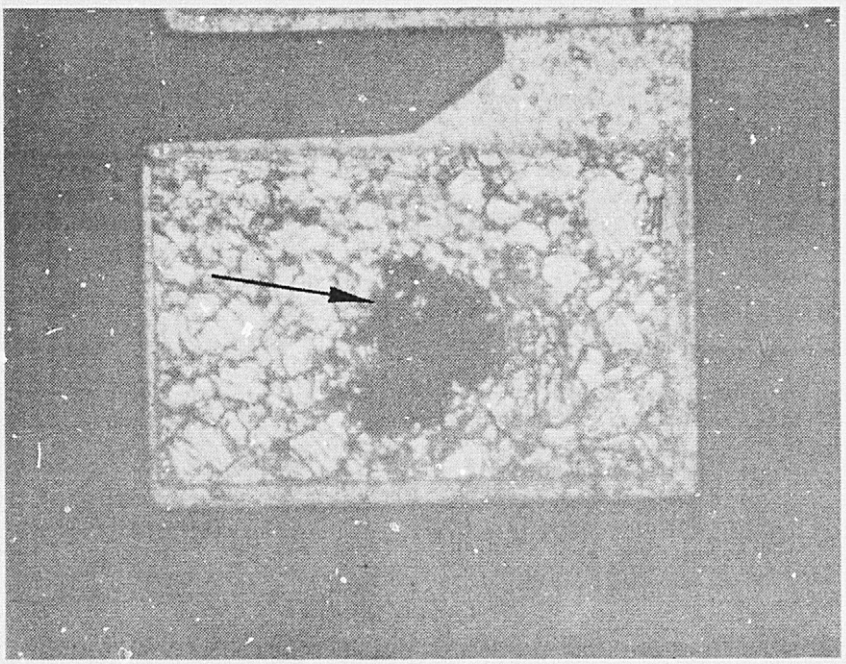

491X S/N 311, GROUP III

FIGURE B12. LIFT-OFF PATTERN OF THE PIN 7 BOND SHOWING THE MOUND OF INTERMETALLICS (ARROW).

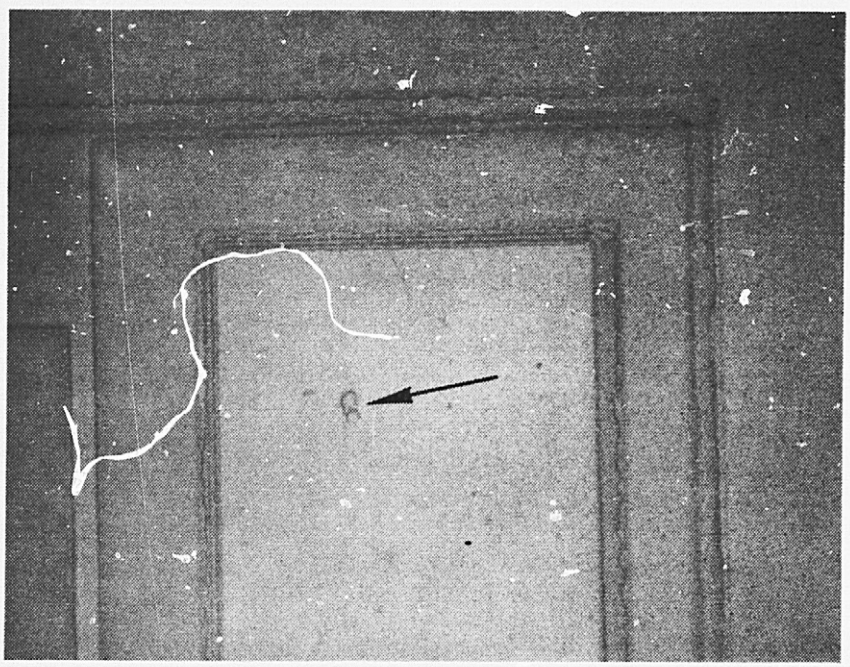

395X S/N 195, GROUP I

FIGURE B13. C1 AFTER ALUMINUM REMOVAL SHOWING THE OXIDE PINHOLES (ARROW).

APPENDIX C

POST-LIFE EVALUATION REPORTS

TABLE OF CONTENTS

APPENDIX C1

POST-LIFE EVALUATION

OF THE

TEXAS INSTRUMENTS SNC54L00T

QUAD 2-INPUT NAND GATE

DATE CODE 7519

I. POST-LIFE EXAMINATIONS - One (1) Texas Instruments 54L00 survivor from each test group was dissected and examined in detail optically and using the SEM for any anomalous condition induced by the test environments. Results were as follows:

A. PACKAGE EXTERIOR: No part exhibited any degradation of the package markings or finish or the lead finish.

B. PACKAGE INTERIOR: No part exhibited any degradation of the internal lead wire dress or the die attach bond.

C. DIE SURFACE: No part showed any sign of degradation of the glassivation as a result of the tests as illustrated in Figure C1.

D. WIRE BONDS: None of the bonds in any of the parts showed any sign of degradation due to the test conditions. A typical wire bond at the die and at the lead frame are shown in Figures C2 and C3.

E. METALLIZATION: The metallization of all test parts was unaffected by the test conditions. The metallization of the die shown in Figure C1 is representative of all six parts.

II. POST-LIFE TESTS: Ten survivors from each test group were leak tested, delidded and optically examined, then subjected to bond pull testing. Results were as follows:

A. LEAK TESTS: The results of the fine and gross leak tests, presented in Table C1, indicated that the package hermeticity had not been degraded by the test conditions.

B. INTERNAL OPTICAL EXAMINATIONS: None of the 60 parts exhibited any anomalous condition induced by the test environment.

C. PULL TESTS: The results of the wire pull tests are presented in Table C2. All breaks occurred in the wire or in the neckdown area above the ball at the specified minimum limit of 2.0 grams or more.

TABLE C1. RESULTS OF THE POST-LIFE LEAK TESTS

TEST GROUP	FINE LEAK RATES (10^{-8} STD CC He/Sec)		NO. OF GROSS LEAKERS
	MEAN	RANGE	
I	0.41	0.35-0.58	0
II	0.26	0.17-0.35	0
III	0.28	0.06-0.38	0
IV	0.32	0.18-0.60	0
V	0.31	0.19-0.38	0
VI	0.16	0.34-0.62	0
PRE-LIFE	0.45	0.34-0.62	0

TABLE C2. RESULTS OF THE POST-LIFE PULL TESTS

TEST GROUP	TOTAL NO. OF WIRES PULLED	MEAN PULL STRENGTH	STD DEVIATION	RANGE	NO. OF FAILURES
I	140	6.20g	1.86g	2.3-13.6g	0
II	140	6.37g	1.59g	3.0-10.0g	0
III	140	6.21g	1.74g	2.0-11.5g	0
IV	140	5.84g	1.44g	2.5-10.3g	0
V	140	6.36g	1.63g	2.7-12.5g	0
VI	140	6.08	1.93g	2.6-12.8g	0
PRE-LIFE	140	5.17g	0.98g	2.0-7.9g	0

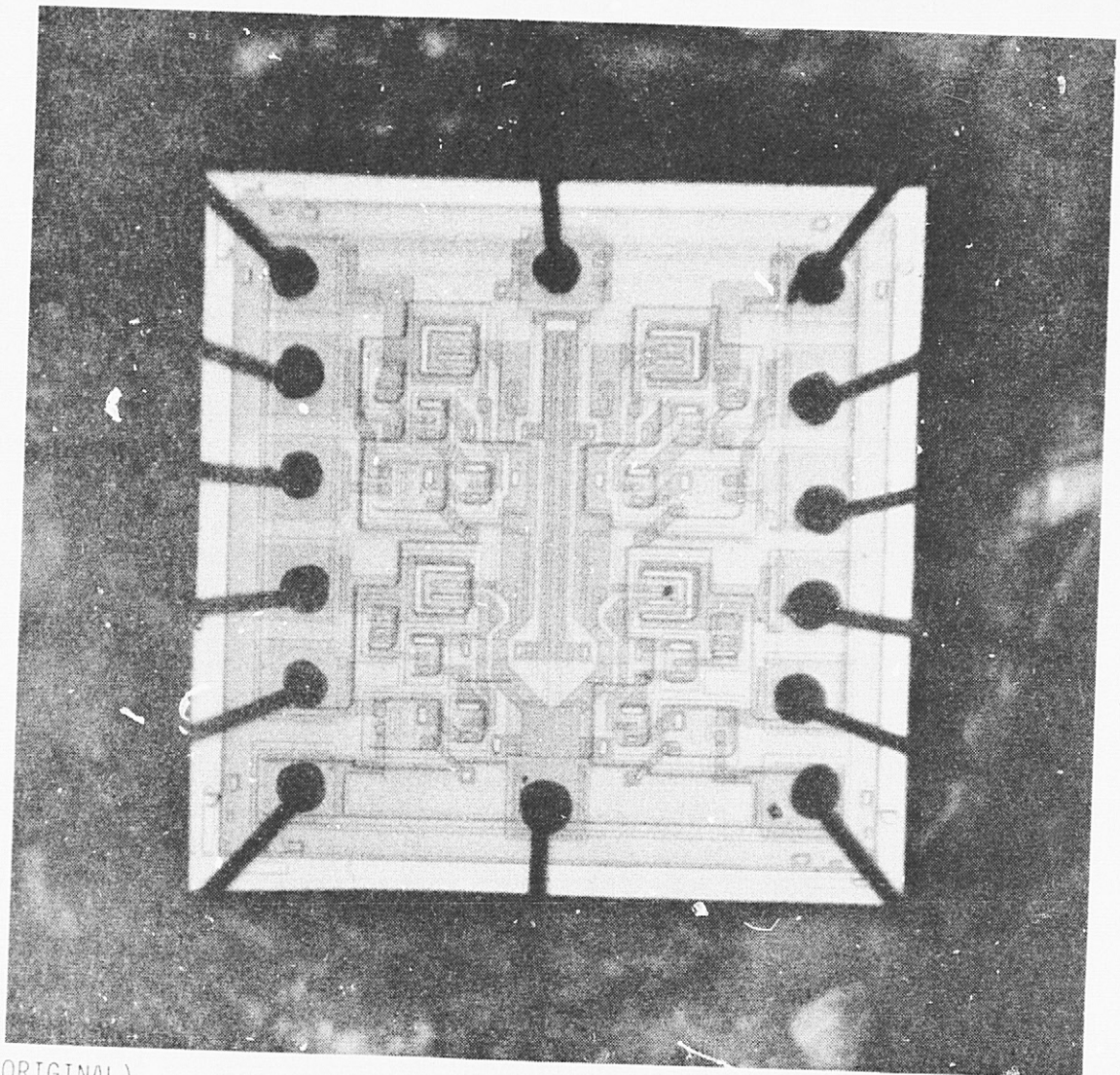

145X (ORIGINAL)

S/N 145, GROUP I

FIGURE C1. PHOTO OF A TYPICAL POST-LIFE DIE.

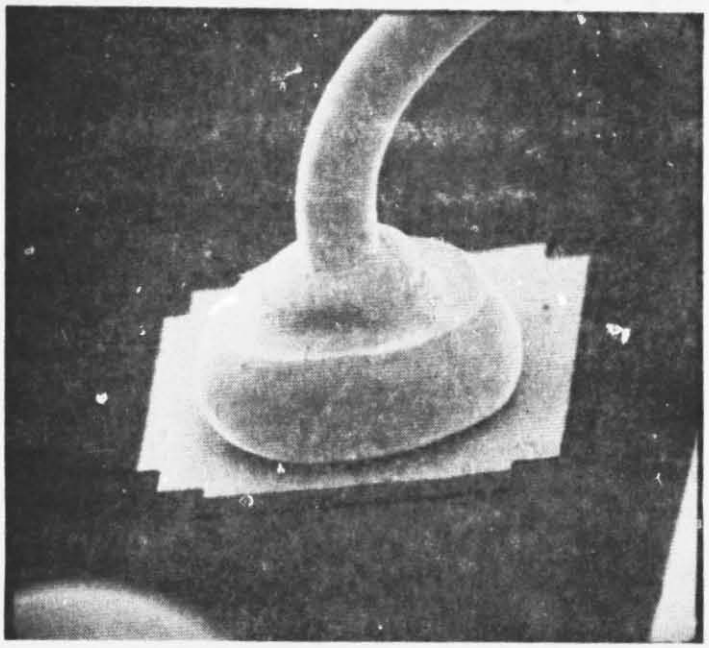

325X S/N 445, GROUP V

FIGURE C2. TYPICAL POST-LIFE WIRE BOND AT THE DIE.

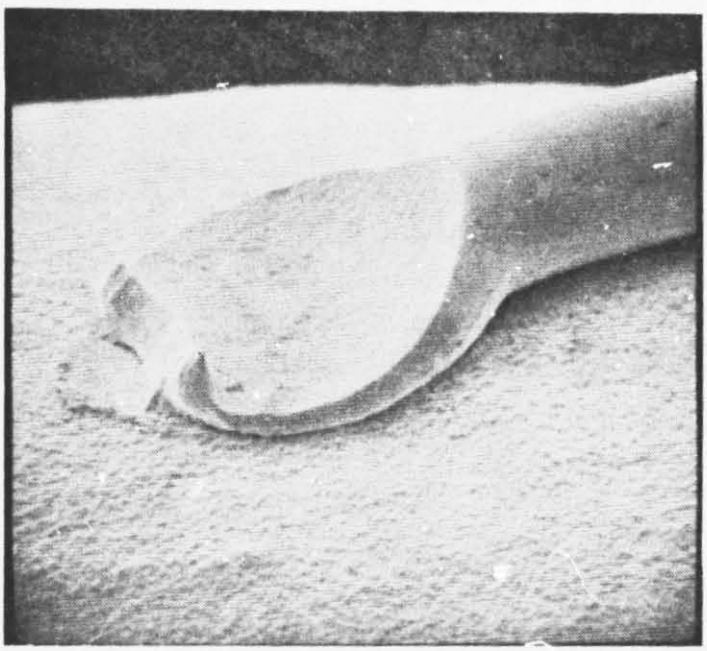

450X S/N 445, GROUP V

FIGURE C3. TYPICAL POST-LIFE WIRE BOND AT THE LEAD FRAME.

APPENDIX C2

POST-LIFE EVALUATION OF THE

NATIONAL SEMICONDUCTOR DM54L00F/883B

QUAD 2-INPUT NAND GATE

DATE CODE 7446

I. POST-LIFE EXAMINATIONS - One (1) National Semiconductor 54L00 survivor from each test group was dissected and examined in detail optically and using the SEM for any anomalous condition induced by the test environments. Results were as follows:

A. PACKAGE EXTERIOR - No part exhibited any degradation of the package markings or the lead finish.

B. PACKAGE INTERIOR - No part exhibited any degradation of the internal wire dress or the die attach bond.

C. DIE SURFACE - None of the parts showed any sign of degradation at the glassivation as a result of the tests, as illustrated in Figure C4.

D. WIRE BONDS - The wire bonds in five of the parts showed no sign of degradation as a result of the test conditions. A typical bond at the die and at the lead frame are shown in Figures C5 and C6. Two of the wire bonds at the lead frame in the group III part appeared to have degraded as a result of the temperature cycling. They contained cracks in the foot of the bond, as illustrated in Figure C7, and faint cracks at the heel, as illustrated in Figure C8.

E. METALLIZATION - The metallization of the three life test parts (Groups IV-VI) was unaffected by the test conditions. The typical post life condition of the metallization of these three parts is illustrated in Figures C9 and C10. The metallization of all three Group I, II and III parts showed evidence of mild aluminum reconstruction as a result of the temperature cycling. Under optical examination the unglassivated aluminum at every bond pad appeared darkened due to roughening, as illustrated in Figure C11. Under SEM examination grain boundary and hillock formations were evident, as illustrated in Figure C12. The aluminum beneath the glassivation was only slightly restructured. Aluminum reconstruction can result in increased sheet resistivity and can promote electromigration. Aluminum reconstruction was not responsible for any failure during the environmental tests and the results of bond pull testing (discussed later) indicated no bond degradation as a result of reconstruction.

II. POST-LIFE TESTS - Ten survivors from each test group were leak tested, delidded and optically examined and then subjected to wire pull testing. Results were as follows:

A. LEAK TESTS - The results of the fine and gross leak tests are presented in Table C3. Two parts had gross leaks at the glass-to-metal seal at the point of lead egress but microscopic examinations of the seal disclosed no reason for the leakage.

B. INTERNAL OPTICAL EXAMINATION - None of the 30 life test parts showed any sign of aluminum reconstruction. All 30 of the temperature cycling test parts exhibited reconstruction of the aluminum bond pads.

C. PULL TESTS - The results of the wire pull tests are presented in Table C4. Twenty-two (22) bonds failed at less than the specified minimum limit of 1.5 grams and are summarized in Table C5. Twenty (20) failures were due to brittle fracture of the heel of the bond at the lead frame, as illustrated in Figure C13. Failed bonds contained evidence of intermetallic growth at the point of the fracture as noted in Figure C13. Removal of the aluminum bond foot with NaOH revealed a mound of gold-rich intermetallics under the entire foot of the bond, as shown in Figure C14. In view of this, the aluminum bonds of five of the pre-life evaluation samples were removed chemically and the lead frames were examined for the presence of intermetallics. All 70 bonds contained gold-rich intermetallics. Since no appreciable intermetallic growth is generated by the ultrasonic bonding operation [1,2], the growth must have resulted from exposure of the bonds to high time/temperature stress during device processing or preconditioning. The 125°C life (Group IV) parts had the lowest average pull strength (2.76 grams) and the highest percentage of heel breaks at the lead frame bond (108/140 or 77%) during the pull tests. The -55°C to 125°C temperature cycle (Group III) parts had the second lowest average pull strength (3.13 grams) and the second highest percentage of heel breaks at the lead frame bond (101/140 or 72%) during the pull tests. The presence of intermetallics would account for these results. The bonds were weakened by continued growth of intermetallics during elevated temperature life and by flexing of the wire at the heel in conjunction with the existing brittle intermetallics during temperature cycling. Low temperature life (Groups V and VI) could not have caused continued growth or flexure of wire, yet seven bonds exhibited low pull strength due to the presence of

intermetallics. Apparently, the few temperature cycles experienced by the parts during insertion and removal from low temperature and during parametric testing at high and low temperature was sufficient to aggravate any bonds weakened by the existing intermetallic growth.

Two (2) failures were due to lift-off of the bond from the pad at the die. The bonds probably had received insufficient ultrasonic energy since welding occurred only around the extreme periphery, as illustrated in Figure C15. This same problem was responsible for the one failure that occurred during the pre-life pull tests.

III REFERENCES

[1] "Purple Plage and Gold Purity", C. W. Horsting, 10th Annual Proceedings, Reliability Physics Symposium, 1972.

[2] "Metallurgical Aspects of Aluminum Wire Bonds to Gold Metallization", J. L. Newsome, R. G. Oswald, and W. R. Rodrigues de Miranda, 14th Annual Proceedings, Reliability Physics Symposium, 1976.

TABLE C3. RESULTS OF THE POST-LIFE LEAK TESTS

TEST GROUP	FINE LEAK RATES (10^{-8} STD CC He/Sec) MEAN	RANGE	NO. OF GROSS LEAKERS
I	1.33	0.81 - 1.74	0
II	1.22	0.81 - 1.62	0
III	0.52 (1)	0.35 - 0.81 (1)	1 (2)
IV	0.62	0.42 - 0.78	0
V	0.38	0.29 - 0.46	0
VI	0.36 (1)	0.19 - 0.83 (1)	1 (3)
PRE-LIFE	0.81	0.46 - 1.13	0

NOTES:

(1) DOES NOT INCLUDE THE GROSS LEAKER

(2) S/N 133 EMITTED THREE LARGE BUBBLES FROM THE GLASS SEAL AT PIN 7

(3) S/N 271 EMITTED THREE LARGE BUBBLES FROM THE GLASS SEAL AT PIN 3

TABLE C4. RESULTS OF THE POST-LIFE PULL TEST

TEST GROUP	TOTAL NO. OF WIRES PULLED	MEAN PULL STRENGTH	STD DEVIATION	RANGE	NO. OF FAILURES
I	140	3.77g	1.21g	1.5-7.0g	0
II	140	4.65g	1.04g	0.9-6.6g	1
III	140	3.13g	0.99g	0.9-5.6g	10
IV	140	2.76g	0.58g	0.5-4.2g	3
V	140	3.46g	0.92g	0.5-5.5g	5
VI	140	3.27g	0.84g	0.6-5.6g	3
PRE-LIFE	140	3.39g	0.86g	0.7-6.0g	1

TABLE C5. SUMMARY OF PULL TEST FAILURES

TEST GROUP	S/N	PIN NO.	PULL STRENGTH (g)	FAILURE MODE	CAUSE OF FAILURE
II	21	6	0.9	HEEL BREAK AT THE POST	Au-Al INTERMETALLICS
III	121	8	1.3		
		14	0.9		
	123	12	0.6		
		13	1.2		
	124	5	0.4		
		7	1.3		
		11	0.7		
		12	1.3		
	131	6	0.0		
	141	13	1.4	BOND LIFTED FROM PAD	UNDERBOND
IV	173	9	1.2	HEEL BREAK AT THE POST	Au-Al INTERMETALLICS
	181	3	1.2		
	185	11	0.5		
V	223	8	1.3		
		9	0.7		
		10	1.2		
	224	11	1.4		
	233	1	0.5		
VI	265	6	1.3		
		9	0.6		
	274	13	1.0	BOND LIFTED FROM PAD	UNDERBOND

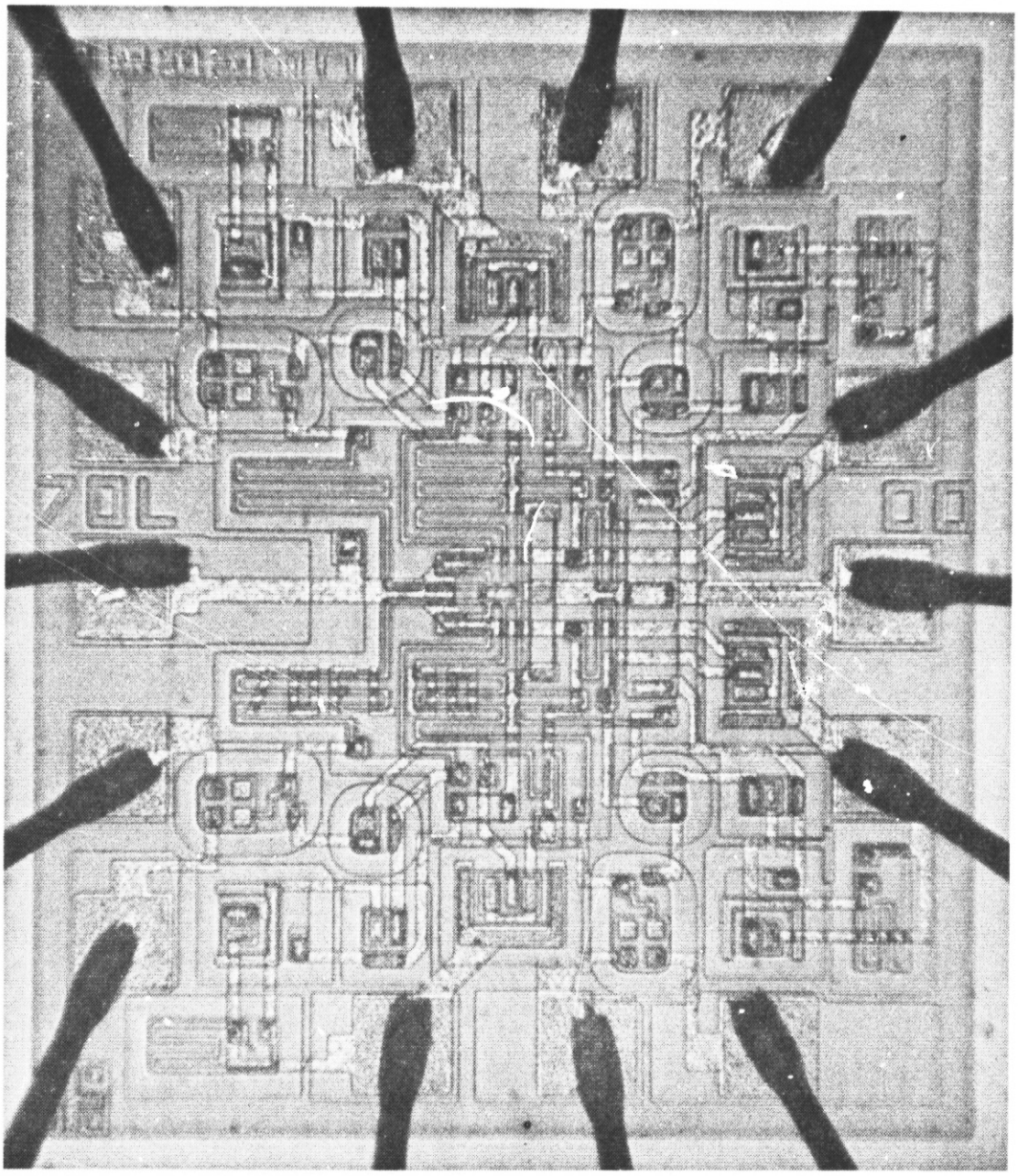

182X (ORIGINAL) S/N 632, GROUP VI

FIGURE C4. DIE PHOTO SHOWING THE TYPICAL CONDITION OF THE GLASSIVATION AFTER THE TESTS.

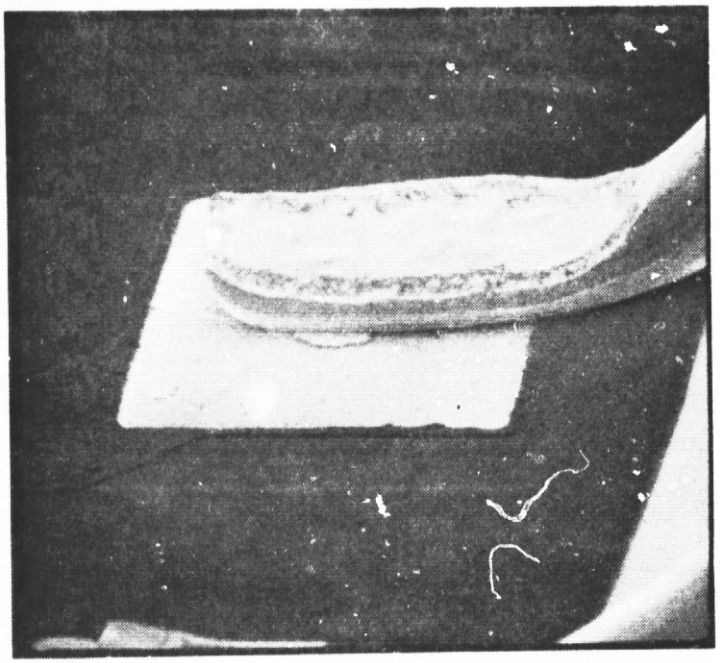

475X S/N 632, GROUP VI

FIGURE C5. TYPICAL WIRE BOND AT THE DIE

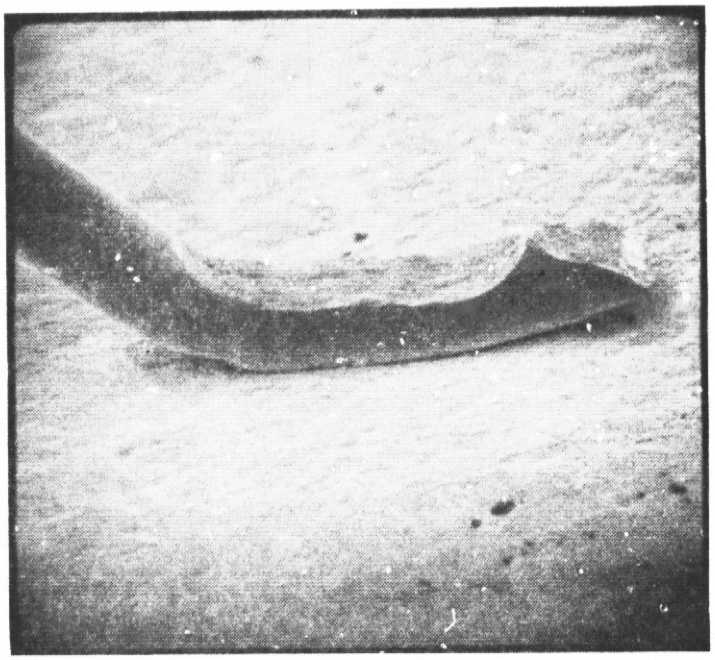

500X S/N 632, GROUP VI

FIGURE C6. TYPICAL WIRE BOND AT THE LEAD FRAME.

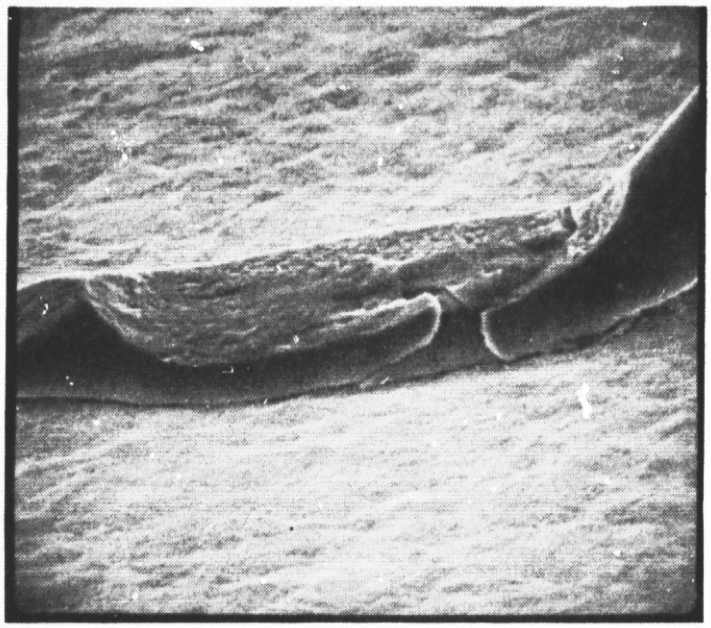

900X S/N 421, GROUP III

FIGURE C7. DEGRADED WIRE BOND AT THE LEAD FRAME (PIN 1).

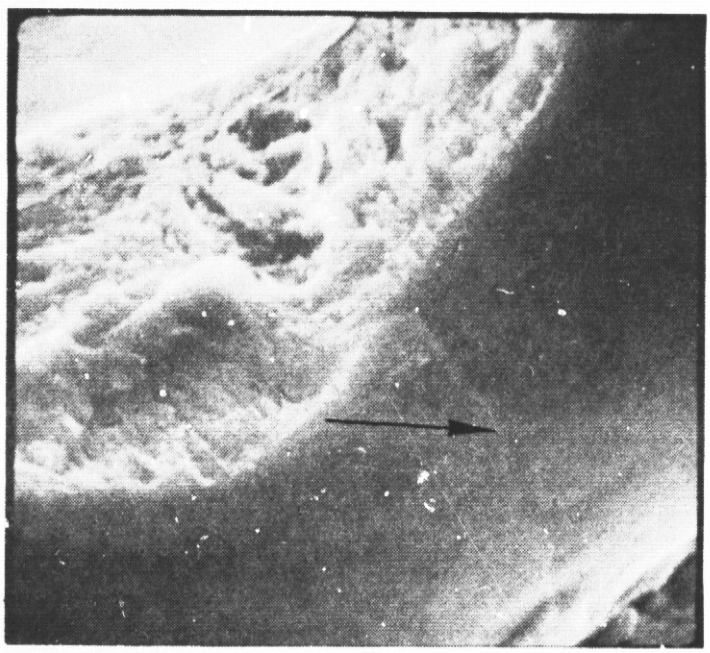

5000X S/N 421, GROUP III

FIGURE C8. FAINT CRACK (ARROW) AT THE HEEL OF THE BOND SHOWN IN FIGURE C7.

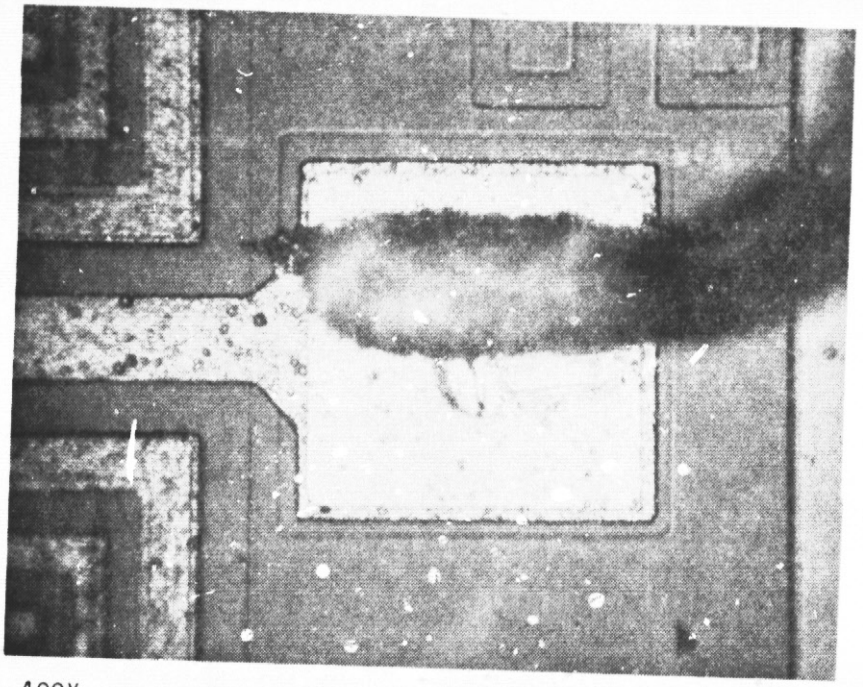

490X S/N 215, GROUP IV

FIGURE C9. V_{CC} (PIN 4) METALLIZATION

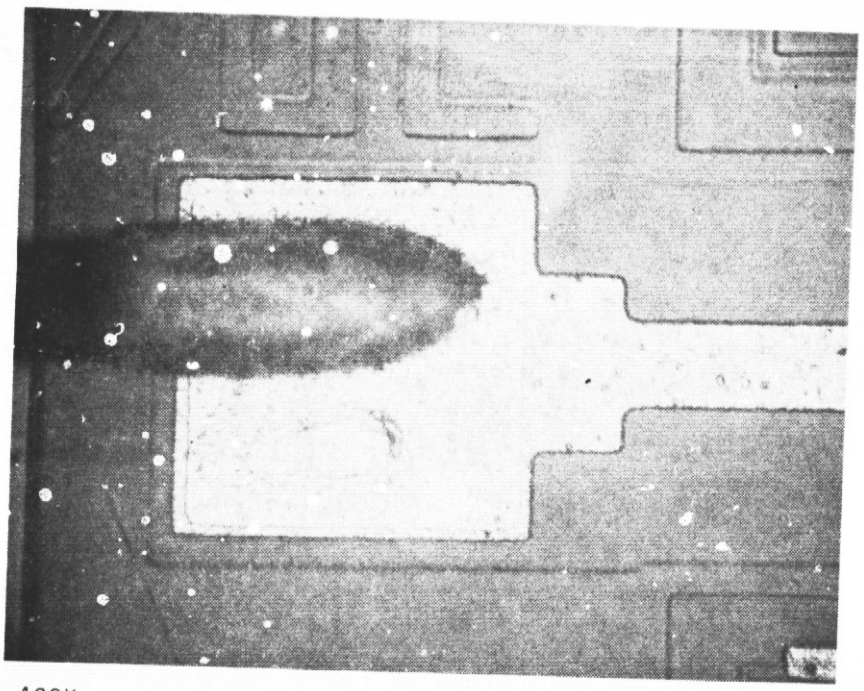

490X S/N 215,

FIGURE C10. GROUND (PIN 11) METALLIZATION.

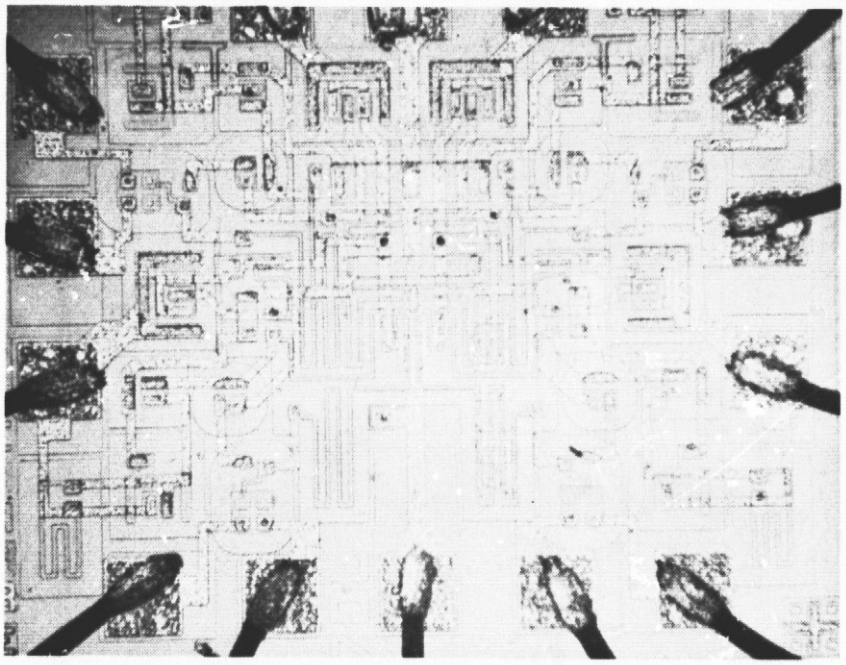

105X S/N 421, GROUP III

FIGURE C11. EXAMPLE OF ALUMINUM RECONSTRUCTION AT BOND PADS.

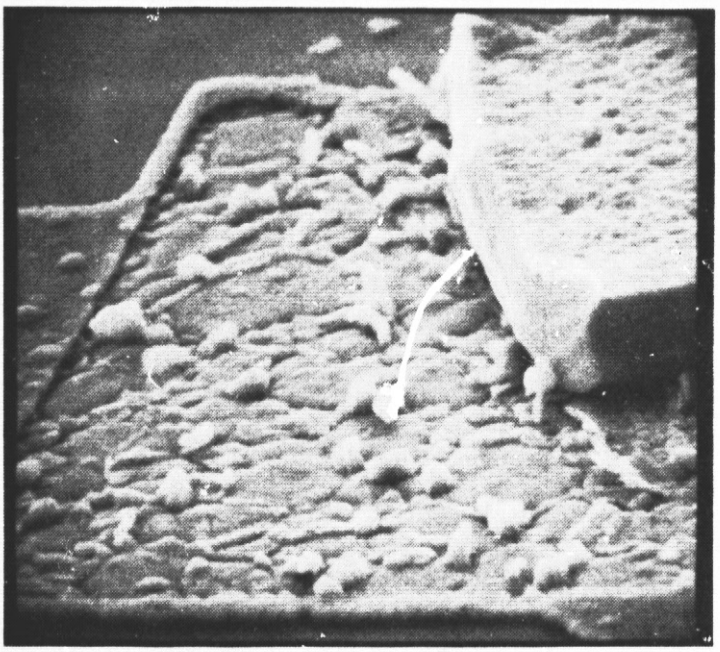

2000X S/N 421, GROUP III

FIGURE C12. SEM PHOTO OF GRAIN BOUNDARY AND HILL FORMATIONS ON THE BOND PADS.

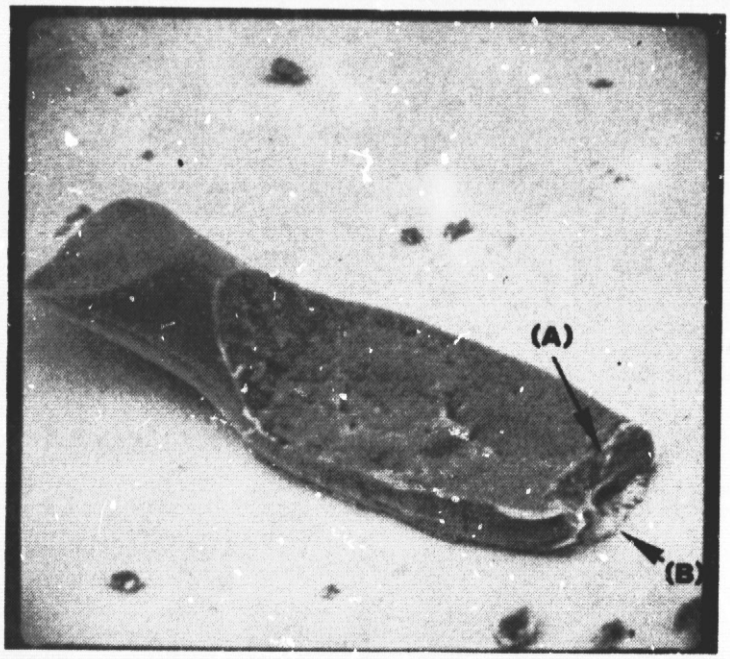

1000X S/N 124, GROUP III

FIGURE C13. FRACTURE POINT (A) OF THE PIN 5 WIRE BOND AT THE LEAD FRAME (PULL STRENGTH = 0.4 GRAM) AND INTERMETALLIC GROWTH (B) AT THE FRACTURE POINT.

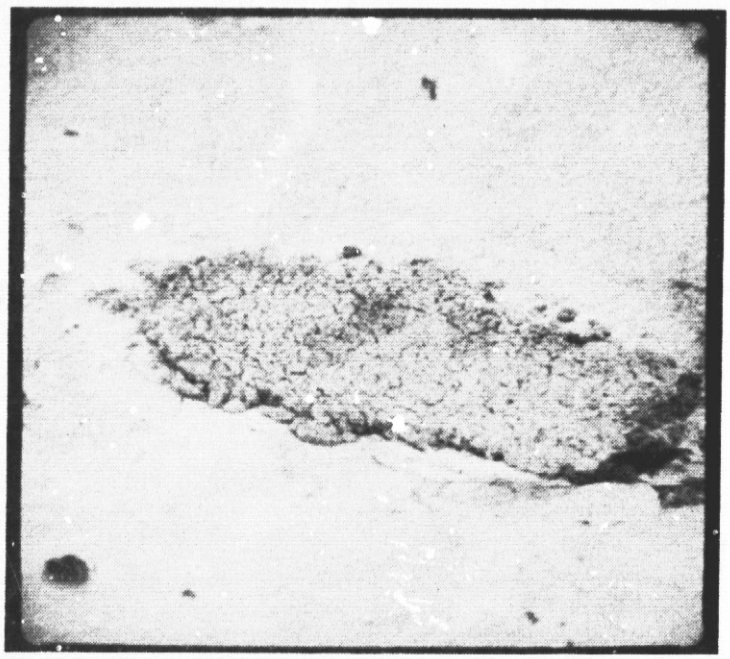

1100X S/N 124, GROUP III

FIGURE C14. INTERMETALLIC GROWTH UNDER THE FOOT OF THE BOND SHOWN IN FIGURE C13

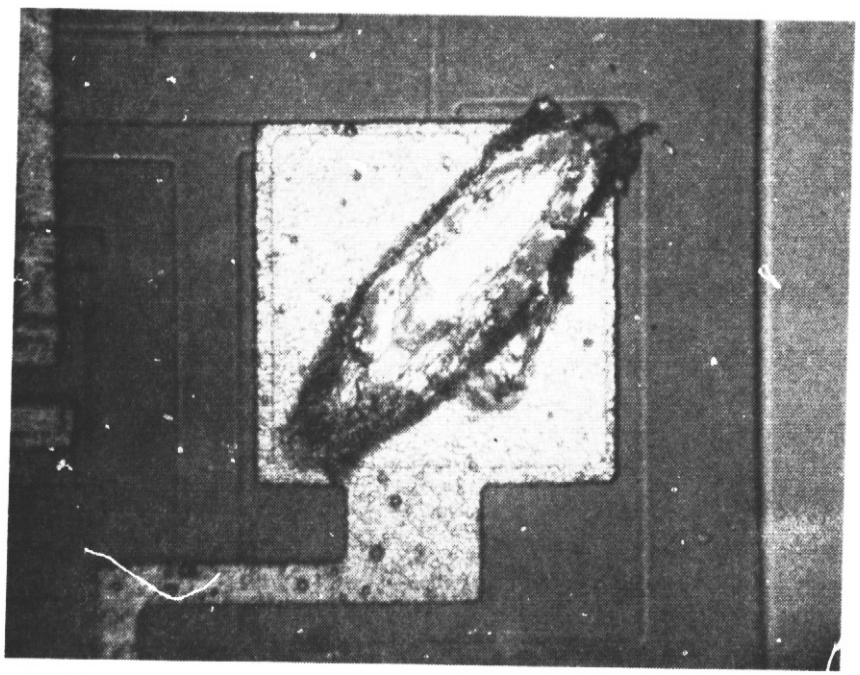

491X S/N 274, GROUP VI

FIGURE C15. LIFT-OFF PATTERN OF THE PIN 13 BOND.

APPENDIX C3

POST-LIFE EVALUATION OF THE

NATIONAL SEMICONDUCTOR LM741H/883B

OPERATIONAL AMPLIFIER

DATE CODE 7545

I. POST-LIFE EXAMINATIONS - One (1) National Semiconductor 741 survivor from each test group was dissected and examined in detail optically and using the SEM for any anomalous condition induced by the test environments. Results were as follows:

A. PACKAGE EXTERIOR - No part exhibited any degradation of the package markings or the lead finish.

B. PACKAGE INTERIOR - No part exhibited any degradation of the internal wire dress or the die attach bond.

C. DIE SURFACE - The Group III (-55°C to +125°C) part contained cracks in the glassivation over the MOS capacitor, as shown in Figure C16. This effect is discussed in a later section of this report. None of the parts from the other five test groups showed any sign of degradation of the glassivation as a result of the tests, as illustrated in Figure C17.

D. METALLIZATION - The metallization of the three life test parts (Groups IV-VI) was unaffected by the test conditions. Typical post-life condition of these three parts is illustrated in Figures C18 and C19. The metallization of all three Group I, II and III parts showed evidence of aluminum reconstruction as a result of the temperature cycling. Under optical examination the unglassivated aluminum at every bond pad appeared darkened due to roughening, as illustrated in Figure C20. Under SEM examination numerous hillock formations were evident, as illustrated in Figure C21. The aluminum beneath the glassivation was slightly restructured, but not as severely as the unglassivated aluminum. Aluminum reconstruction can result in increased sheet resistivity and can promote electromigration. Aluminum reconstruction was not responsible for any failure during temperature cycling or life tests and the results of bond pull testing (discussed later) indicate that no bond degradation occurred as a result of reconstruction of the pad.

E. WIRE BONDS - The wire bonds in five of the parts showed no sign of degradation as a result of the test conditions. A typical bond at the die and at the post are shown in Figures C22 and C23. All of the bonds at the die in the Group III part had deteriorated. As illustrated in Figure C24, the feet of the bonds were wrinkled and depleted of aluminum. This effect was apparently due to a form of aluminum reconstruction because the unbiased pins (1 and 5) exhibited the same degree of deterioration, as did the pins that were biased during temperature cycling

(pins 2, 3, 4, 6 and 7). The bonds also contained tears above the heel and wrinkles or cracks below the heel, as illustrated in Figure C25. The condition of the wire under the heel was caused by flexure of the wire during temperature cycling, but the tears above the heel could have been generated by the bonding operation. No tears at the heel of the bonds were present in the one unstressed part examined in detail during the pre-life evaluation. Therefore, a second unstressed sample was delidded and its wire bonds were examined in the SEM. This part contained tears at the heel of each bond from battering of the ultrasonic bonding tool, as illustrated in Figure C26. Closer examination disclosed that the tears were relatively benign since none contained any sharp metallurgical cracks propagating into the aluminum as shown in Figure C27.

Reconstruction of the bond foot and fatigue of the heel was not responsible for any failure during life test or temperature cycling, but the results of bond pull testing (discussed later) indicate that the bonds were weakened as a result of the condition of the heel.

II. POST-LIFE TESTS - Ten survivors from each test group were leak tested, delidded and optically examined and then subjected to a wire pull test. Results were as follows:

A. LEAK TESTS - The results of the fine and gross leak tests presented in Table C6, indicated that the package hermeticity was not degraded by the test conditions.

B. INTERNAL OPTICAL EXAMINATION - Nine of the Group III parts contained cracks in the glassivation over the MOS capacitor. No part in the other five groups displayed any crazing over the capacitor. This indicated that the crazing was caused by thermal expansion mismatch of the glass and the large aluminum area of the capacitor during the -55°C to +125°C temperature cycling. The crazing also indicates a possible lack of or insufficient level of phosphorous doping in the glassivation.

None of the 30 Group IV, V and VI (life test) parts showed any sign of aluminum reconstruction. All 30 of the Group I, II and III (temperature cycling) parts exhibited reconstruction of the aluminum bond pads. The foot of the bonds in nine of the Group III parts was depleted due to reconstruction. Similar bond degradation was noted in the Group II and the Group I parts but to a progressively lesser degree.

C. PULL TESTS - The results of the wire pull tests are presented in Table C7. Seven bonds broke at less than the specified minimum limit of 1.5 grams and are summarized in Table C8. All seven weak bonds occurred in Group III parts and all were due to breaks at the heel, as illustrated in Figures C28 and C29. The low pull strengths were attributed to weakening of the heel caused by flexing of the wire during temperature cycling. It did not appear that reconstruction of the bond foot contributed to the weakness. However, since all seven failures occurred at either pin 6 (output) or pin 7 (V+), it appeared that electromigration of aluminum may have been a contributing factor. As shown in Table C9, Groups II and III the mean pull strengths of the pins that were biased and conducted current (pins 4, 6 and 7) during temperature cycling were significantly lower than the pull strengths of the pins that were unbiased (pins 1 and 5) during cycling. This pattern did not exist in the pre-life samples.

TABLE C6. RESULTS OF THE POST-LIFE LEAK TESTS

TEST GROUP	FINE LEAK PARTS (10^{-8} STD CC He/Sec)		NUMBER OF GROSS LEAKERS
	MEAN	RANGE	
I	1.63	1.34-2.20	0
II	1.12	0.85-1.46	0
III	0.87	0.65-1.11	0
IV	1.69	1.20-2.22	0
V	0.77	0.65-0.91	0
VI	0.66	0.40-0.80	0
PRE-LIFE	ALL LESS THAN 3.80		0

TABLE C7. RESULTS OF THE POST-LIFE PULL TESTS

TEST GROUP	TOTAL NO. OF WIRES PULLED	MEAN PULL STRENGTH	STD DEVIATION	RANGE	NO. OF FAILURES
I	70	2.76g	0.41g	1.7-4.0g	0
II	70	2.66g	0.42g	1.9-4.1g	0
III	70	2.26g	0.59g	0.5-3.4g	7
IV	70	2.45g	0.35g	1.7-3.2g	0
V	70	2.92g	0.51g	1.8-4.4g	0
VI	70	2.89g	0.49g	2.0-4.4g	0
PRE-LIFE	70	2.75g	0.45g	2.0-4.0g	0

TABLE C8. SUMMARY OF PULL TEST FAILURES

TEST GROUP	S/N	PIN NO.	PULL STRENGTH (g)	FAILURE MODE	CAUSE OF FAILURE
III	223	6	1.4	Heel Break	Heel Fatigue
		7	1.3	↓	↓
	225	6	1.1		
		7	1.4		
	232	7	0.9		
	233	6	0.5		
		7	0.9		

TABLE C9. MEAN PULL STRENGTHS AS A FUNCTION OF PIN NUMBER

PIN NUMBER: / TEST GROUP	1	2	3	4	5	6	7
III	2.42g	2.08g	2.55g	2.29g	2.75g	1.92g	1.78g
II	3.33g	2.48g	2.77g	2.69g	3.05g	2.65g	2.42g
PRE-LIFE	2.64g	2.50g	2.89g	2.72g	3.22g	2.59g	2.66g

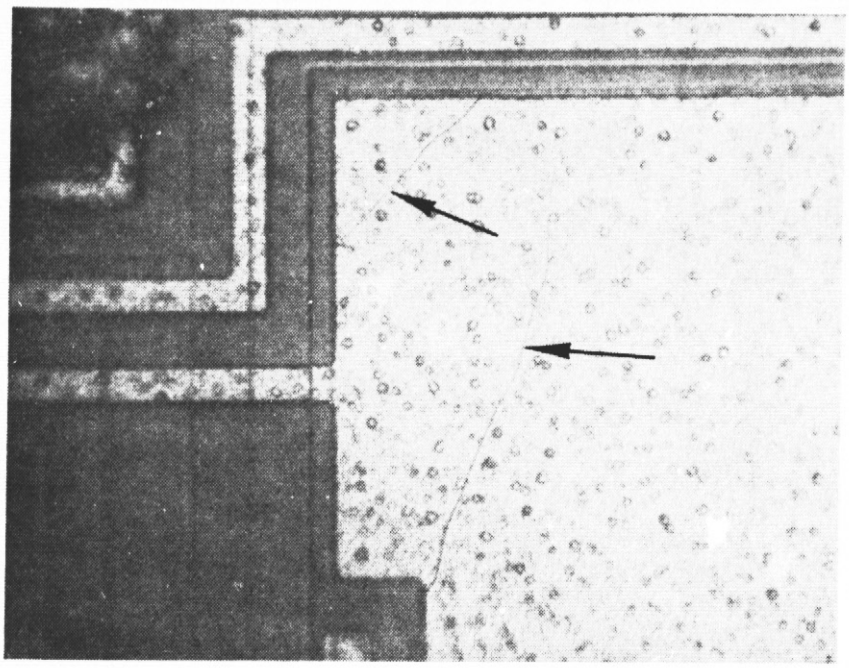

395X S/N 274, GROUP III

FIGURE C16. CRACKS IN THE GLASSIVATION OVER THE MOS CAPACITOR OF THE GROUP III PART.

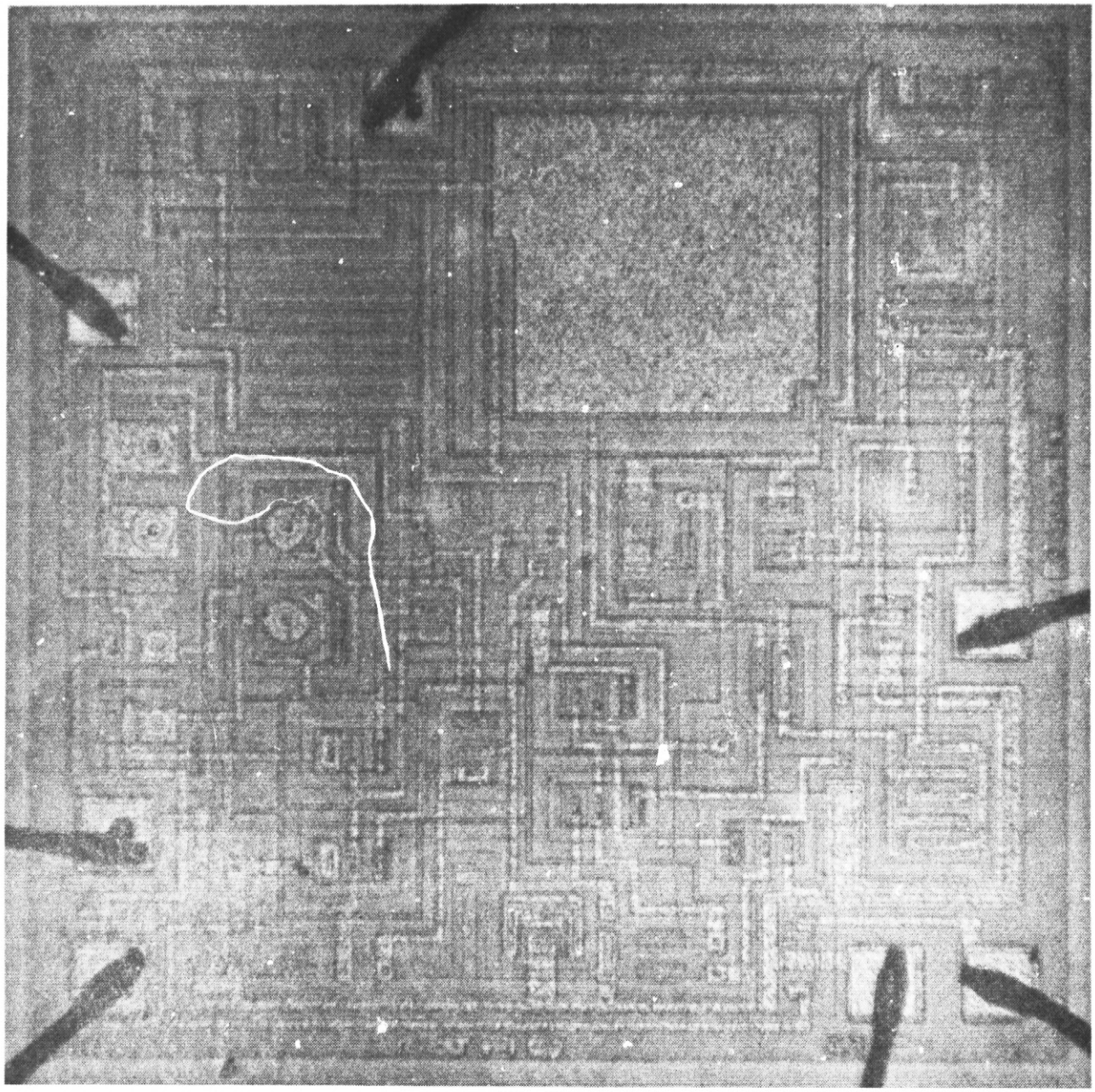

130X (ORIGINAL) S/N 491, GROUP V

FIGURE C17. PHOTO OF A DIE WHICH ILLUSTRATES THE CONDITION OF THE GLASSIVATION, TYPICAL OF GROUP I, II, IV, V AND VI PARTS.

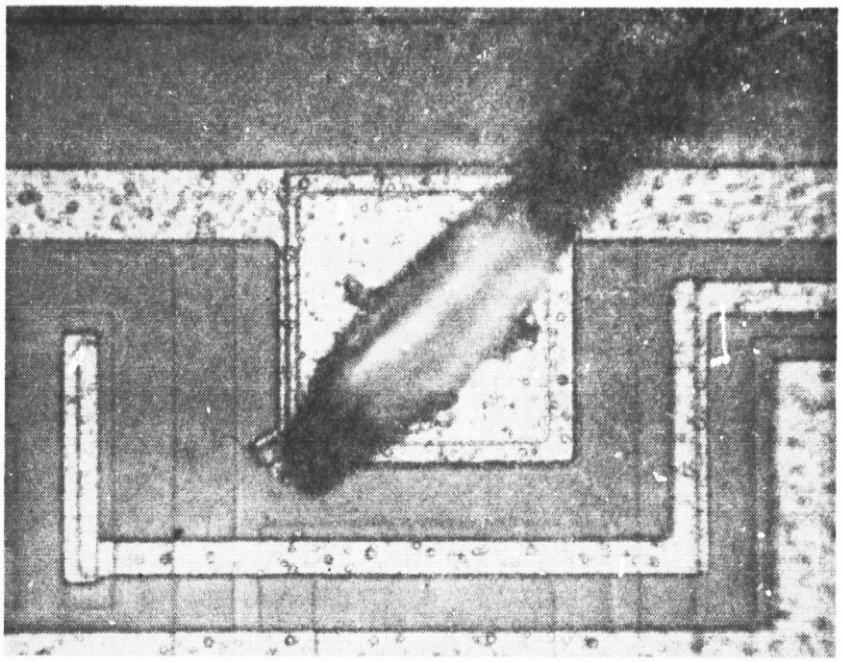

395X S/N 603, GROUP VI

FIGURE C18. V+ (PIN 7) METALLIZATION.

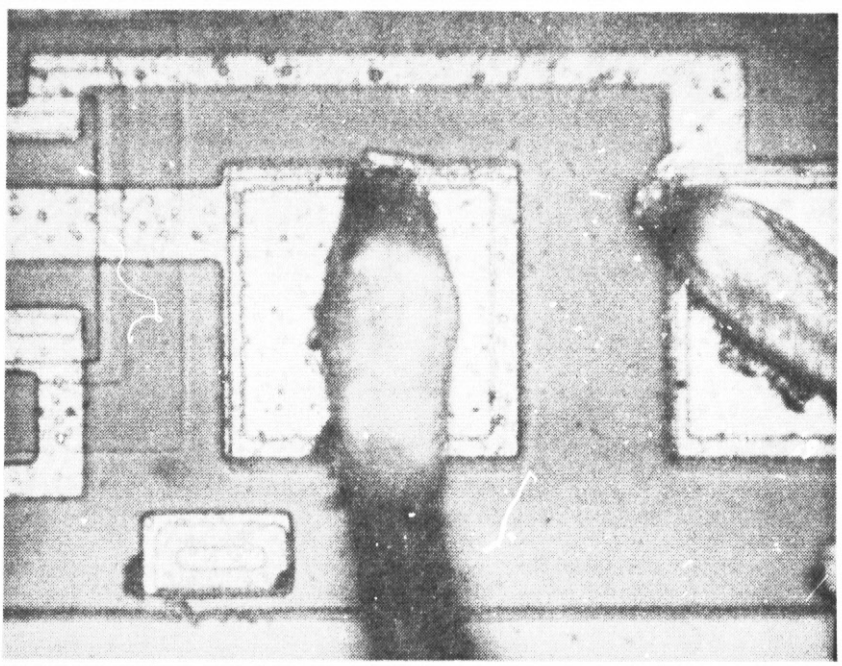

395X S/N 603, GROUP VI

FIGURE C19. V- (PIN 4) METALLIZATION.

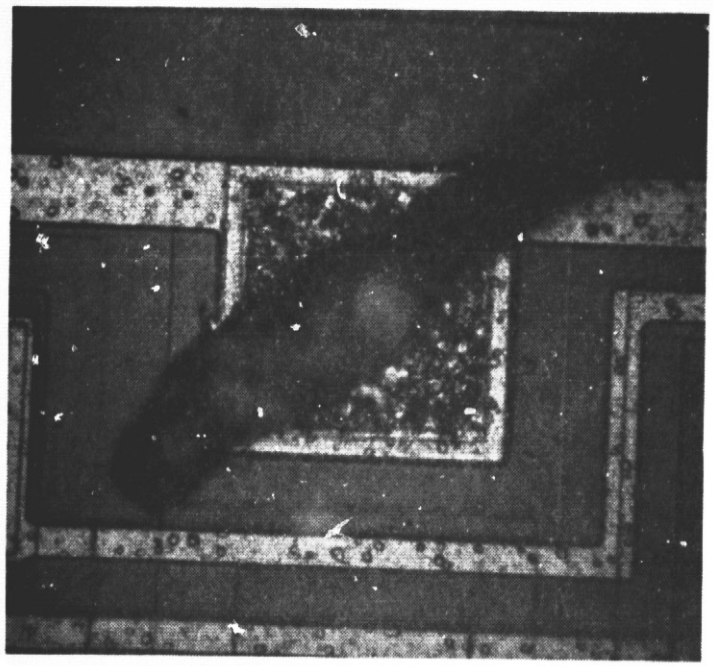

395X X/N 274, GROUP III

FIGURE C20. EXAMPLE OF ALUMINUM RECONSTRUCTION AT THE BOND PAD (PIN 7).

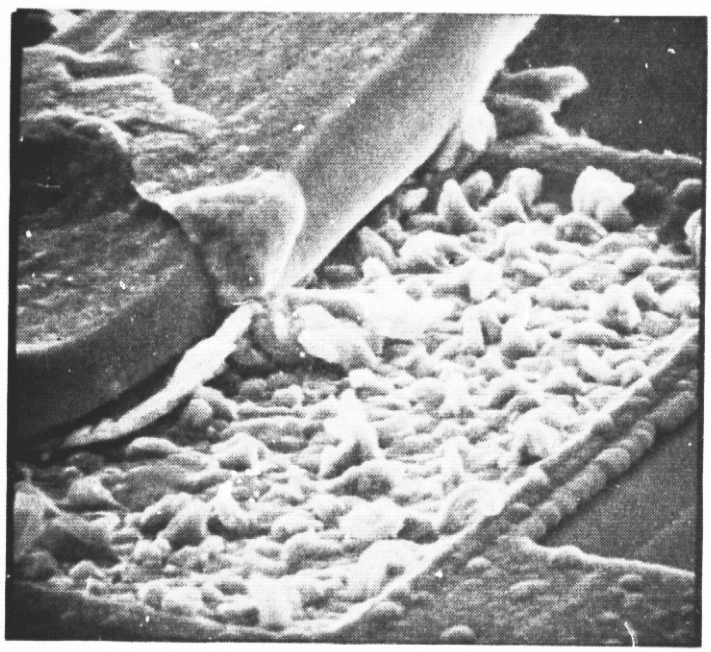

1500X S/N 274, GROUP III

FIGURE C21. SEM PHOTO OF ALUMINUM RECONSTRUCTION AT THE BOND PAD (PIN 4).

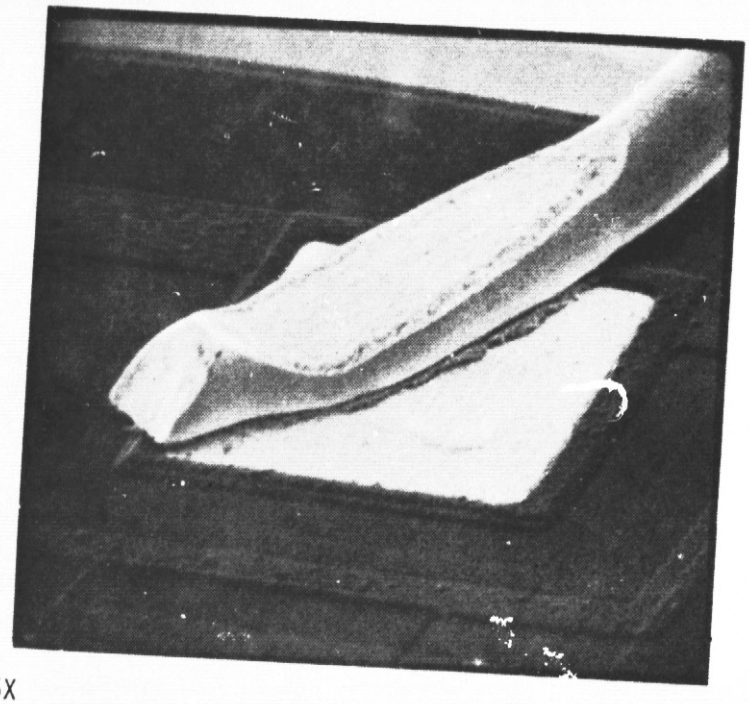

475X

S/N 491, GROUP V

FIGURE C22. WIRE BOND AT THE DIE.

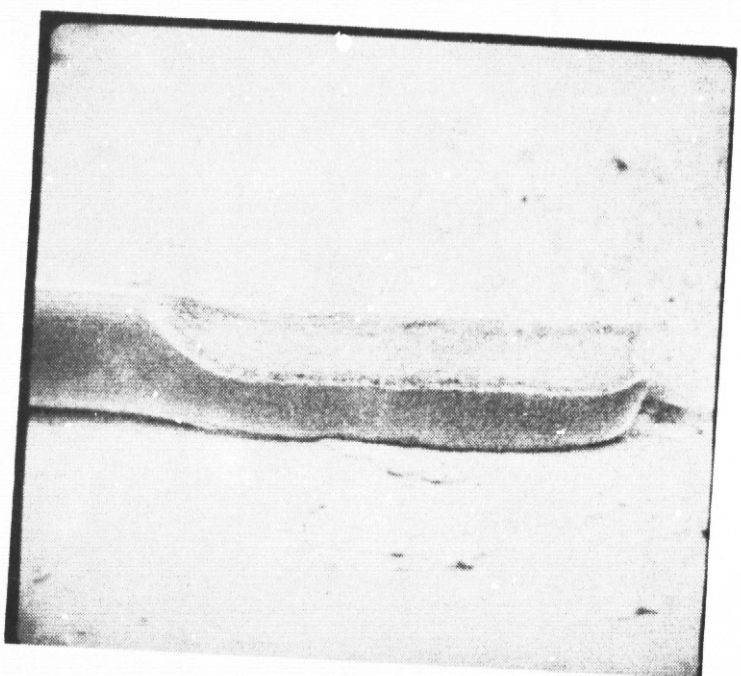

475X

S/N 65, GROUP II

FIGURE C23. WIRE BOND AT THE POST.

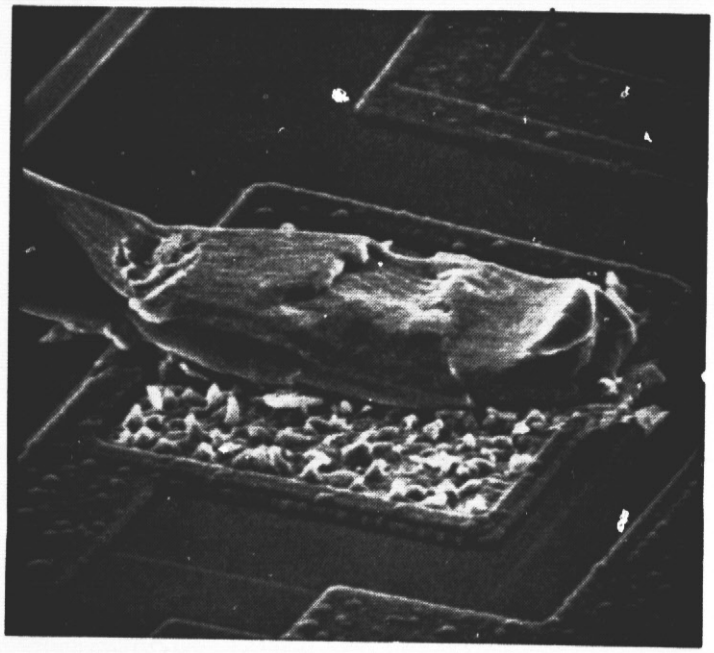

750X S/N 274, GROUP III

FIGURE C24. DEGRADED BOND AT PIN 6.

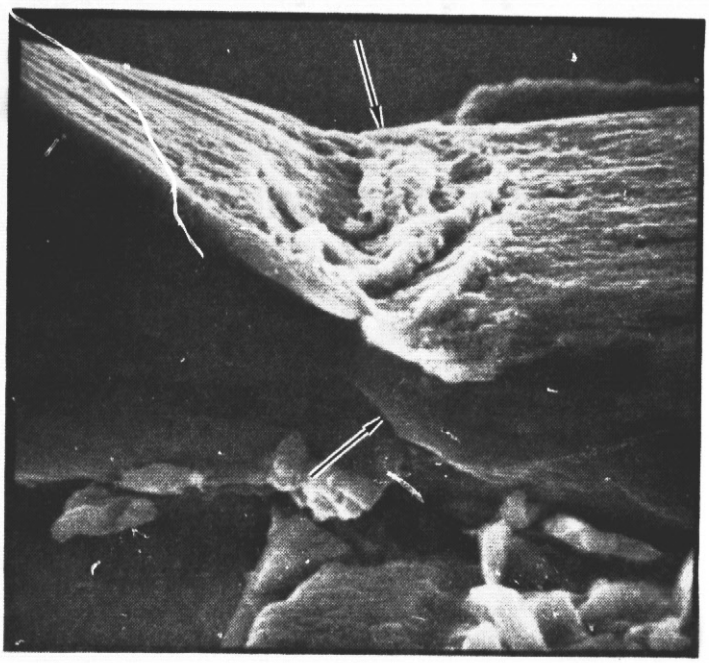

3000X S/N 274, GROUP III

FIGURE C25. CLOSE-UP OF THE HEEL OF THE PIN 6 BOND SHOWING THE TEAR AND WRINKLE (ARROWS).

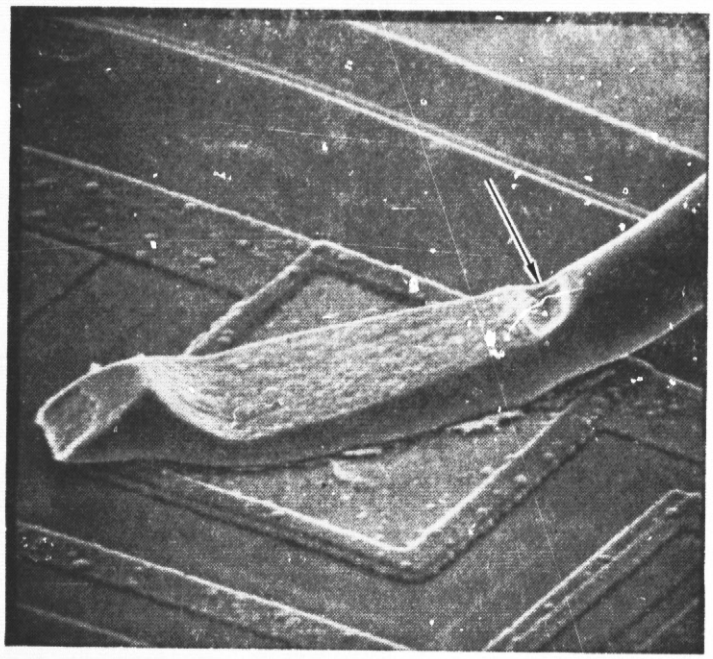

700X S/N 641 (UNSTRESSED)

FIGURE C26. WORST CASE EXAMPLE OF A TEAR AT THE HEEL (ARROW) FOUND IN THE UNSTRESSED SAMPLE (PIN 7).

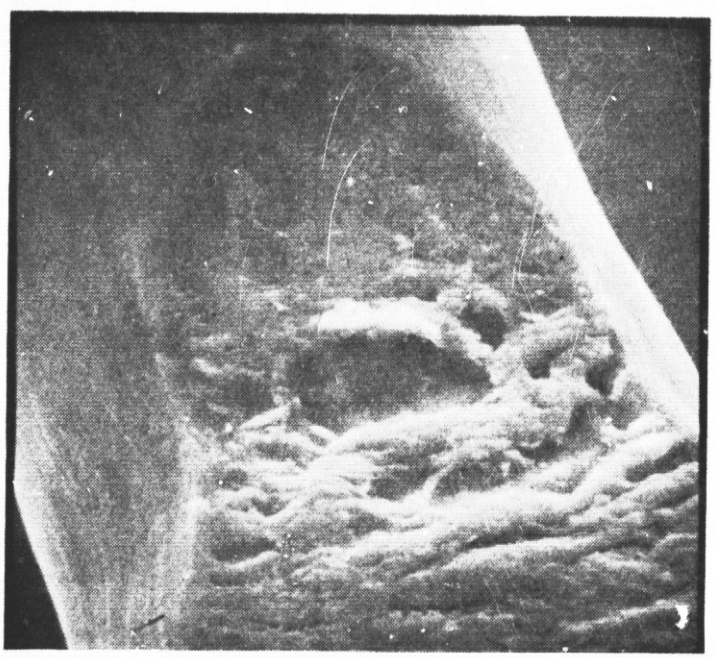

4000X S/N 641 (UNSTRESSED)

FIGURE C27. CLOSE-UP OF A TYPICAL TEAR AT THE HEEL OF A BOND IN THE UNSTRESSED SAMPLE.

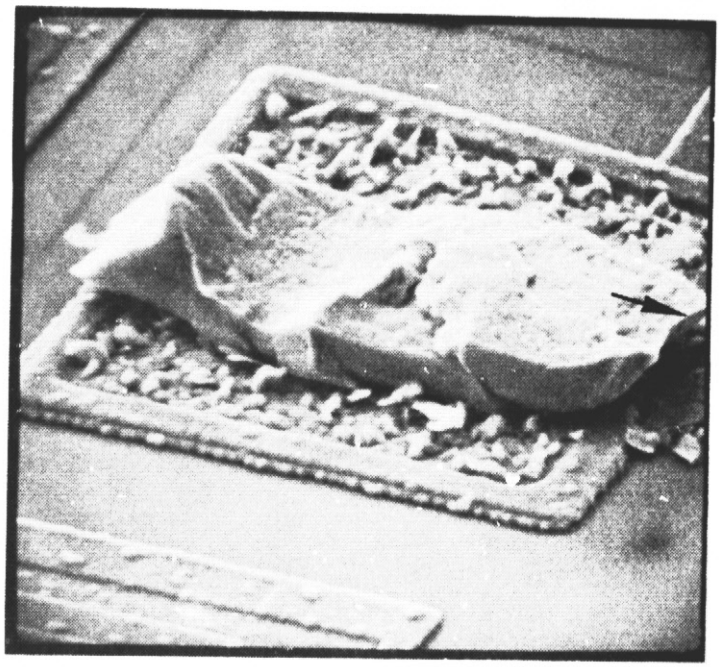

750X S/N 223, GROUP III

FIGURE C28. EXAMPLE OF FAILED BOND (PIN 6) SHOWING THE LOCATION OF THE BREAK (ARROW).

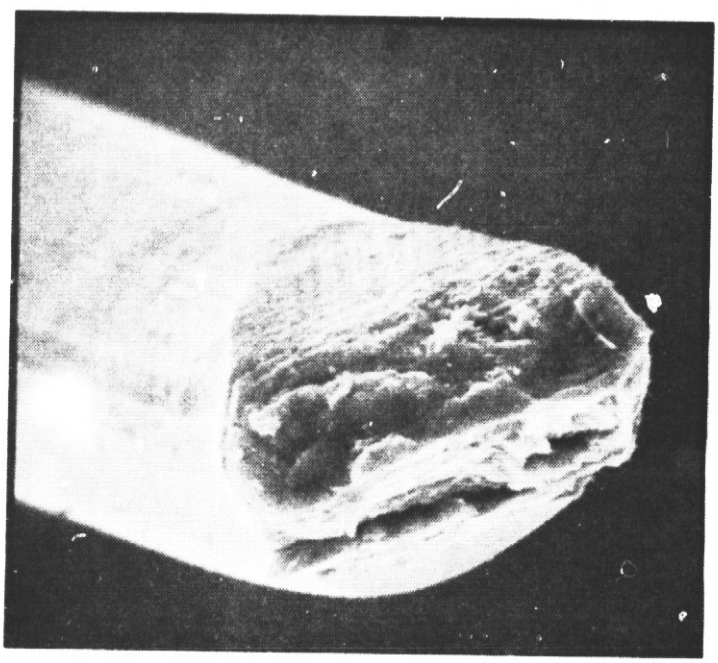

2000X S/N 223, GROUP III

FIGURE C29. WIRE END OF THE BREAK SHOWN IN FIGURE C28.

APPENDIX C4

POST-LIFE EVALUATION OF THE

RAYTHEON RM741T883B

OPERATIONAL AMPLIFIER

DATE CODE 5737

I. POST-LIFE EXAMINATIONS - One (1) Raytheon 741 survivor from each test group was dissected and examined in detail optically and using the SEM for any anomalous condition induced by the test environments. Results were as follows:

A. PACKAGE EXTERIOR: No part exhibited any degradation of the package markings or finish or the lead finish.

B. PACKAGE INTERIOR: No part exhibited any degradation of the internal wire dress or the die attach bond.

C. DIE SURFACE: None of the parts showed any sign of degradation of the glassivation as a result of the tests. A photograph of a typical die is presented in Figure C30. The test Group II and III parts contained a noteworthy anomaly which was not related to the test condition. The surface of the glassivation of each part contained drops of contamination above the stripes, as shown in Figure C31. The droplets would swell up and burst when examined at high magnification in the SEM as illustrated by the sequence shown in Figures C32 through C34. The contaminant more than likely was introduced during manufacturing and, since the material did not result in any degradation or failure of a part, no attempt was made to identify its composition or source.

D. WIRE BONDS: The wire bonds in five of the parts showed no sign of degradation as a result of the test conditions. A typical bond at the die and at the post are shown in Figures C35 and C36. The Group IV (125°C Life) part contained some intermetallic growth around most of the Au-Al bonds at the die as illustrated in Figure C37.

E. METALLIZATION: The metallization of the three life test parts (Groups IV-VI) was unaffected by the test conditions. Typical post life condition of these three parts is shown in Figures C38 and C39. The metallization of all three Group I, II, and III parts showed evidence of mild aluminum reconstruction as a result of the temperature cycling. Under optical examination the unglassivated aluminum at every bond pad appeared darkened due to roughening as illustrated in Figure C40. Under SEM examination grain boundary formations and fatigue striations were evident as illustrated in Figure C41. The aluminum beneath the glassivation was also restructured as illustrated in Figure C42 but not as severely as was the unglassivated aluminum. Aluminum reconstruction can result in increased sheet resistivity and can promote electromigration. However, the results of the

failure analyses and the bond pull tests (discussed below) indicate that the aluminum reconstruction was not responsible for any device failure and did not degrade the bond strength.

II. POST-LIFE TESTS - Ten survivors from each test group were leak tested, delidded and optically examined and then subjected to a wire pull test. Results were as follows:

A. LEAK TESTS: The results of the fine and the gross leak tests, presented in Table C10, indicated that the package hermeticity was not degraded by the test conditions. One Group I part had a relatively high fine leak rate of 58 X 10^{-8} cc/sec. The mean leak rate of the other nine Group I parts was 0.94 X 10^{-8} cc/sec. Another Group I part had a gross leak but this was caused by a defect in the glass seal introduced during manufacturing.

B. Internal Optical Examination: All 30 of the Group I, II and III (temperature cycling) parts exhibited aluminum reconstruction. None of the 30 Group IV, V, and VI life test parts showed any signs of aluminum reconstruction. None of the 60 parts showed any optically visible intermetallic growth around their ball bonds. One part, S/N 333, of Group IV contained a lifted ball bond at pin 5 (discussed in next section).

C. PULL TESTS: The results of the wire pull tests are presented in Table C11. Seventeen bonds and two wires failed at less than the specified minimum limit of 2.0 grams and these failures are summarized in Table C12. Eleven bonds lifted (separated) from the aluminum pad at the Au/Al interface. Examination of the pad disclosed that in ten instances, the aluminum was compressed under the ball, but the inprint area contained little or no sign of intermetallic formation as illustrated in Figure C43. This indicated that these failures were the result of underbonding, probably caused by insufficient heat or dwell time during the bonding operation or possibly incomplete glassivation removal. This same problem was responsible for three failures during the pre-life pull tests. In one instance, the pad was badly smeared as shown in Figure C44, indicating that this failure was caused primarily by tool slippage during the bonding operation. Two bonds failed due to separation of the bond pad aluminum from the SiO_2 passivation

as shown in Figure C45. The two failures were probably due to poor adhesion of the aluminum to the SiO_2. Four bonds separated in the gold-aluminum intermetallic zone. In each instance the pad was covered with a mound of gold colored intermetallics as illustrated in Figure C46. This indicated that the failure was the result of Kirkendall voiding in Au_5Al_2. The other six bonds in each of the four packages exhibited satisfactory pull strengths ranging from 2.9 grams to 6.4 grams (mean = 4.40 grams). This indicates that the excessive intermetallic growth which led to the four bond failures was caused by an isolated bonding error, such as excessive dwell time, rather than by excessive test temperatures. In two instances, the low pull strength was the result of a wire breaking at less than 2 grams. In both cases the wire broke above the ball, contained no deficiency, and was necked down at the break in the same manner as all of the other wires which broke at satisfactory levels as illustrated in Figure C47. Therefore these two breaks were not considered significant. The results of these pull tests indicated that no anomalous condition was induced by the environmental tests. The post-life pull strengths were essentially the same as the pre-life pull strength. However, the results also indicate that the environmental tests in conjunction with periodic electrical testing did not effectively detect weak bonds. Only two parts failed due to open bonds during the environmental tests, yet the pull test revealed seven bonds with zero gram pull strength in parts that had passed all electrical testing. In each case the bond was open and lifted (pin 5 of S/N333) or open and barely contacting the pad. Three of the zero strength bonds involved a V_{IO}ADJ pin (pins 1 and 5) and thus could not have been detected electrically (these pins were not tested and were not biased), but four involved V+, V-, or an input or output pin and could have been detected. Temperature cycling and elevated temperature life are needed to accelerate or aggravate to failure any weak or marginal bond, but the pull test results indicate that these tests must be supplemented with a centrifuge or a monitored shock/vibration type of test to detect the weak bond.

TABLE C10. RESULTS OF THE POST-LIFE LEAK TESTS

Test Group	FINE LEAK RATES(10^{-8}STD CC He/Sec) Mean	Range	Numbers of Gross Leakers
I	6.65	0.34-58.00 ⚠1	1 ⚠2
II	0.86	0.35-1.51	0
III	0.81	0.62-1.05	0
IV	1.33	0.96-2.04	0
V	0.56	0.43-0.62	0
VI	1.26	0.85-1.83	0
PRE-LIFE	1.22	1.06-1.46	0

⚠1 S/N 121 had a leak rate of 58 x 10^{-8}cc/sec

⚠2 S/N 122 emitted a steady stream of bubbles from a pinhole or dimple in the glass seal that was introduced during manufacturing.

TABLE C11. RESULTS OF THE POST-LIFE PULL TESTS

Test Group	Total No. of Wires Pulled	Mean Pull Strength	STD Deviation	Range	No. of Failures
I	70	4.60g	1.16g	0.0-6.5g	2
II	70	4.78g	1.09g	0.7-7.0g	2
III	70	4.13g	1.38g	0.0-6.9g	6
IV	70	3.73g	1.43g	0.0-6.4g	7
I	70	4.65g	0.87g	1.7-6.7g	1
VI	70	4.74g	0.85g	1.8-6.8g	1
PRE-LIFE	70	4.75g	1.48g	0.2-7.8g	4

TABLE C12. SUMMARY OF PULL TEST FAILURES

Test Group	S/N	P/N No.	Pull Strength (Grams)	Failure Mode	Failure Cause
I	121	7	0.9	Ball lifted from pad	Underbonded
	123	1	0.0	"	"
II	92	6	0.7	Ball broke in intermetallics	Bonding error
	94	5	1.7	Ball lifted from pad	Underbonded
III	222	6	0.0	Ball lifted from pad	Underbonded
		7	0.1	"	"
	223	1	0.6	Aluminum lifted from SiO_2	Poor aluminum adhesion
	225	5	1.4	Ball broke in intermetallics	Bonding error
	231	1	1.7	Aluminum lifted from SiO_2	Poor aluminium adhesion
		7	0.0	Ball lifted from pad	Pad damaged by bond tool
IV	331	3	0.0	Ball broke in intermetallics	Bonding error
	332	1	0.0	Ball lifted from pad	Underbonded
		7	0.1	"	"
	333	5	0.0	"	"
		6	0.0	"	"
		7	0.4	"	"
	335	7	0.4	Ball broke in intermetallics	Bonding error
V	421	1	1.7	Wire broke	None
VI	581	6	1.8	Wire broke	None

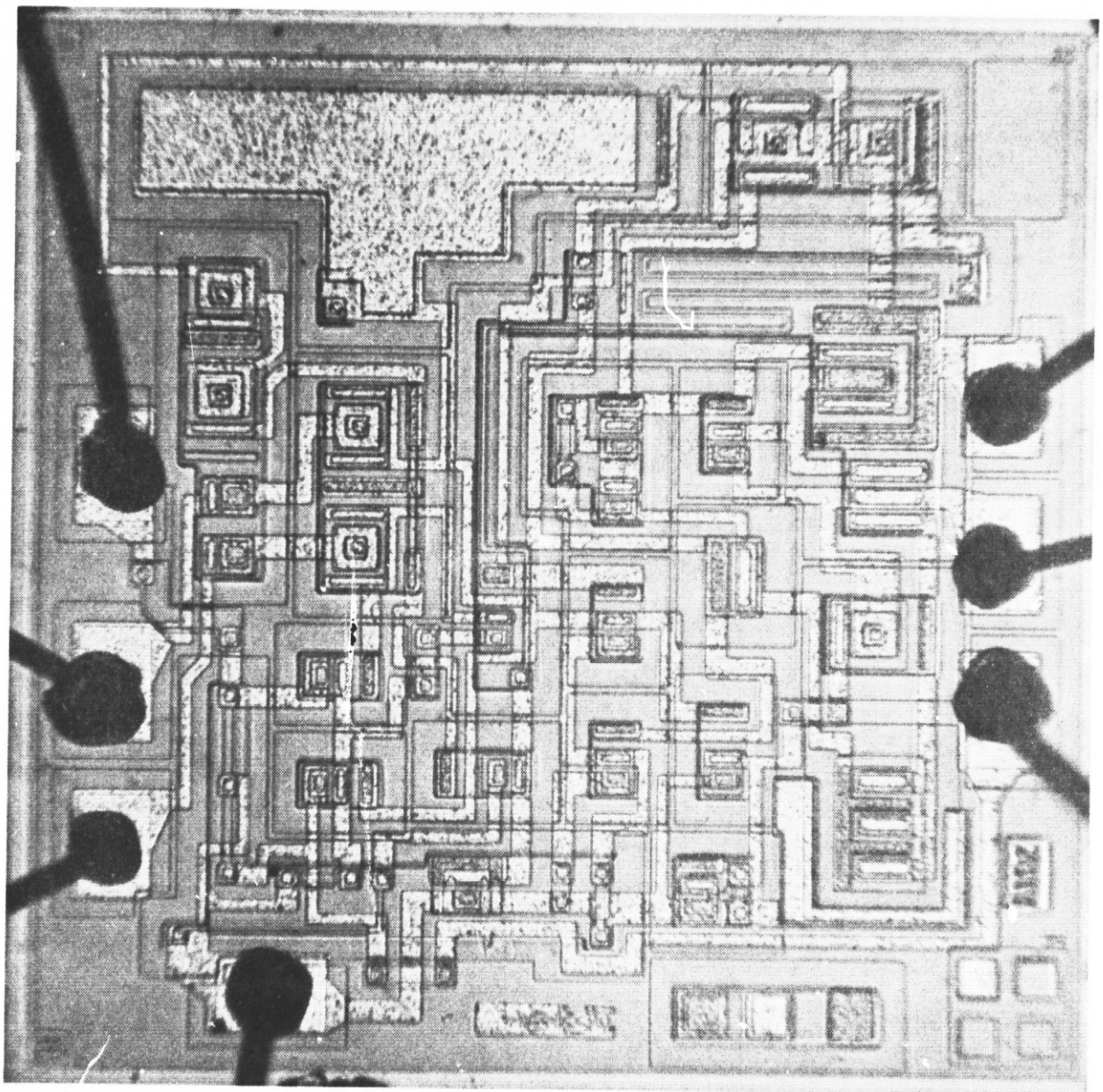

125X (ORIGINAL) S/N 504, GROUP VI

FIGURE C30. PHOTO OF A DIE WHICH ILLUSTRATES THE CONDITION OF THE GLASSIVATION TYPICAL OF ALL SIX TEST GROUPS.

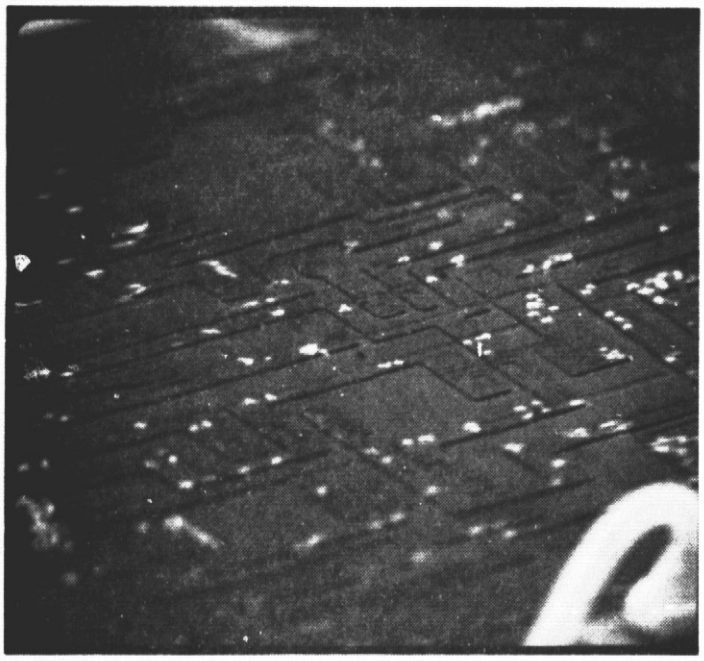

S/N 241, GROUP III

FIGURE C31. SEM PHOTO OF THE SURFACE OF A PART CONTAMINATED WITH DROPS OF FOREIGN MATTER (WHITE SPOTS).

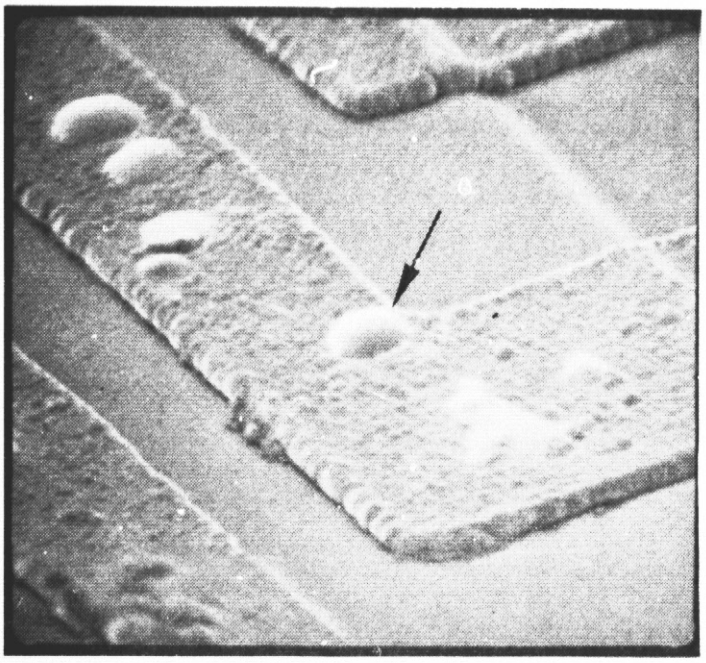

1250X S/N 241, GROUP III

FIGURE C32. SEM CLOSE UP OF THE DROPLETS SHOWING THE INITIAL SHAPE OF THE DROPLET (ARROW) TO BE INVESTIGATED.

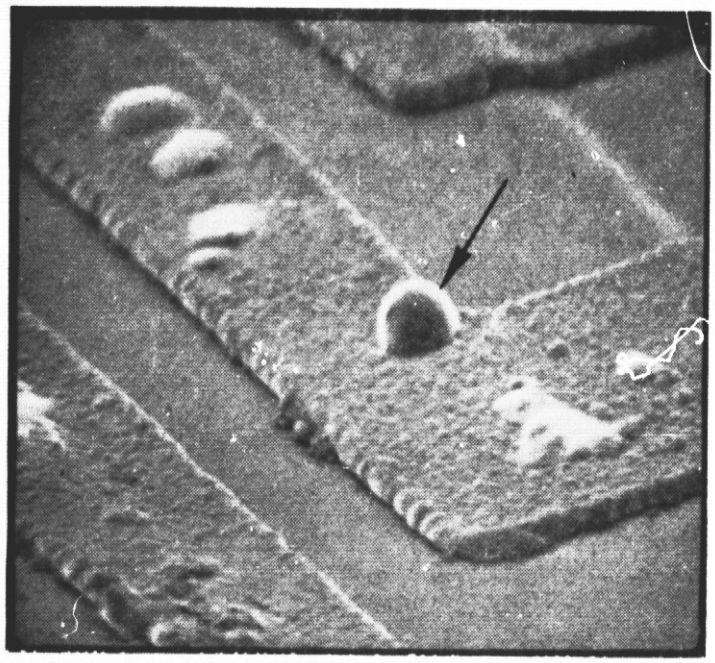

1250X S/N 241, GROUP III

FIGURE C33. SEM PHOTO SHOWING THE SWELLING INDUCED IN ONE DROPLET (ARROW) AFTER EXAMINING IT AT HIGHER MAGNIFICATIONS.

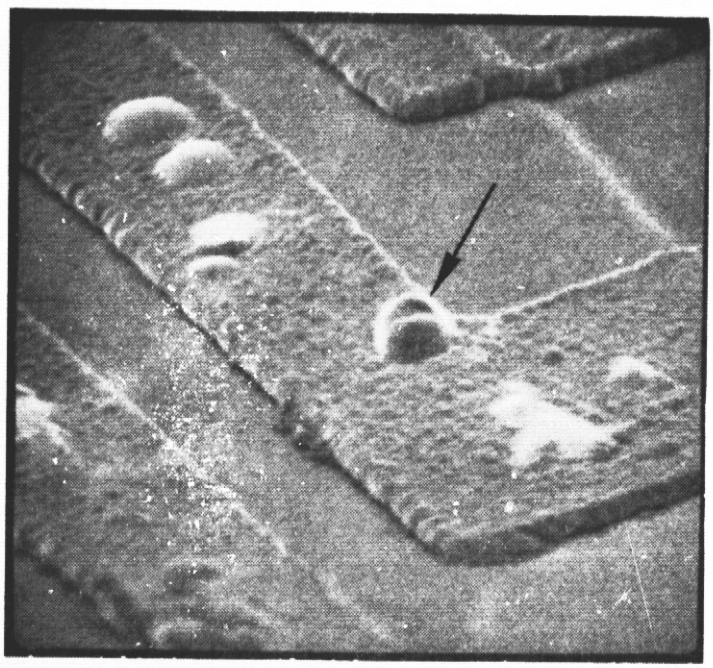

1250X S/N 241, GROUP III

FIGURE C34. SEM PHOTO TAKEN A FEW SECONDS AFTER FIGURE C33 WAS TAKEN SHOWING THAT THE SWOLLEN DROPLET (ARROW) HAS COLLAPSED.

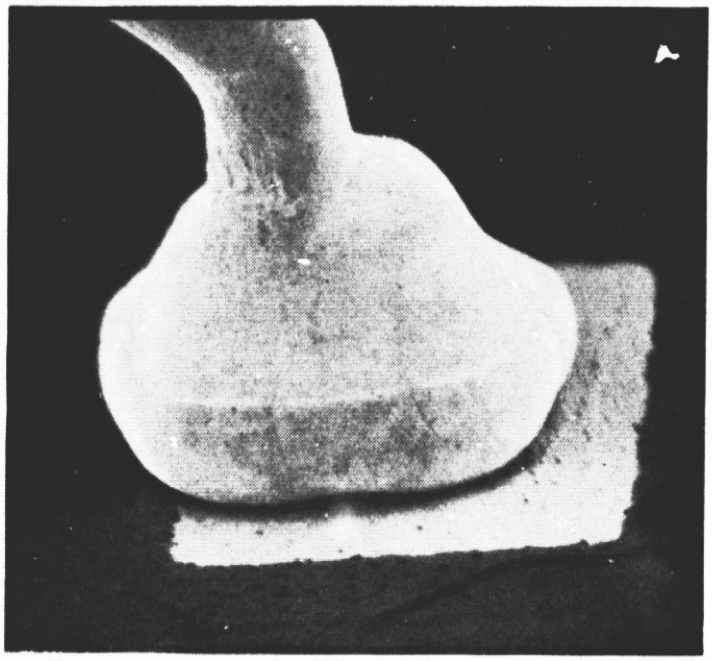

500X S/N 481, GROUP V

FIGURE C35. WIRE BOND AT THE DIE.

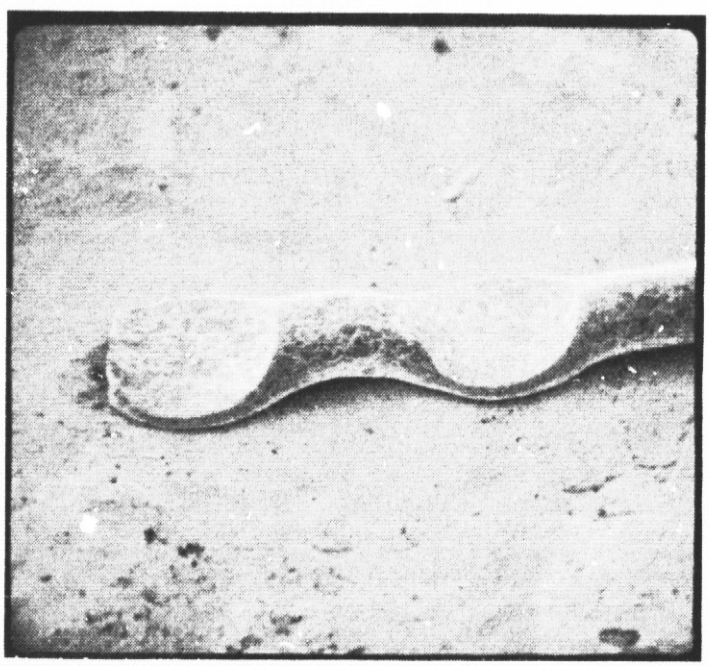

250X S/N 481, GROUP V

FIGURE C36. WIRE BOND AT THE POST.

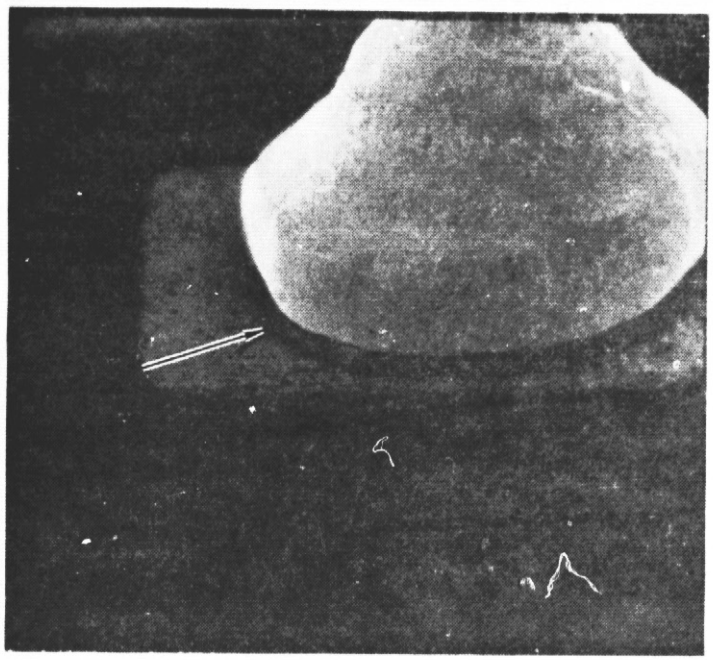

580X S/N 362, GROUP IV

FIGURE C37. PIN 8 BOND SHOWING RING OF INTERMETALLICS (ARROW).

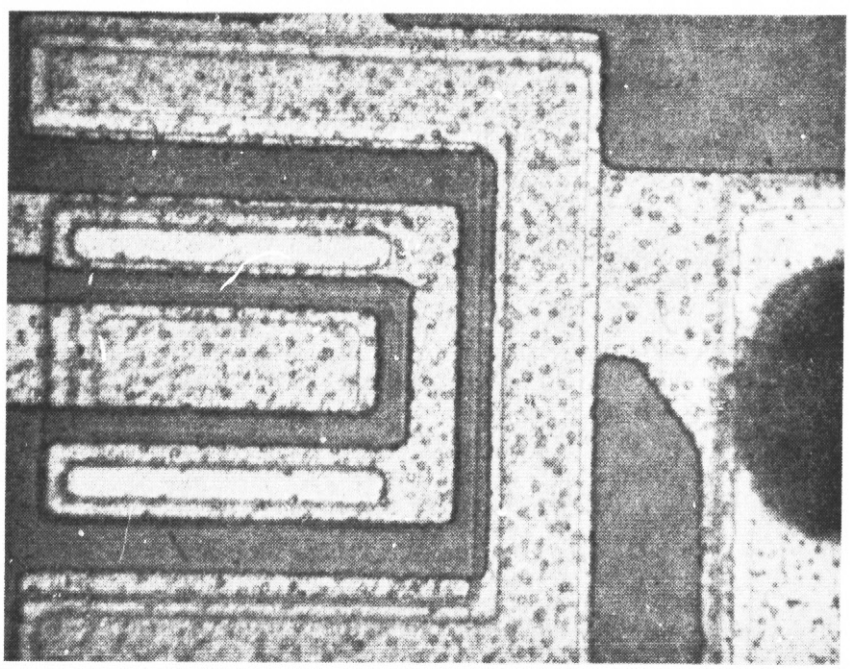

490X S/N 362, GROUP IV

FIGURE C38. V+ (PIN 7) METALLIZATION

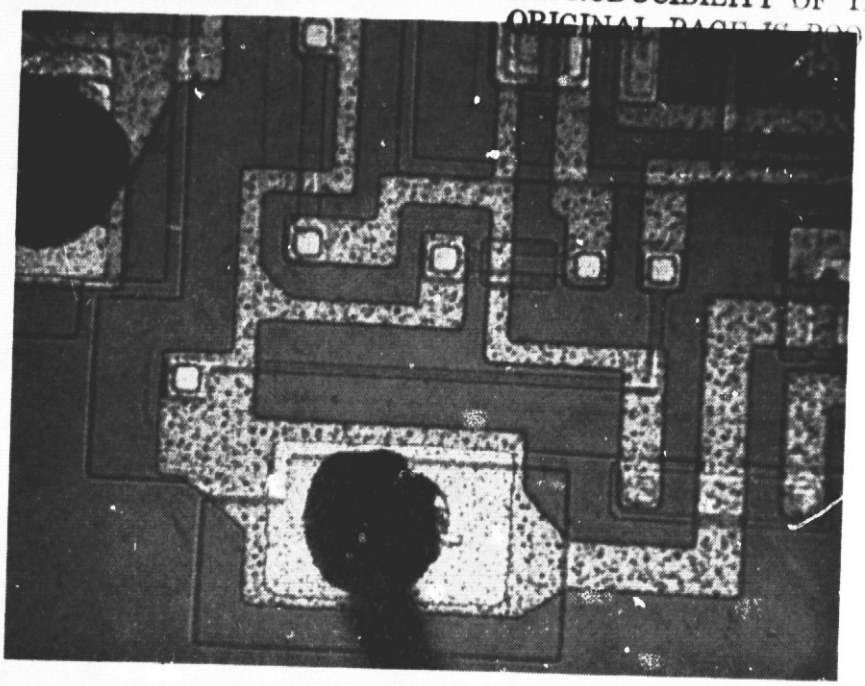

250X

S/N 362, GROUP VI

FIGURE C39. V- (PIN 4) METALLIZATION

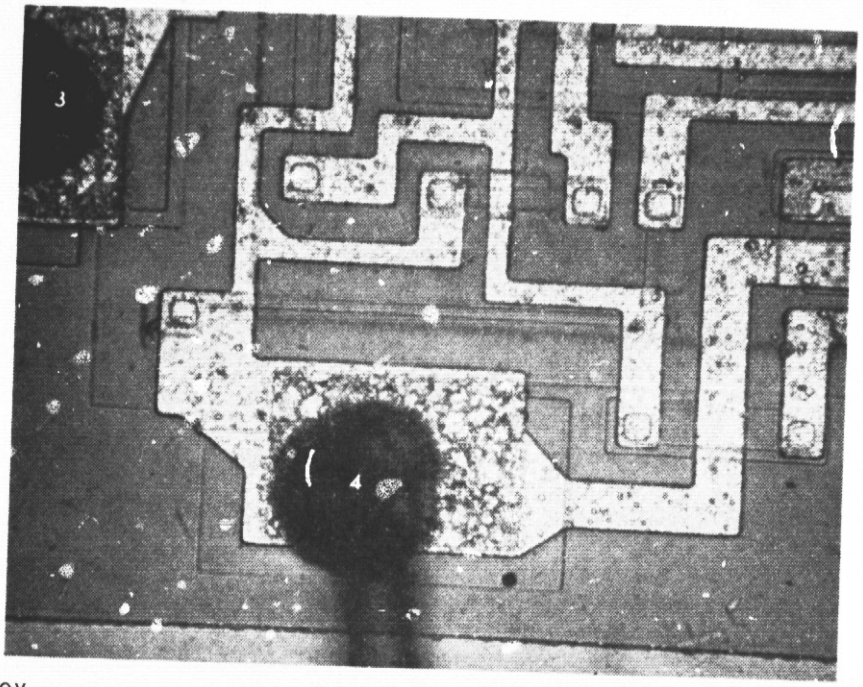

250X

S/N 241, GROUP III

FIGURE C40. EXAMPLE OF ALUMINUM RECONSTRUCTION AT THE BOND PADS.

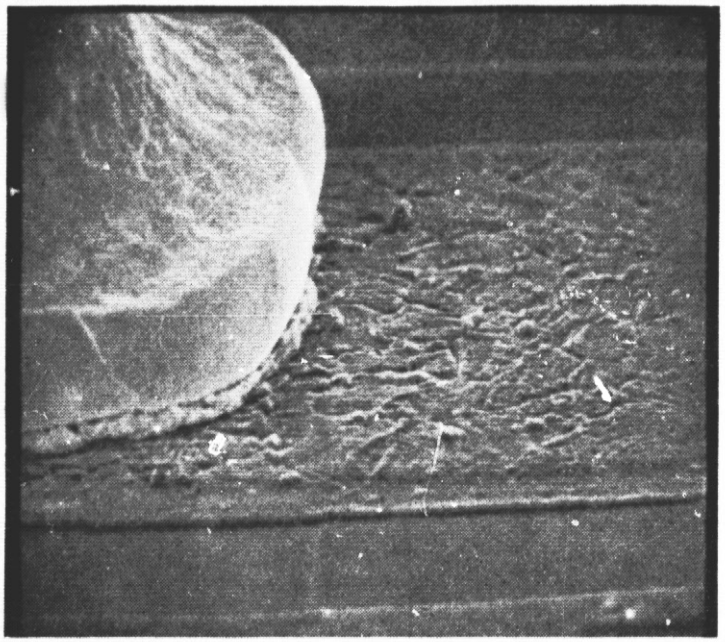

650X S/N 85, GROUP II

FIGURE C41. SEM PHOTO OF ALUMINUM RECONSTRUCTION AT THE PIN 5 BOND PAD.

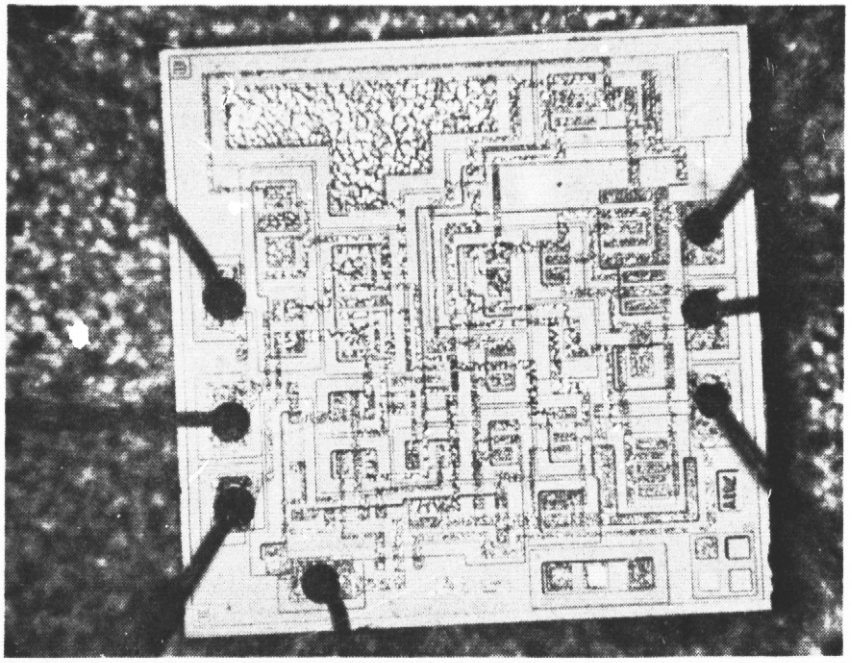

57X S/N 184, GROUP I

FIGURE C42. EXAMPLE OF THE EXTENT OF ALUMINUM RECONSTRUCTION REVEALED BY GLASSIVATION REMOVAL.

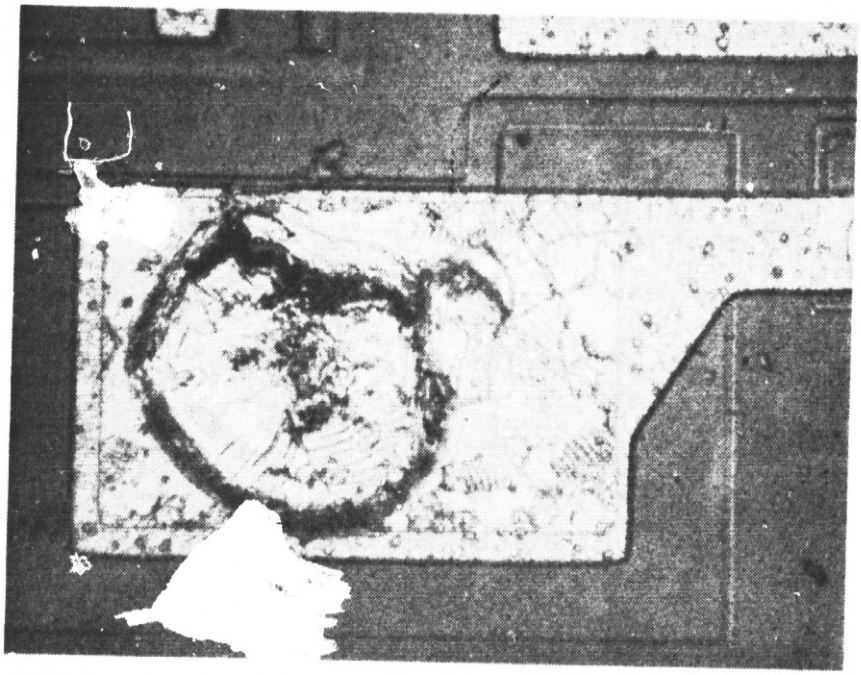

490X S/N 123, GROUP I

FIGURE C43. LIFT-OFF PATTERN OF THE PIN 1 BOND

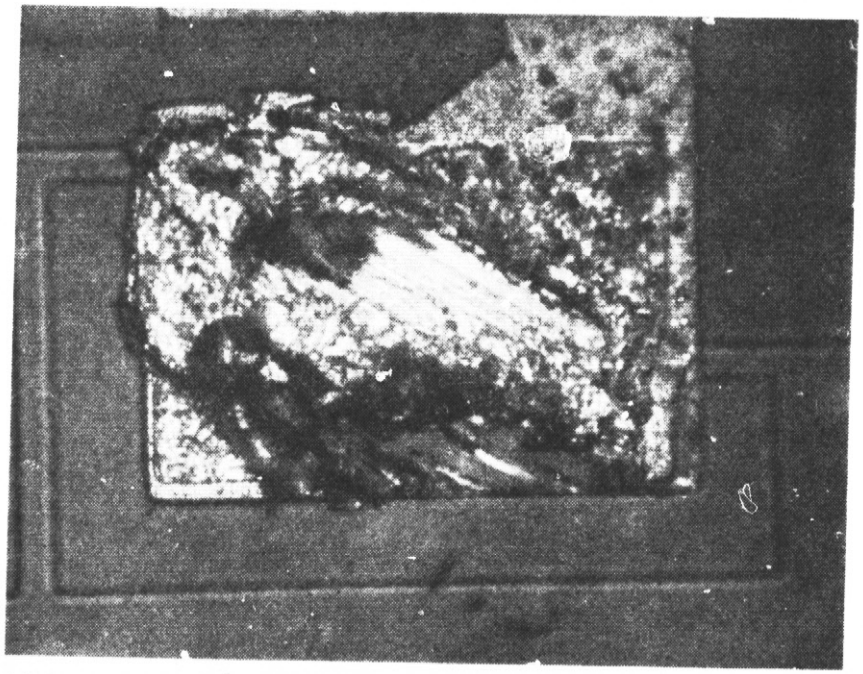

490X S/N 231, GROUP III

FIGURE C44. SMEARED PIN 7 BOND PAD.

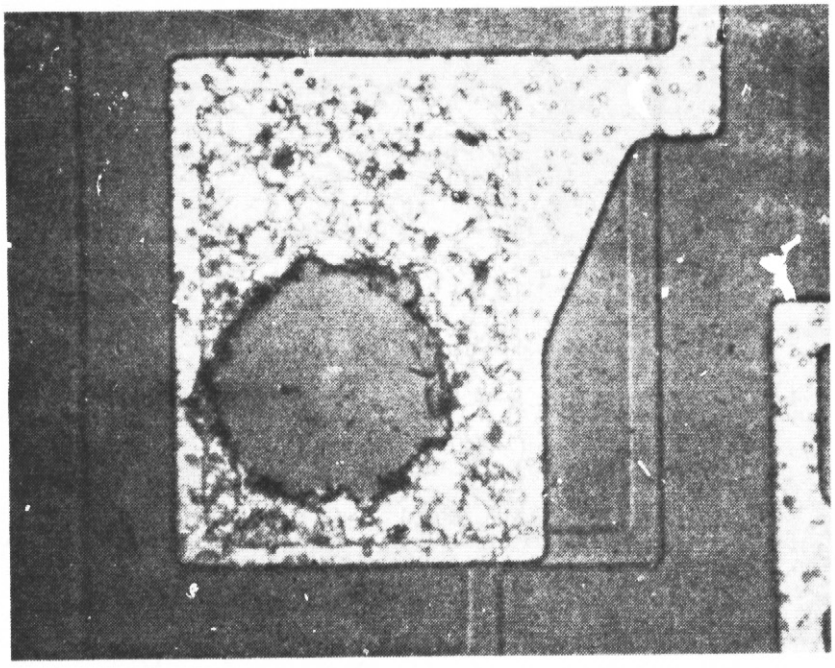

490X S/N 223, GROUP III

FIGURE C45. EXAMPLE OF BOND FAILURE DUE TO SEPARATION OF THE ALUMINUM FROM THE SiO_2 (PIN 1).

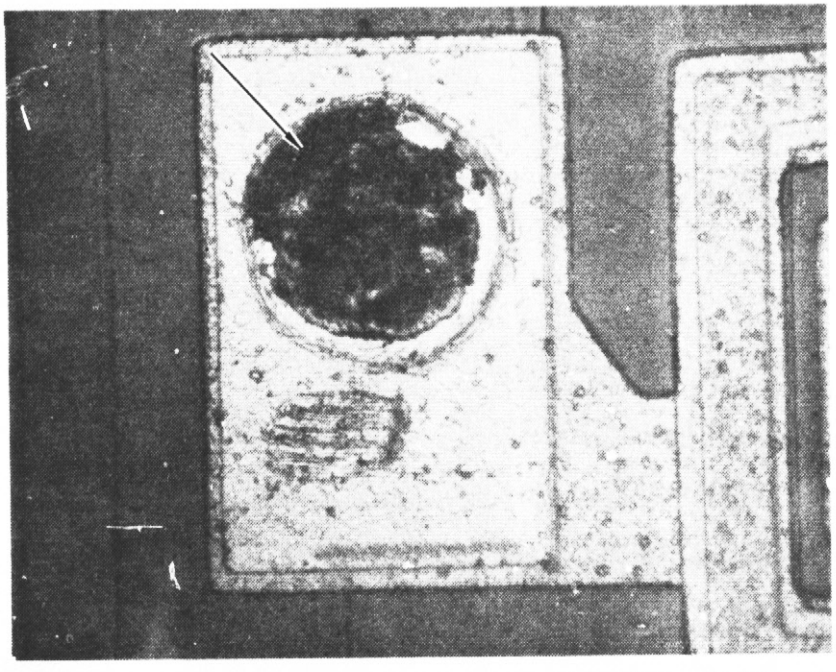

490X S/N 335, GROUP IV

FIGURE C46. LIFT-OFF PATTERN OF PIN 7 SHOWING THE MOUND OF INTERMETALLICS (ARROW).

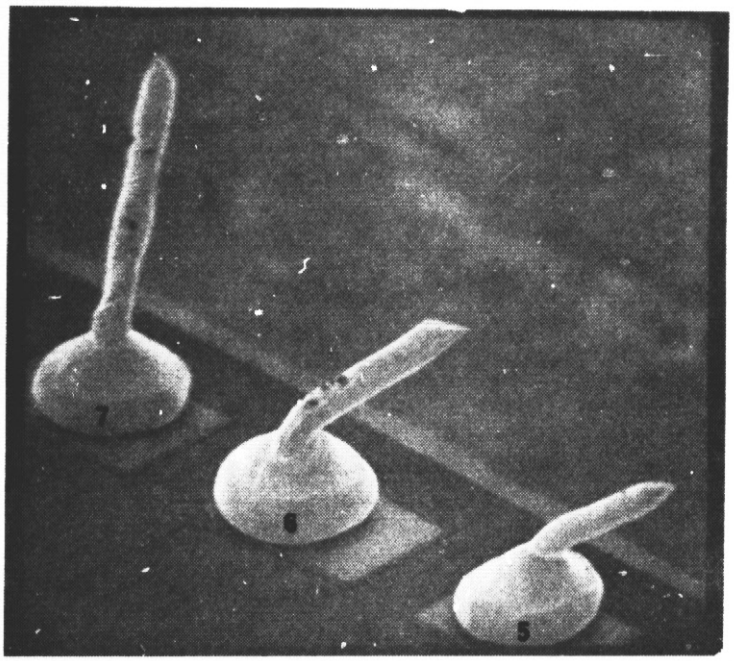

170X S/N 581, GROUP VI

FIGURE C47. SEM PHOTO OF THE FAILED PIN 6 WIRE (CENTER) WHICH BROKE AT 1.8 GRAMS. THE L/H WIRE BROKE AT 3.8 GRAMS AND THE R/H WIRE BROKE AT 4.4 GRAMS.